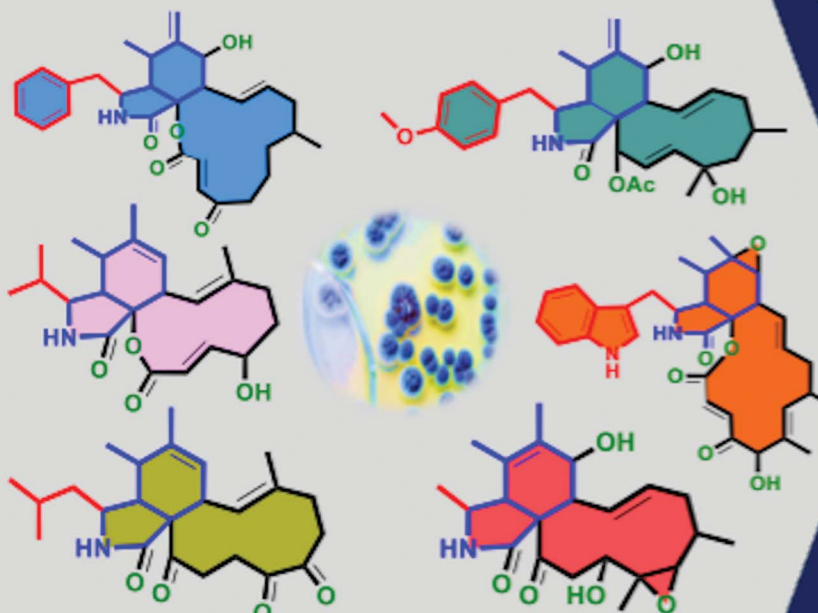


Natural Product Reports

rsc.li/npr

Cytochalasans



PKS-NRPS



Chemistry
Biology



Biosynthesis
Pharmacokinetics

ISSN 0265-0568



Cite this: *Nat. Prod. Rep.*, 2025, **42**, 788

The cytochalasans: potent fungal natural products with application from bench to bedside†

Mohamed A. Tammam, ^a Florbela Pereira, ^b Elizabeth Skellam, ^c Stefan Bidula, ^d A. Ganesan ^d and Amr El-Demerdash ^{*def}

Covering: 2000–2023

Cytochalasans are a fascinating class of natural products that possess an intricate chemical structure with a diverse range of biological activities. They are known for their complex chemical architectures and are often isolated from various fungi. These compounds have attracted attention due to their potential pharmacological properties, including antimicrobial, antiviral, and anticancer effects. For decades, researchers have studied these molecules to better understand their mechanisms of action and to explore their potential applications in medicine and other fields. This review article aims to shed light over the period 2000–2023 on the structural diversities of 424 fungal derived cytochalasans, insights into their biosynthetic origins, pharmacokinetics and their promising therapeutic potential in drug discovery and development.

Received 24th December 2024

DOI: 10.1039/d4np00076e

rsc.li/npr



1. **Introduction**
2. **Recent advances in cytochalasan biosynthesis**
- 2.1. **Biosynthetic gene clusters (BGCs)**
- 2.2. **Enzymes required for the synthesis of the perhydroisoindolone core**
- 2.3. **Oxidative modifications by tailoring enzymes and non-enzymatic processes**
3. **Structural diversity and biological activities of cytochalasans derived from fungi**
 - 3.1. **Fungi of the class Agaricomycetes**
 - 3.1.1. **Fungi of the undenied subclass**
 - 3.1.1.1. **Fungi of the order Polyporales**
 - 3.1.2. **Fungi of the class Dothideomycetes**
 - 3.2.1. **Fungi of the subclass Pleosporomycetidae**
 - 3.2.1.1. **Fungi of the order Pleosporales**
 - 3.3. **Fungi of the class Eurotiomycetes**
 - 3.3.1. **Fungi of the subclass Eurotiomycetidae**
 - 3.3.1.1. **Fungi of the order Eurotiales**
 - 3.4. **Fungi of the class Leotiomycetes**
 - 3.4.1. **Fungi of the subclass Leotiomycetidae**
 - 3.4.1.1. **Fungi of the order Helotiales**
 - 3.5. **Fungi of the class Sordariomycetes**
 - 3.5.1. **Fungi of the subclass Sordariomycetidae**
 - 3.5.1.1. **Fungi of the order Diaporthales**
 - 3.5.2. **Fungi of the subclass Hypocreomycetidae**
 - 3.5.2.1. **Fungi of the order Hypocreales**
 - 3.5.2.2. **Fungi of the order Sordariales**
 - 3.5.3. **Fungi of the subclass Xylariomycetidae**
 - 3.5.3.1. **Fungi of the order Xylariales**
 4. **Pharmacokinetics and ADMET of cytochalasans derived from fungi**
 5. **Applications of cytochalasans in imaging and drug discovery**
 - 5.1. **Cytochalasans as illuminating probes**
 - 5.1.1. **Illuminating the cellular landscape**
 - 5.1.2. **Journeying into the molecular landscape**
 - 5.2. **The epic quest in drug discovery**
 - 5.2.1. **Targeted therapy**
 - 5.2.2. **Navigating the seas of drug delivery systems**
 - 5.3. **Current stage of clinical development of cytochalasans**
 - 5.3.1. **Cardiovascular applications**
 - 5.3.2. **Oncology and cancer therapy**
 - 5.3.3. **Inflammatory and autoimmune diseases**

^aDepartment of Biochemistry, Faculty of Agriculture, Fayoum University, Fayoum 63514, Egypt

^bLAQV REQUIMTE, Department of Chemistry, NOVA School of Science and Technology, Universidade Nova de Lisboa, 2829516 Caparica, Portugal

^cDepartment of Chemistry and BioDiscovery Institute, University of North Texas, 1155 Union Circle, Denton, TX, 76201, USA

^dSchool of Chemistry, Pharmacy and Pharmacology, University of East Anglia, Norwich Research Park, Norwich NR4 7TJ, UK. E-mail: A.Eldemerdash@uea.ac.uk

^{*}Division of Organic Chemistry, Department of Chemistry, Faculty of Sciences, Mansoura University, Mansoura 35516, Egypt

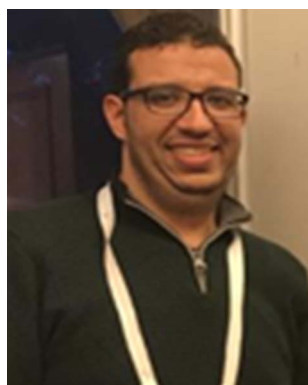
[†]Department of Biochemistry and Metabolism, The John Innes Centre, Norwich Research Park, Norwich NR4 7UH, UK. E-mail: Amr.El-Demerdash@jic.ac.uk

† Electronic supplementary information (ESI) available. See DOI: <https://doi.org/10.1039/d4np00076e>

- 5.3.4. Infectious diseases
- 5.3.5. Modulators of stem cell differentiation
- 6. Conclusion, future directions opportunities and challenges
- 7. Abbreviations
- 8. Data availability
- 9. Author contributions
- 10. Conflicts of interest
- 11. Acknowledgements
- 12. References

1. Introduction

Microbial natural products have long been recognized as a valuable source of bioactive compounds with diverse chemical structures and potent biological activities. These organic



Mohamed A. Tammam

mentorship of Prof. Vassilios Roussis and Prof. Efstathia Ioannou. Dr Tammam is currently a postdoctoral researcher at NKUA, continuing his work on bioactive natural products from marine organisms.



Florbela Pereira

learning techniques to predict molecular properties based on DFT data, aiding in early-stage screening for drug and materials design. She serves on the editorial boards of Computational and Structural Biotechnology Journal, In Silico Methods for Drug Discovery, and Marine Drugs.

compounds, produced by microorganisms such as bacteria and fungi, play a crucial role in drug discovery and development.^{1,2} Indeed, they have evolved intricate biosynthetic pathways, allowing them to produce an array of secondary metabolites that serve various ecological functions, including defence against competitors and communication within microbial communities.^{3,4}

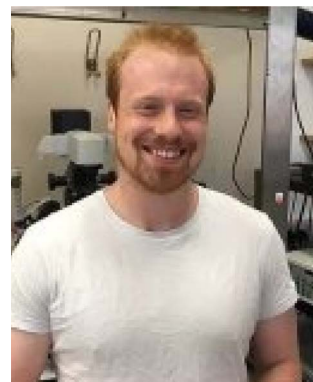
Moreover, microbial natural products have demonstrated unique chemical scaffolds with a wide range of biological activities, including antimicrobial, anticancer, immunomodulatory, and antiviral properties making them promising candidates for drug discovery.⁵ These compounds have served as the basis for the development of numerous clinically important drugs, such as antibiotics (e.g., Penicillin, Erythromycin), immunosuppressants (e.g., Cyclosporine), and anticancer agents (e.g., Doxorubicin).^{6,7}

Fungi, a diverse group of microorganisms, have long captured the interest of scientists and researchers for their ability to produce an astonishing variety of natural products.^{8,9}



Elizabeth Skellam

Dr Elizabeth Skellam received an MChem degree from Swansea University, a master's in business administration from the University of North Carolina at Wilmington, and a PhD in Chemistry from the University of Bristol. She has worked as a Technical Writer at ID Business Solutions and as an Akademischer Rat in Leibniz University Hannover. She is currently an Assistant Professor at the University of North Texas, and her research focuses on elucidating and engineering biosynthetic pathways in microorganisms to discover new enzymes and generate novel natural products.



Stefan Bidula

Dr Stefan Bidula holds a BSc (Hons) in Genetics and Molecular Biology and a PhD in Biomedicine from the University of East Anglia (2011). He completed his first postdoctoral position at the University of Aberdeen (2014–2016), studying C-type lectins in antifungal immunity. Dr Bidula then held two postdoctoral positions at UEA (2016–2022), investigating ATP-gated ion channels. In 2022, he established his own group in the School of Pharmacy at UEA, focusing on non-canonical nucleic acid structures, fungal secondary metabolism, novel antifungal targets, and host–fungal interactions. He also serves as an editor for Virulence and Critical Reviews in Microbiology.

These fungal natural products, also known as secondary metabolites, exhibit a wide range of chemical structures and biological activities, making them valuable resources for drug discovery.^{10–12}

Fungal natural products have played a significant role in the development of therapeutic agents. Many well-known approved drugs as well as these under preclinical or clinical investigations, such as antibiotics [e.g. Penicillin and Cephalosporins],^{13,14} immunosuppressants [e.g. Cyclosporine A and Mycophenolic acid],^{15,16} anticancers [e.g. Taxol],^{17,18} anti-inflammatories [e.g. Cordycepin and Gliotoxin],^{19,20} and cholesterol-lowering agents [e.g. Lovastatin and Pravastatin],^{21,22} owe their origins to fungal sources. These compounds have revolutionized medicine and have been instrumental in combating various diseases.^{23–25} Indeed, the remarkable diversity of fungal species offers an extensive repertoire of natural products waiting to be explored.^{26,27} Fungi possess unique biosynthetic pathways and have the capacity to produce complex molecules with intricate chemical scaffolds.^{28–30} This structural complexity often translates into a wide array of biological activities, including antimicrobial, anticancer, anti-inflammatory, and antiviral properties.^{31–34}

One of the key advantages of fungal natural products in drug discovery is their novelty. Fungi can produce compounds that are not found in other organisms, making them a rich source of untapped chemical diversity.^{35–37} This inherent novelty opens new avenues for developing innovative therapeutics and addressing unmet medical needs.^{13,38,39} Furthermore, the increasing threat of drug-resistant pathogens has underscored the urgent need for new antimicrobial agents.^{40–42} Additionally, fungal natural products have shown promise in combating multidrug-resistant bacteria, providing potential solutions to the global health challenge posed by antibiotic resistance.^{43–45}

Cytochalasans are a class of fungal metabolites that have a wide range of biological activities. The name “cytochalasans” comes from the Greek words “cytos” meaning cell and “chalasis”

meaning relaxation, referring to their ability to disrupt actin filaments in cells.^{46,47} Historically, the first cytochalasans, namely phomin and cytochalasans A–D were discovered in the 1960s from cultures of *Helminthosporium dematioideum* and *Metarrhizium anisopliae*.^{48,49} Since then, they have been isolated mainly from various fungal genera including *Aspergillus*,⁵⁰ *Chaetomium*,⁵¹ and *Phomopsis*.⁵²

Chemically, cytochalasans have a unique tricyclic core structure consisting of a polyketide-derived 11, 13 or 14-membered macrocyclic ring fused to various aromatic or heteroaromatic rings (e.g. an isoindolone moiety). The unique chemistry of cytochalasans arises from their incorporation of numerous amino acids and the presence of functional groups, such as hydroxyl, methyl, and acyl groups, which further enhance their chemical complexity, structural diversity, and biomedical potentialities. Additionally, the presence of these functional groups allows for potential modifications and derivatizations to fine-tune the biological activity of cytochalasans.^{53,54} Furthermore, the stereochemistry of cytochalasans plays a crucial role in their biological properties, with specific configurations at key positions influencing their interactions with biological targets.^{55–57}

Structurally, cytochalasans are generally classified into six main groups (G1–G6) based on the specific amino acids involved in their formation (Chart 1). These groups include “Cytochalasins” which contain a phenylalanine residue, “Pyrichalasins” which incorporate a tyrosine or a related derivative residue, “Chaetoglobosins” which feature a tryptophan residue, “Aspochalasins” which include a leucine residue, “Alachalasins” which have an alanine residue, and “Trichalasin” which involves α -valine residue.^{58–60} To date, over 400 different naturally occurring cytochalasans have been identified, particularly from fungal species of The Ascomycota and Basidiomycota.^{53,58}

The pharmacological profile of cytochalasans encompasses a wide range of biological activities, making them promising candidates for various therapeutic applications. These



A. Ganesan

Southampton in 1999 and to UEA in 2011 as Chair of Chemical Biology. Prof. Ganesan is co-founder of Karus Therapeutics and Chair of EU COST Action CM1406. His research focuses on chemical biology, medicinal chemistry, and epigenetics.



Amr El-Demerdash

Dr Amr El-Demerdash holds a BSc (2004) and MSc (2009) in chemistry from Mansoura University, Egypt, and a PhD in organic chemistry from CNRS-ICSN, University of Paris-Saclay, France (2016), focusing on pharmacologically active marine natural products and biomimetic synthesis. He completed postdoctoral training at CNRS/MNHN, Sorbonne Universities (2017–2019), and the John Innes Centre-UK (2019–2024). In 2021, he was promoted to Associate Professor in Organic Chemistry at Mansoura University, Egypt. In August 2024, he joined the University of East Anglia-UK, as a Group Leader and Assistant Professor in Chemical Biology. His lab specializes in natural products-based drug discovery.



compounds have demonstrated cytotoxic effects, meaning they can inhibit the growth and proliferation of cancer cells. This property has garnered significant interest in the development of cytochalasans as potential anticancer agents.^{61–63}

In addition to their cytotoxicity, cytochalasans have also shown antimicrobial activity against bacteria, fungi, and parasites. They can inhibit the growth and reproduction of these microorganisms, making them valuable in the search for new antimicrobial agents.⁶⁴

Furthermore, certain cytochalasans exhibit antiviral properties, with the ability to interfere with viral replication and infection processes.⁶⁵ This makes them potential candidates for the development of antiviral therapies.⁶⁶ The anti-inflammatory effects of cytochalasans have also been investigated. These compounds can modulate inflammatory responses by inhibiting the production of inflammatory mediators and reducing the activation of immune cells.⁶⁷ Such anti-inflammatory properties may have implications for the treatment of inflammatory disorders and autoimmune diseases.⁶⁸

Moreover, cytochalasans have demonstrated immunosuppressive effects. This property can be beneficial in cases where immune hyperactivity needs to be controlled, such as following organ transplantation or in autoimmune conditions.^{69,70}

Biosynthetically, cytochalasans are synthesized through polyketide synthase–nonribosomal peptide synthetase (PKS–NRPS) hybrid pathways. These pathways play a pivotal role in constructing the intricate molecular architecture of these metabolites. PKS–NRPS pathways represent distinctive modular enzymatic systems that orchestrate the integration of both polyketide and peptide building blocks.

Additionally, within these pathways, the PKS components are responsible for assembling the polyketide backbone, while the NRPS components incorporate amino acid residues into the growing PKS chain. This hybrid nature of PKS–NRPS systems

enables the incorporation of diverse building blocks, fostering structural and biological diversification.^{60,71–74}

Previously, Hertweck and his co-workers,⁵⁸ outlined a comprehensive overview of the chemistry and biology of fungal cytochalasans. They explored the diverse chemical structures, biological activities, biosynthesis, structure–activity relationships, modes of action, with focused examination of their impact on cellular processes and their potential as therapeutic agents.

Additionally, Zhu *et al.*, presented a book chapter discussing the recent progress in the chemistry of fungal-derived cytochalasans. They provided an updated overview on isolation, structural determination, biological activities, biosynthesis and the recent strategies employed in the total synthesis and modifications of these fungal natural products.⁵³

Furthermore, Lambert *et al.*, reported on the impact of cytochalasans on actin filament remodelling, a crucial process in cell motility and shape changes. They highlighted the structural diversity of a total of 136 cytochalasans, their capacity to modulate actin dynamics and organization in eukaryotic cells, and their potential as future therapeutic tools, particularly in the context of employing click chemistry.⁷⁵

In line with our continuous research efforts on identifying biologically active natural products,^{76,77} particularly focusing on pharmacologically active fungal-derived natural products (FNPs),^{78–83} herein we present a comprehensive and up-to-date literature review on cytochalasans exclusively isolated from different fungal strains.

The review encompasses the period from 2000–2023 and aims to provide a thorough comprehensive examination of the chemical and structural diversities, pharmacological activities, biosynthesis, pharmacokinetics and druglikeness properties associated with these fungal derived metabolites. Throughout the review, we systematically documented the distribution of a total of 424 cytochalasans among various fungal genera, shedding light on their unique chemical profiles and

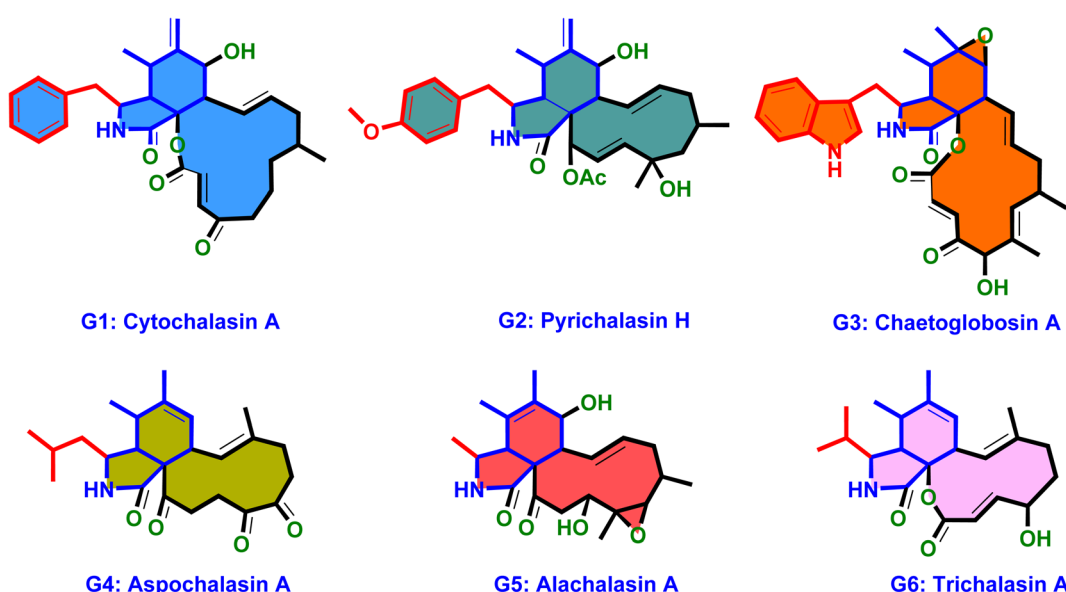


Chart 1 The molecular architecture of the six main cytochalasans (G1–G6).



therapeutic potentialities. This in-depth analysis allows us to gain insights into the remarkable diversity of cytochalasans derived from fungal sources and their significance in drug discovery and development.

Additionally, the review discusses recent advances in the biogenesis of cytochalasans, offering insights into the mechanisms underlying their formation within fungal strains. Indeed, we hope that this comprehensive literature review serves as a valuable resource for researchers and scientists interested in the field of fungal cytochalasans and their potential applications in the development of novel therapeutic agents.

2. Recent advances in cytochalasan biosynthesis

2.1. Biosynthetic gene clusters (BGCs)

Extensive isotope-labelled feeding studies performed during the 1970–1990s indicated that cytochalasans are biosynthesized

from acetate/malonate, *S*-adenosylmethionine, *L*-amino acids, and molecular oxygen.^{84–88} In fungi, polyketide-peptide hybrids are typically synthesized by giant multi-functional multi-domain-containing polyketide synthase/non-ribosomal peptide synthetase (PKS-NRPS) enzymes.^{74,89} The understanding of PKS-NRPS enzymes in fungi led to the identification of biosynthetic gene clusters (BGCs) encoding chaetoglobosin A (199),⁹⁰ cytochalasans E (376)/K (329),⁹¹ and cryptic cytochalasans,^{92–96} in quick succession (Chart 2).

BGCs encoding pyrichalasin H (I),⁹⁷ phomacins D/E/F (II, III and IV),⁹⁸ aspochalasins C, E, M and flavichalasines F and G (77), (69), (70), (79) and (80),⁹⁹ cytochalasin H (116) and related cytochalasins,¹⁰⁰ aspergillin PZ (81),¹⁰¹ chaetoglobosin P (V),¹⁰² cytoglobosin X (VI),¹⁰³ have also been identified recently. These BGCs share a high level of homology, where the PKS-NRPS, *trans*-acting enoylreductase (*trans*-ER), α,β -hydrolase (α,β -HYD), and Diels–Alder (DA) genes are considered to be the core genes,¹⁰⁴ yet all BGCs identified to date also

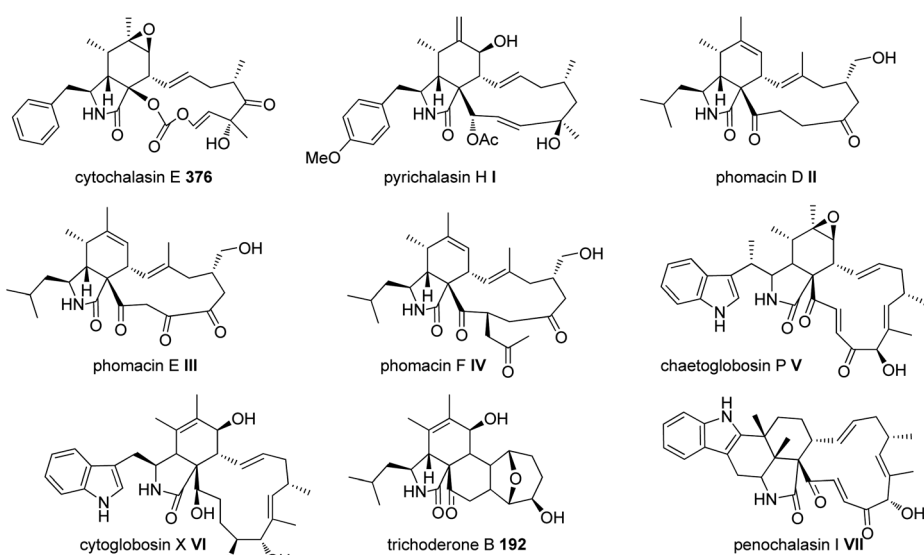


Chart 2 Chemical structures of biosynthetically investigated cytochalasans 192, 376, and I–VII.

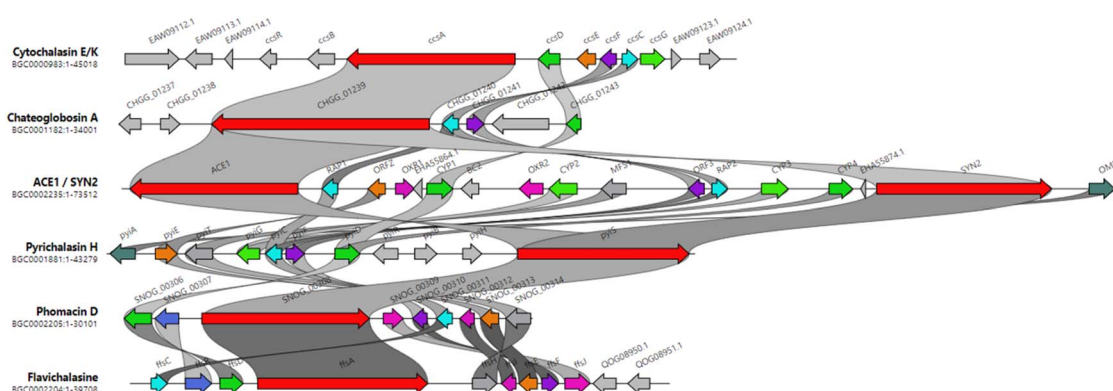
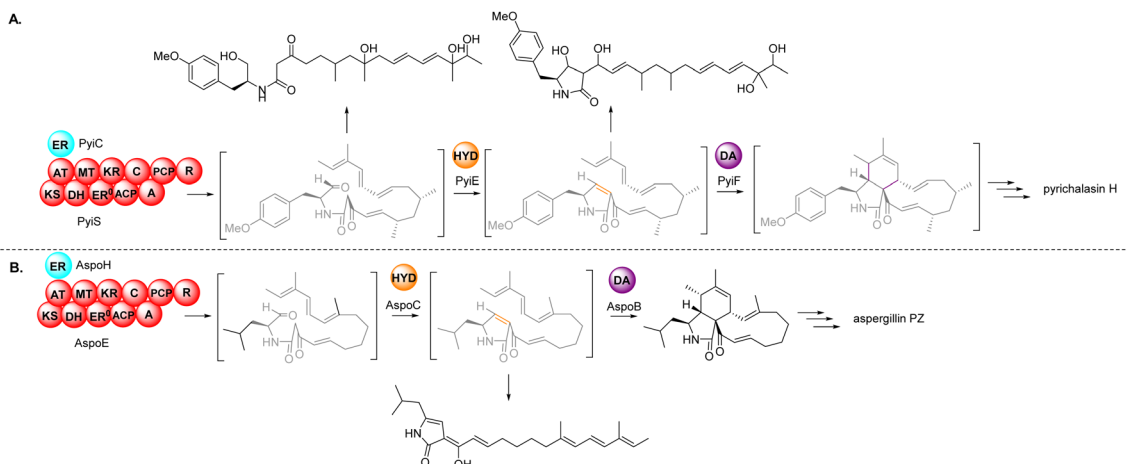


Chart 3 Clinker comparison of experimentally validated cytochalasan BGCs.¹⁰⁷ Abbreviations: OMeT = O-methyltransferase; α,β -HYD = α,β -HYD and *trans*-ER; MFS = major facilitator superfamily transporter; *trans*-ER = *trans*-acting enoyl reductase; DA = Diels–Alderase; P450 = cytochrome P450 monooxygenase; PKS-NRPS = polyketide synthase/non-ribosomal peptide synthetase; OXR = oxidoreductase; TF = transcription factor.





Scheme 1 Overview of the core enzymes, and their deduced roles, in the biosynthesis of the characteristic perhydroisoindolone moiety of cytochalasans. (A) *In vivo* experimental results from the investigation of pyrichalasin H (I); (B) *In vivo* experimental results from the investigation of aspergillin PZ (81).

encode several additional tailoring enzymes such as: cytochrome P450 monooxygenases (P450); oxidoreductases (OXR); Baeyer–Villiger monooxygenases (BVMO); and transferases (Chart 3). Typically, BGCs also encode transcription factors (TF) which have mostly been shown to function as positive regulators of cytochalasan biosynthesis.^{91,98,105,106} The precise role of the major facilitator superfamily (MFS) transporter is unknown.

2.2. Enzymes required for the synthesis of the perhydroisoindolone core

Based on the chemical structures of cytochalasans, biosynthetic proposals suggested that after the polyketide chain had reached the length and level of reduction defined by the PKS module, it is condensed with a specific amino acid, dictated by the NRPS module, and released from the PKS–NRPS *via* reduction to generate an aldehyde.^{91,108} The resulting aldehyde undergoes Knoevenagel condensation, followed by [4 + 2] cycloaddition to generate the characteristic perhydroisoindolone core (Scheme 1). Gene disruption (also knock-out; KO) and/or heterologous expression experiments determined that the PKS–NRPS gene was essential for biosynthesis of the carbon backbone during the biosynthesis of cytochalasans.^{90,91,97–99,101} Similarly, KO of the *trans*-ER confirmed that the PKS–NRPS cannot function successfully without its partner,^{90,97} analogous to other studies of fungal PKS–NRPS systems.

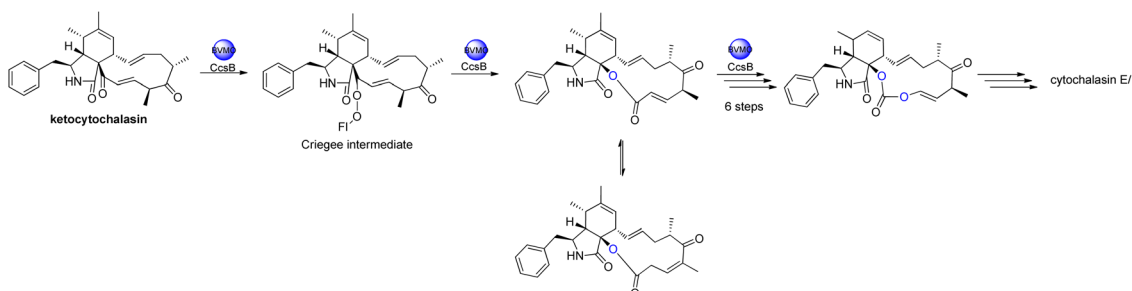
In-depth studies of the terminal reductase (R) domain of PyiS, the PKS–NRPS required for pyrichalasin H (I) biosynthesis, determined the precise chain release mechanism is a two-electron NADPH-mediated reduction of the covalently bound polyketide thiolester.¹⁰⁹ Although this mechanism had long been suspected, several *in vivo* investigations had led to identification of an alcohol thought to result from over-reduction of the aldehyde by unknown enzymes in the fungal host,^{72,95} however a four-electron reduction mechanism could not be ruled out until now.

Additionally, studies of PyiS indicated that the adenylation (A) domain of the NRPS can be quite flexible towards a range of amino acid substrates.^{73,97} Pyrichalasin H (I) possesses a *para*-methoxy group, presumed to arise *via* methylation of tyrosine. KO experiments determined that a dedicated O-methyltransferase (–OMeT) methylated tyrosine which is then condensed with the growing polyketide chain.⁹⁷ Indeed, in the absence of the –OMeT, a range of unnatural *para*-substituted phenylalanine analogues can be fed to the fungal host generating a library of new-to-nature functionalized cytochalasans.⁷³ *In vivo* experiments determined the role of the α,β -HYD in facilitating formation of the pyrrolinone moiety.¹¹⁰ Synthetic aldehyde analogues were shown to be reactive and spontaneously hydrolyze to give a pyrrolinone, however the double bond was not in the position required for a subsequent [4 + 2] cyclization.¹¹⁰ This tautomerization was also observed during heterologous co-expression of the PKS–NRPS and *trans*-ER genes in certain fungal hosts.^{98,101} Therefore, the α,β -HYD appears to prevent reduction of the aldehyde and ensures correct tautomerization of the resulting five-membered heterocyclic ring. Similarly, KO experiments of the DA gene confirmed its role as facilitating [4 + 2] cycloaddition of the polyketide terminal diene and the correctly tautomerized pyrrolinone core.¹⁰⁵ Heterologous expression of the PKS–NRPS, *trans*-ER, α,β -HYD, and DA from the aspergillin PZ (72) into *Aspergillus nidulans* led to the production of the characteristic cytochalasan core.¹⁰¹

2.3. Oxidative modifications by tailoring enzymes and non-enzymatic processes

The oxidative modifications associated with cytochalasans are typically observed around the cyclohexene moiety such as epoxidation or hydroxylation (e.g. 115–117), and around the macrocycle including oxygen insertion, hydroxylation, and epoxidation (e.g. 119, 73, 314). Additionally, there are numerous examples of cytochalasans that possess more elaborate modifications and lead to significant structural divergence including halogenation (e.g. xylarichalasin A (387)), penta- and hexacyclic





Scheme 2 Overview of oxygen insertion into the cytochalasan backbone *via* a Baeyer–Villiger monooxygenase.

fused ring systems tricoderone B (192) and penochalasin I (VII), spiro-cytochalasans (*e.g.* trichodermone (193)), merocytochalasans (*e.g.* 57–60, 64, and 74–76), and open-chain cytochalasans (*e.g.* 109, 297, 298, 310). Of the cytochalasan BGCs interrogated to date, each contains one or more P450s (Chart 3); one family epoxidizes the cyclohexene moiety, and the other hydroxylates the macrocycle.^{90,97,100,101} In some instances, the P450 that hydroxylates the macrocycle is known to be, or suspected to be, iterative introducing two consecutive hydroxyl groups at adjacent carbon atoms (*e.g.* 376, 81, 199, 329).^{90,91,101} There are various examples of cytochalasans that exhibit either single or double oxygen atom insertion into the macrocycle to form a lactone (*e.g.* 119, 95, 3), or carbonate (*e.g.* 376, 110, 111, 329, 330), respectively, and typically both are co-isolated from the same culture. The mechanism of oxygen insertion was investigated in the biosynthesis of E (376)/K (329) and found to be mediated by CcsB, a flavin-dependent monooxygenase (FMO) designated as a Baeyer–Villiger Monooxygenase (BVMO).¹¹¹ *In vitro* studies of CcsB confirmed that this single enzyme could catalyze both single and double oxygen insertion on the substrate ketocytochalasin (328) and demonstrated that a vinylgous 1,5-diketo system is essential for carbonate formation (Scheme 2).¹¹¹

Aside from P450s and BVMOs, cytochalasan BGCs often contain one or more oxidoreductases (OXR) that are either FAD- or NAD(P)H dependent. PyiH, the NAD(P)H-dependent short-chain dehydrogenase (SDR) involved in pyrichalasin H (I) biosynthesis simply reduces a ketone to an alcohol, enabling acetyl transfer by the acetyltransferase PyiB.⁹⁷ Similarly, AspoD, the NAD(P)H-dependent SDR involved in flavichalasine G (80) biosynthesis, also reduces a ketone to an alcohol. In contrast, the flavin-dependent monooxygenases (FMO) CHGG_01242-1 and AspoA, required for chaetoglobosin A (199) and aspergilin PZ (81) biosynthesis respectively, convert specific hydroxyl groups to ketones.^{90,101} However, AspoA displays a rather unusual mechanism as the oxidase is involved in keto-enol tautomerization. Without isomerization of the C-19/C-20 double bond, acid-conditions mediate formation of intramolecular cyclizations, oxygen-bridges, and merocytochalasans.¹⁰¹ AspoA therefore represents a significant enzymatic strategy for controlling metabolic flux between intended and competing (*i.e.*, non-enzymatic) modifications. Exploiting acid-catalyzed intramolecular conversions, a series of

novel cytochalasans *e.g.*, cytochalasans J₁ to J₅ and H₁/H₂ were rapidly generated in a separate study.^{55,112}

3. Structural diversity and biological activities of cytochalasans derived from fungi

3.1. Fungi of the class Agaricomycetes

3.1.1. Fungi of the undenied subclass

3.1.1.1. Fungi of the order Polyporales

3.1.1.1.1. *Fungi of the family Polyporaceae.* 3.1.1.1.1.1. **Genus Perenniporia (Mycobank ID 18204).** A chemical investigation of the organic extract of the fungus *Perenniporia subacida*, collected from Jinlin Province, China, in the mountain of Changbai, afforded the isolation of the previously reported cytochalasans Z2 (1), B (2), and dihydrocytochalasin B (3), along with three previously undescribed analogues namely perenniporins A (4), B (5) and C (6) (Fig. 1). Compounds 4–6 were examined for their cytotoxic effects against SMMC-7721, A549 and MCF-7 cancer cell lines, using Taxol as positive control with IC₅₀ value of >0.008 μM, among them, 4 and 6 showed weak effect only against SMMC-7721 and A549 with IC₅₀ values of 23.3 and 37.6 μM, respectively. Additionally, they were examined for their anti-inflammatory effect through the examination for their ability to inhibit NO production in LPS-activated macrophages. Only 6 displayed an inhibition effect with IC₅₀ value of 18.4 μM, when compared to MG-132 (Sigma) as positive control which displayed IC₅₀ value of 0.14 μM.¹¹³ Even though the successful trial of the Guo *et al.*, led to the isolation of the above mentioned cytochalasin derivatives from the genus of *Perenniporia*, but we must express our doubts regarding the ability of this genus to produce such compounds.

3.2. Fungi of the class Dothideomycetes

3.2.1. Fungi of the subclass Pleosporomycetidae

3.2.1.1. Fungi of the order Pleosporales

3.2.1.1.1. *Fungi of the family Didymellaceae.* 3.2.1.1.1.1. **Genus Boeremia (Mycobank ID 515621).** Seven previously undescribed analogues namely boerechalasins A–G (7–13) (Fig. 2), along with the previously mentioned (2), were isolated from the EtOAc extract of the plant derived fungus *Boeremia exigua*, isolated from the healthy potato. Compounds 7–13 were examined for their cytotoxicity against MCF-7 cancer cell line,



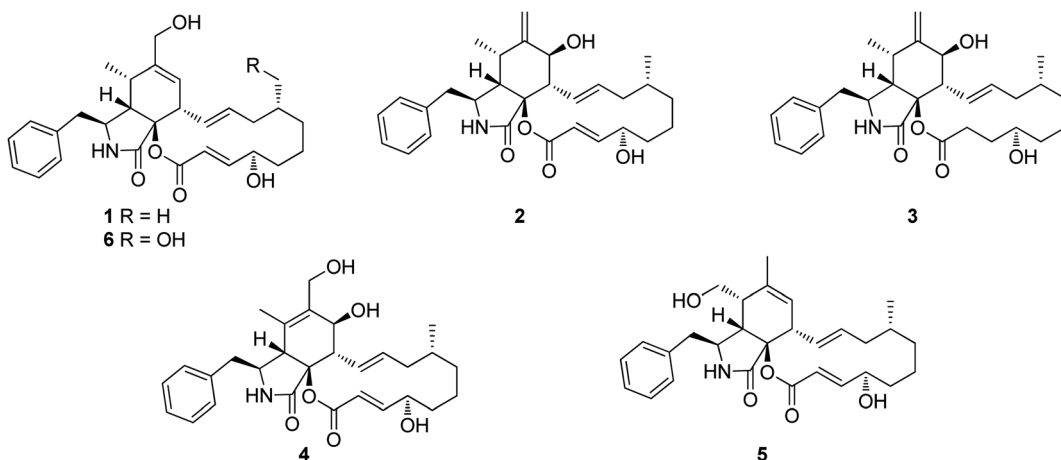


Fig. 1 Chemical structures of 1–6.

among them, boerechalasin F (**12**), displayed moderate cytotoxic activity with IC_{50} value of 22.8 μM , when compared to the positive control Paclitaxel ($IC_{50} < 0.008 \mu\text{M}$). Moreover, they were examined for their anti-inflammatory activity, where boerechalasins A (**7**) and E (**11**), showed an anti-inflammatory potential through the inhibition of NO production with IC_{50} values of 21.9 and 5.7 μM , respectively.¹¹⁴

3.2.1.1.2. Genus Phoma (Mycobank ID 9358). A chemical investigation of the plant derived fungus *Phoma exigua* var. *heteromorpha* [taxonomically updated as *Boeremia exigua*], isolated from *Nerium oleander* L. leaves necrotic spots, collected in Italy from Bari, led to the isolation of the previously mentioned (**1**) and (**2**), along with the previously reported cytochalasans A (**14**), F (**15**), T (**16**), Z3 (**17**), 7-O-acetylcytochalasin B (**18**), and deoxaphomnin (**19**), together with three previously unreported cytochalasans Z4 (**20**), Z5 (**21**), and Z6 (**22**), (Fig. 3). Whilst **20** and **21**, were proven as inactive phytotoxins, compound **22**, displayed weak inhibitory activity of root elongation on tomato

seedlings at concentration of 10^{-4} M. Moreover, only **21** caused 20% mortality of brine shrimp.¹¹⁵ Additionally, the previously mentioned cytochalasans derivatives **1**, **2**, **15**, **17**, and **19** were isolated from the organic extract of the plant derived fungus *P. exigua* var *exigua*, isolated from the lesions that exist on the leaves of *C. arvense* and *S. arvensis*, which was collected from different areas. Whilst **1**, **2**, **15** and **17** exhibited lower phytotoxic activity on *C. arvense* leaves, deoxaphomnin (**19**) showed the highest level of toxicity on *S. arvensis* leaves.¹¹⁶ Further four previously unreported analogues namely phomachalasins A (**23**), B (**24**), C (**25**), and D (**26**), (Fig. 3), were isolated from the organic extract of the plant derived fungus *P. exigua* var. *exigua*, obtained from the necrotic lesions of *C. arvense* and *S. arvensis* leaves, collected from Norway (Oslo) and Russia (St. Petersburg). Phomachalasins A-D (**23–26**) represent the first examples of cytochalasans which possessing 1,2,3,4,6,7-hexasubstituted bicyclo[3.2.0]heptene connected to the macrocyclic ring. None of the isolated metabolites was proven active neither as

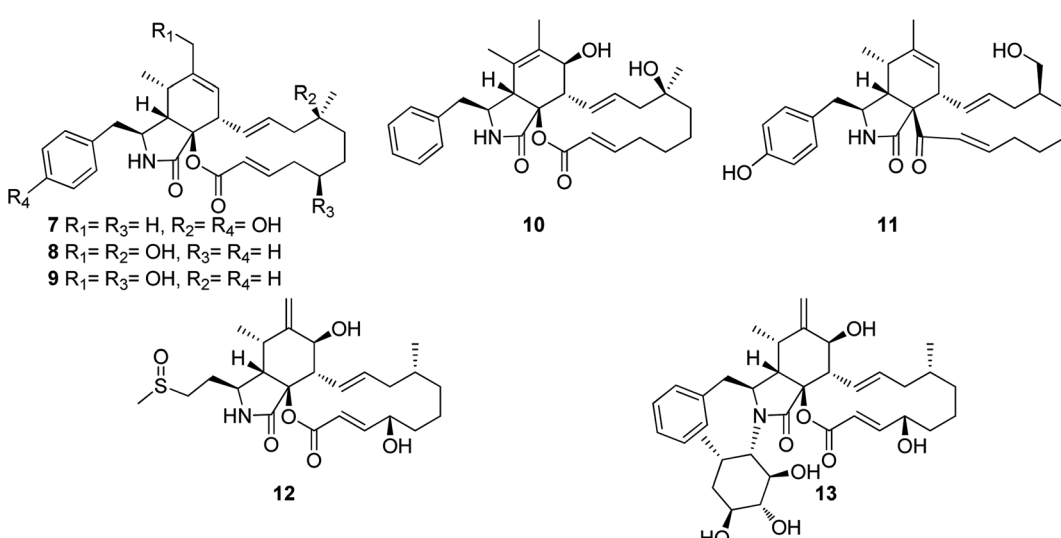


Fig. 2 Chemical structures of 7–13.



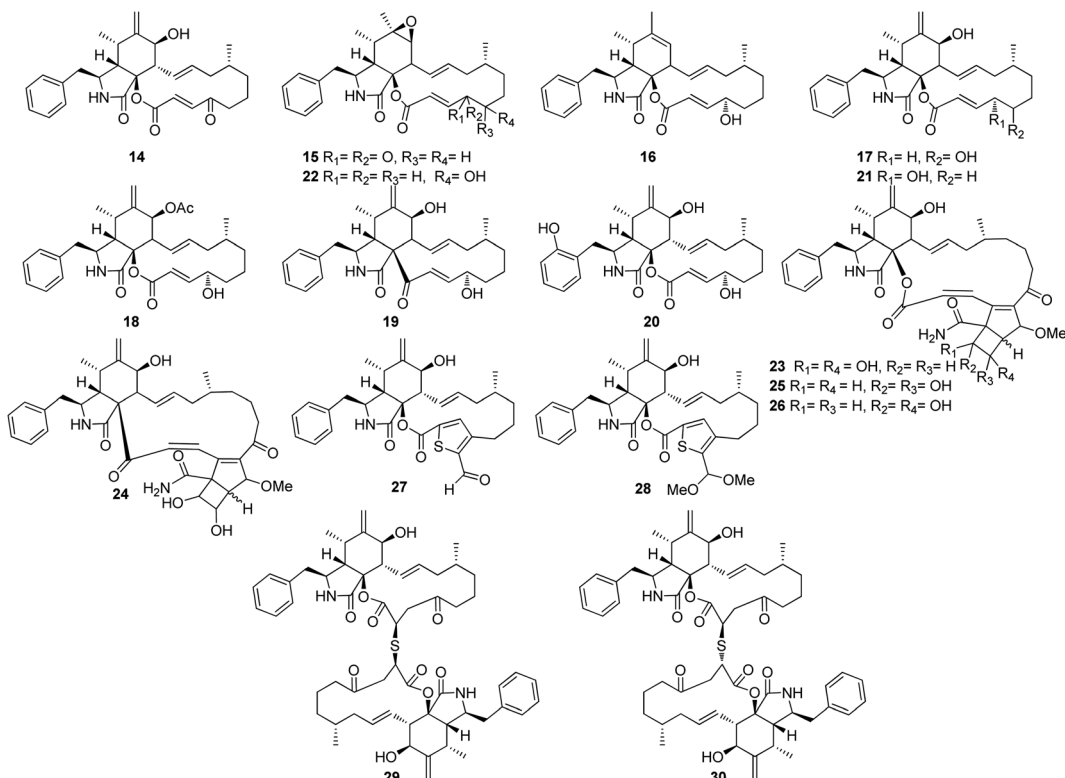


Fig. 3 Chemical structures of 14–30.

a phytotoxic agent when tested on *L. esculentum*, *C. arvense*, and *E. repens*, nor antifungal against *C. tropicalis*.¹¹⁷ Additional chemical investigation of the endophytic derived fungus *P. multirostrata* XJ-2-1, isolated from *Parasenecio albus* collected in China, Xinning County Province, Hunan, led to the isolation of four previously undescribed sulphur-containing cytochalasans derivatives namely thiocytochalasans A (27), B (28), C (29) and D (30), (Fig. 3). Structurally, it is worth to mention that

thiocytochalasans A (27) and B (28), represent the first cytochalasan derivatives containing a thiophene moiety, possessing a novel 5/6/14/5 tetracyclic scaffold. Whilst thiocytochalasans C (27) and D (28), are homodimers epimers, formed through a thioether bridge. Compounds 27–30 were examined for their cytotoxic effects against HepG2, MCF-7, A549, CT26 and HT-29 cancer cell lines. Whilst 27 and 28, exhibited moderate cytotoxic effect against the examined cell lines with IC_{50} values ranging

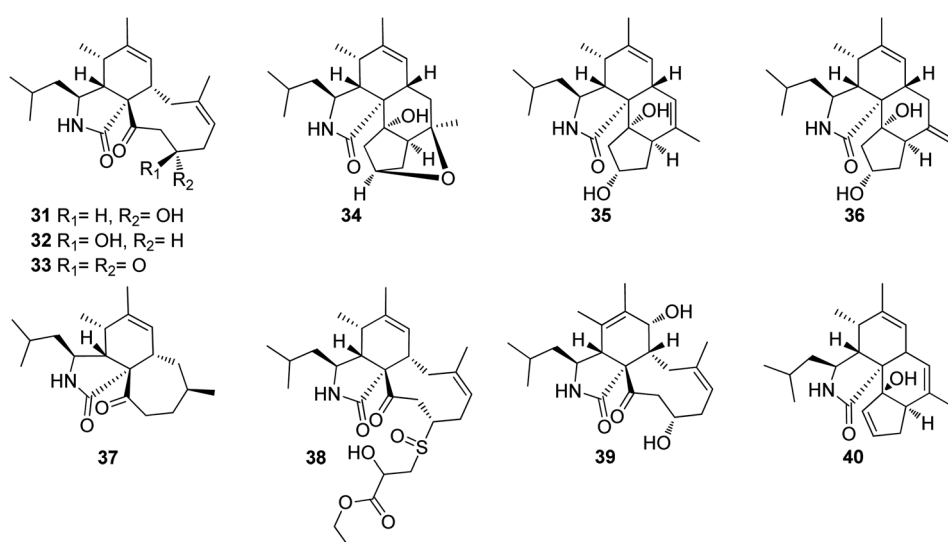


Fig. 4 Chemical structures of 31–40.



from 4.17 to 23.41 $\mu\text{mol L}^{-1}$. Additionally, **29** and **30** displayed potent cytotoxicity against the tested cells with IC_{50} values ranging from 0.76 to 7.52 $\mu\text{mol L}^{-1}$, when compared to Doxorubicin hydrochloride as positive control displayed IC_{50} values of 1.37, 1.07, 1.05, 1.01 and 0.48 $\mu\text{mol L}^{-1}$, against the tested tumour cells, respectively. Furthermore, the investigation of **28–30** examined their impact on cell cycle progression in CT26, A549, and HT29 cells. The findings suggested that these compounds have the potential to induce concentration-dependent G2/M cell cycle arrest in these cells. Notably, **29** and **30** exhibited significant G2/M phase arrest in CT26 cells at a concentration of 1 $\mu\text{M L}^{-1}$.¹¹⁸

3.2.1.1.2. Fungi of the family Periconiaceae. **3.2.1.1.2.1. Genus Periconia (MycoBank ID 9263).** Three previously unreported cytochalasans derivatives possessing an unusual 9/6/5 tricyclic ring system, namely periconiasins A–C (**31–33**) (Fig. 4), were isolated from the endophytic derived fungus *Periconia* sp., isolated from the leaves of *A. muricata*, a medicinal plant, collected in China, Hainan Province. Compounds **31–33** were investigated for their cytotoxic effects against A549, BGC-823, Bel-7402, HCT-8, and A2780 human cancer cell lines, using Camptothecin as positive control (IC_{50} values of 0.001, 0.04, 6.3, 3.6, and 0.9 μM , respectively), where **33** was inactive against all the examined cells with IC_{50} values of $>10 \mu\text{M}$, **31** displayed potent selective cytotoxicity against HCT-8 and BGC-823 tumour cell lines with IC_{50} values of 0.9 and 2.1 μM , respectively. Whilst **32**, displayed significant cytotoxic activity towards HCT-8, Bel-7402 and BGC-823, with IC_{50} values of 0.8, 5.1 and 9.4 μM . Indeed, **31** and **32**, might considered to be lead cytotoxic agents against HCT-8 tumour cell line, due to their prominent cytotoxic activity in comparison with the positive control with IC_{50} value of 3.6 μM .¹¹⁹

Later, further investigation of the same fungal strain by the same group resulted in the isolation of three additional previously undescribed cytochalasans derivatives namely periconiasins D–F (**34–36**) (Fig. 4). Compounds **34–36** were found inactive when examined for their cytotoxic potential against HCT-8, Bel-7402, BGC-823, A549 and A2780 tumour cell lines. Additionally, these compounds were found inactive when evaluated for their anti-inflammatory activity. Furthermore, only **35** showed a weak anti-HIV activity when compared with the positive control Efavirenz, with IC_{50} values of 29.2 and 1.4 nM, respectively.¹²⁰ Moreover, a re-examination of the same fungus by the same group afforded the isolation of two additional previously unreported cytochalasan derivatives namely periconiasins G–H (**37–38**) (Fig. 3). Structurally, periconiasin G (**37**) possess an unusual 7/6/5 tricyclic ring system. Whilst periconiasin H (**38**) bears unpredicted sulfoxide group. Compounds **37–38** were found inactive when examined for their cytotoxic activity against A549, A2780, Bel-7402, HCT-8, and BGC 823 cell lines, at concentration of 10^{-5} M , compared with Camptothecin as positive control. Furthermore, when both compounds were examined for their antiviral activity against HIV, using Efavirenz as the positive control, only **37** exhibited weak activity with IC_{50} value of 67.0 μM .¹²¹ Additionally, the same group through a further chemical investigation managed to isolate further two

previously unreported analogues namely periconiasins I–J (**39–40**) (Fig. 4), which possesses 9/6/5 tricyclic ring and 5/6/6/5 tetracyclic ring systems, respectively. Whilst **40** displayed no cytotoxicity against MCF-7 cells, **39** displayed potent cytotoxic effect against the same cancer cell line when compared with Paclitaxel as positive control with IC_{50} values of 4.8 and 0.0002 μM , respectively. Moreover, **39** showed no antiviral activity towards HIV, but **40** was found active as antiviral agent when compared to the positive control Efavirenz with IC_{50} values of 25.0 and 0.0014 μM , respectively.¹²²

3.2.1.1.3. Fungi of the family Pleosporaceae. 3.2.1.1.3.1.

Genus Pyrenophora (MycoBank ID 4596). A chemical examination of the wheat derived fungus *Pyrenophora semeniperda*, led to the isolation of the previously mentioned cytochalasans derivatives **1**, **2**, **15**, **16**, **17** and **19**, along with the previously unreported cytochalasin Z1 (**41**) (Fig. 5). Cytochalasans B (**2**), F (**15**) and deoxaphomnin (**19**), displayed a remarkable inhibition activity towards root elongation, when compared to cytochalasans Z1 (**41**), Z2 (**1**), and Z3 (**17**).¹²³

3.2.1.1.4. Fungi of the family Sporormiaceae. 3.2.1.1.4.1.

Genus Preussia (MycoBank ID 4363). Chemical investigation of the medicinal plant derived fungus *Preussia similis*, isolated from the roots of *Globularia alypum*, collected in Algeria from the city of Batna, resulted in the isolation of the previously mentioned metabolites **1**, **2**, **15**, and **19**. While **2** and **19** caused complete actin disruption at a concentration of 1 $\mu\text{g mL}^{-1}$, this effect was reversible for **2** and irreversible for **19**. The effects of **1** and **15** were found to be incomplete and reversible at a concentration of 5 $\mu\text{g mL}^{-1}$.¹²⁴

3.2.1.1.4.2. Genus Pycnidiophora (MycoBank ID 4563). Four previously undescribed cytochalasans derivatives sharing the rare 5/6/6/5 pentacyclic skeleton, namely pycnidiophorones A–D (**42–45**) (Fig. 6) were reported from the wetland derived fungus *Pycnidiophora dispersa*, isolated from the soil sample collected in China, at Hebei Province, from the Lake of Baiyangdian. Compounds **42–45** were examined for their cytotoxicity against the HeLa, PC-3, A549, HepG-2 and HL-60 cells. Whilst no cytotoxicity was observed for **43** against A549 cells, **44** showed no cytotoxicity against PC-3 and HepG-2 cells, and **45** displayed no cytotoxicity against PC-3, HepG-2, and HL-60 cells. However, the examined compounds exhibited weak to mild cytotoxic effects against the tested cells, with IC_{50} values ranging from 7.0 to 99.0 μM , when compared to the positive control, *Cis*-platin (IC_{50} values of 11.7, 5.6, 11.8, 9.3 and 15.7 μM , respectively).¹²⁵

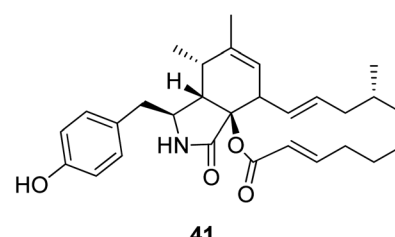


Fig. 5 Chemical structure of **41**.

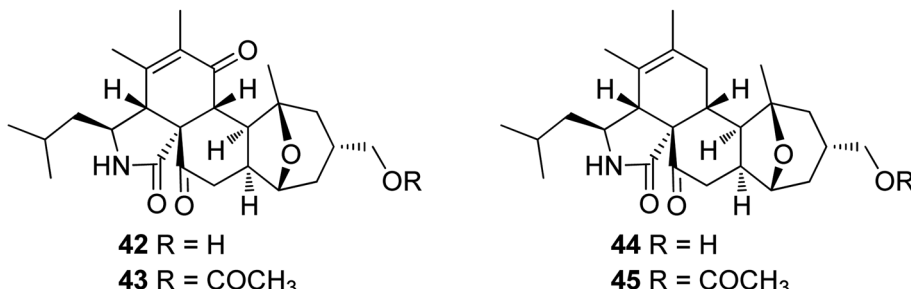


Fig. 6 Chemical structures of 42–45.

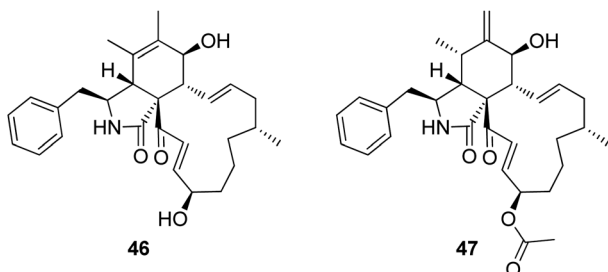


Fig. 7 Chemical structures of 46–47.

3.2.1.1.4.3. Genus *Sparticola* (Mycobank ID 551921). The previously mentioned cytochalasin derivative (2), along with the previously described deoxaphomnin B (46) together with the previously unreported triseptatin (47) (Fig. 7) were isolated from the decayed branch derived fungus, *Sparticola triseptata* obtained from *Tofieldia calyculata* (L.) Wahlenb. Compounds 2, 46 and 47, were examined for their antiproliferative ability against HUVEC and K562 cells using Imatinib as positive control (GI₅₀ values of 18.5 and 0.17 μ M, respectively), where they displayed significant antiproliferative activity against the examined cells with GI₅₀ values ranging from 1.08 to 8.31 μ M. Furthermore, 46 and 47 were tested against L929, HeLa, MCF-7, A549, PC-3 SKOV-3 and A431 cancer cell lines, using Epothilone B as positive control (IC₅₀ values of 0.0014, 0.000089, 0.00024, 0.000065, 0.0016, 0.00028 and 0.000079 μ M, respectively). Both

compounds displayed strong cytotoxicity with IC₅₀ values of 1.55 to 6.91 and 1.80 to 11.28 μ M, respectively. Additionally, 46 and 47 displayed an inhibition effect towards F-actin network.¹²⁶

3.2.1.1.4.4. Genus *Westerdykella* (Mycobank ID 5772). The chemical examination of the marine derived fungus *Westerdykella dispersa*, obtained from the marine sediment, collected from Guangdong Province, China, from the South China Sea, afforded the isolation of six previously unreported cytochalasans analogues, namely 18-oxo-19,20-dihydrophomacin C (48), 18-oxo-19-methoxy-19,20-dihydrophomacin C (49), 18-oxo-19-hydroxy-19,20-dihydrophomacin C (50), 19,20-dihydrophomacin C (51), 19-methoxy-19,20-dihydrophomacin C (52), and 19-hydroxy-19,20-dihydrophomacin C (53) along with the previously reported analogue phomacin B (54) (Fig. 8). Compounds 48–54 were examined for their cytotoxicity effect against MCF-7, HepG2, A549, HT-29 and SGC-7901 tumour cancer lines using 5-Fluorouracil as positive control (IC₅₀ values of 63.98, 58.10, 66.82, 67.13 and >100 μ M, respectively). Compounds 48–50 showed no cytotoxicity against the examined cancer lines, however 51 and 53 displayed a selective mild cytotoxicity against HT-29 with IC₅₀ values of 55.5 and 49.1 μ M, respectively. Furthermore, 52 and 54 exhibited moderate cytotoxicity with IC₅₀ values ranging from 25.6 to 83.7 μ M. Additionally, all the isolated compounds were found inactive when tested for their antibacterial activity against the Gram-negative bacterial strains (*S. typhimurium*, *P. vulgaris*, *E. aerogenes* and *E. coli*) and the Gram-positive bacteria

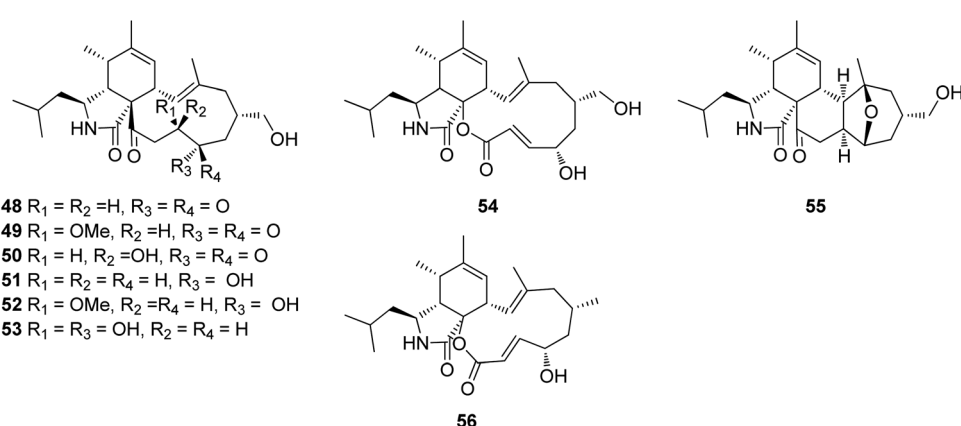


Fig. 8 Chemical structures of 48–56.



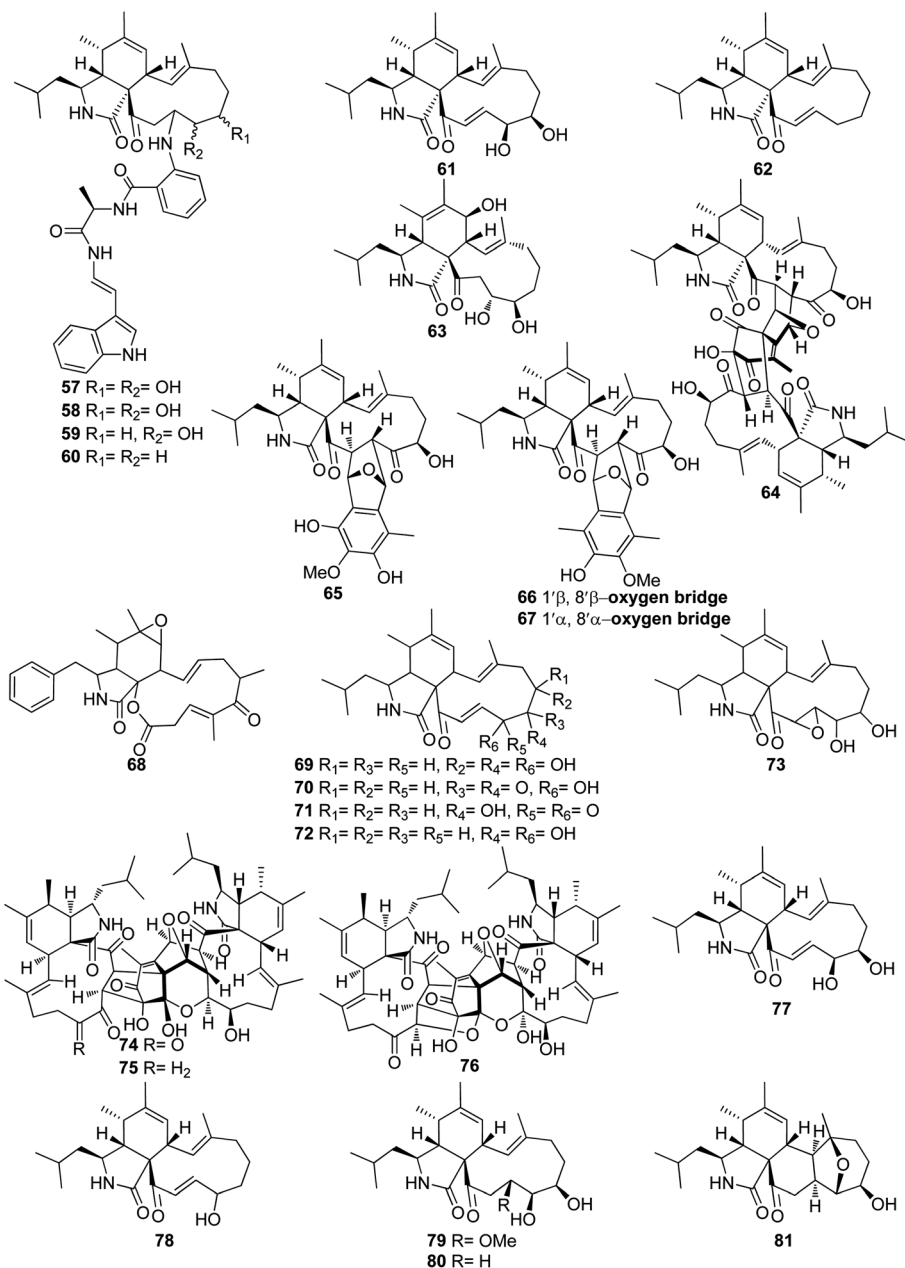


Fig. 9 Chemical structures of 57–81.

strains (*S. enterica*, *B. anthracis*, *M. luteus* and *B. subtilis*),¹²⁷ when compared to Ciprofloxacin as positive control (MIC value of $0.78125 \mu\text{g mL}^{-1}$ against the tested bacterial strains). Further examination for the same fungal strain by the same group resulted in the isolation of another two previously unreported cytochalasans derivatives, namely 16-hydroxymethylaspergillin PZ (55) and, 16 α -methylaspochalasin J (56) (Fig. 8). Both compounds were examined for their antibacterial activity against *Proteus vulgaris*, *Enterobacter aerogenes*, *Escherichia coli*, *Salmonella enterica*, *Micrococcus luteus*, and *Bacillus subtilis*, using Ciprofloxacin as positive control (MIC value of $0.78125 \mu\text{g mL}^{-1}$ against the tested bacterial strains), where they displayed moderate antibacterial effect against (*P. vulgaris* and *E.*

aerogenes) and *B. subtilis*, respectively with MIC values of $50 \mu\text{g mL}^{-1}$.¹²⁸ The previously mentioned cytochalasin derivatives (53), (54), and (55), were reported from the mangrove derived fungus *W. nigra*, isolated from the roots of *Avicennia marina*, collected in the Red Sea, Egypt from the port of Safaga. Compounds 53–55 were examined for their inhibition effect towards the activity of acetylcholine esterase using Donepezil ($\text{IC}_{50} 0.035 \mu\text{M}$) as positive control, where 53 exhibited the most promising activity with IC_{50} value of $0.056 \mu\text{M}$, followed by 55 and 56, with IC_{50} values of 0.088 and $0.140 \mu\text{M}$, respectively.¹²⁹

3.3. Fungi of the class Eurotiomycetes

3.3.1. Fungi of the subclass Eurotiomycetidae

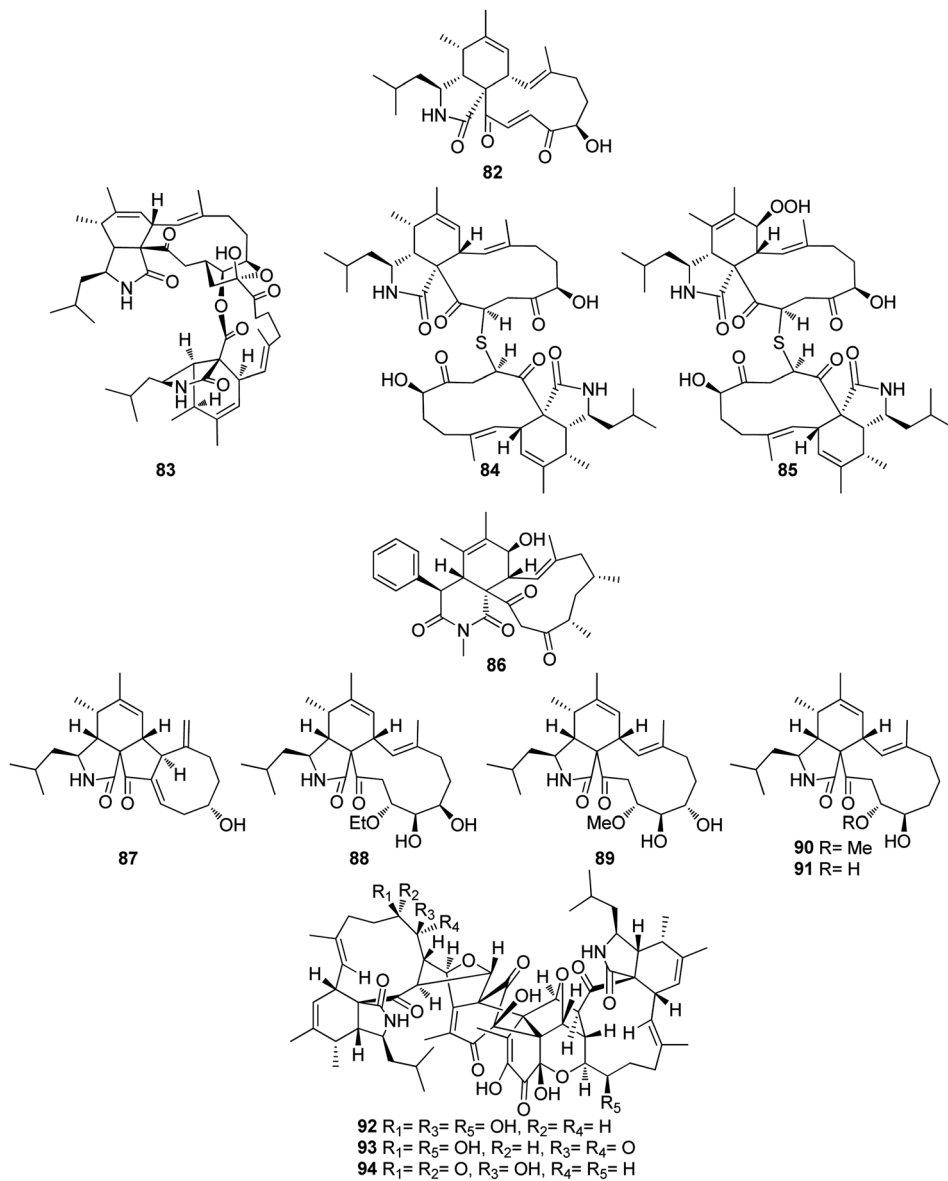


Fig. 10 Chemical structures of 82–94.

3.3.1.1. Fungi of the order Eurotiales

3.3.1.1.1. Fungi of the family Aspergillaceae. **3.3.1.1.1.1. Genus Aspergillus (Mycobank ID 7248).** Chemical examination of the endosymbiotic derived fungus *Aspergillus niveus* LU 9575, isolated from woodlouse, collected near Konigsheide in Germany, led to the isolation of the previously undescribed aspochalamins A (57), B (58), C (59) and D (60) along with the previously reported aspochalasins D (61), and Z (62) (Fig. 9). Compounds 57–62 were examined for their cytotoxic effects against HMO2, MCF7, HepG2 and Huh7 cells, where 57–60 and 62, displayed weak to mild cytotoxic effect against the examined cells. Additionally, these compounds were evaluated for their antimicrobial activity against *A. globiformis* DSM 20124, *A. aurescens* DSM 20116, *A. oxydans* DSM 6612, *A. pascens* DSM 20545, *B. subtilis* DSM 10, *B. brevis* DSM 30, *R. erythropolis* DSM 1069, and *S. aureus* DSM 20231, where 57–60, showed weak

antibacterial effect against the examined Gram-positive bacteria.^{130,131} Aspochalasin U (63), a previously unreported cytochalasin derivative was isolated from the marine derived fungus *Aspergillus* sp., obtained from Dongshi Saltern, Fujian Province (China), (Fig. 9). Aspochalasin U (63), showed mild effect against the necrotic cell death induced by TNF- α .¹³² A chemical investigation of methanolic extract of the river derived fungus *A. flavipes*-507, resulted in the isolation of a previously unpreceded cytochalasan dimer featuring the decacyclic ring system, namely asperchalasine A (64), along with asperchalasines B (65), C (66) and D (67), a three related biogenetically intermediates (Fig. 9), compounds 64–67, were examined for their cytotoxic effects against (HL-60, SMMC-7721, A-549, MCF-7, and SW-480), cancer cell lines, where all of them displayed weak antitumour effect against all the examined cancer cell lines, when compared to *Cis*-platin (IC_{50} values of 1.16, 8.08,

7.10, 10.45, and 8.88 μM) and Taxol (IC_{50} values of <0.0008 μM) as positive controls. Additionally, compound **64** was proven to be effective cytoskeletal inhibitor, when examined for its ability to disturb F-actin microfilaments. Furthermore, **64** exhibited a reasonable G1-phase cell cycle arrest in the four tested cancer cell lines and interestingly with no effect on the normal cell lines.¹³³ The chemical exploration of the marine derived fungus *A. flavipes* co-cultured with the actinomycete *Streptomyces* sp., isolated from Nanji Islands, sediments, (China), led to the detection of six previously reported cytochalasin derivatives, namely rosellichalasin (**68**) aspochalasin E (**69**), aspochalasin M (**70**), aspochalasin P (**71**), 19,20-dihydro-aspochalasin D (**72**), and aspochalasin H (**73**) (Fig. 9). Compounds **68**–**73** displayed strong inhibition ability against *Streptomyces* sp, growth with an inhibition rate of 50–80% at concentration ranged from 2 to 16 $\mu\text{g mL}^{-1}$, it is worth mention that the above-mentioned cytochalasans derivatives support the fungus *A. flavipes* when competing with *Streptomyces* sp.¹³⁴ The aforementioned findings regarding the antibacterial activity of the obtained cytochalasin derivatives must be considered with great caution, as they contradict all other reports in the literature. Additionally, three previously unreported heterotrimers cytochalasan analogues namely amichalasines A (**74**), B (**75**), and C (**76**) (Fig. 9), together with the previously mentioned analogues (**61**) and (**64**), were obtained through the chemical examination of the organic extract of the endophytic fungus *A. micronesiensis* PG-1, isolated from *Phyllanthus glaucus* roots. Compounds **74**–**76** were examined for their cytotoxicity against HL60, U87MG, MDA-MB-231, A549, Hep3B, and SW480 cancer cell lines, where they displayed mild to potent cytotoxic effect against the examined cancer cell lines with IC_{50} values ranging from 1.71 to 35.84 μM . It is worth noting that amichalasine B (**75**), was more active than the model compounds, cytochalasans B (**2**) and D (**366**).¹³⁵ A chemical investigation of the marine derived fungus *A. flavipes* CNL-338, isolated from the red alga *Laurencia* sp. collected from the Bahamas, led to the isolation of the previously mentioned derivatives (**69**) and (**71**), along with five previously reported analogues namely aspochalasin C (**77**), TMC-169 (**78**), flavichalasines F (**79**) and G (**80**) and aspergillin PZ (**81**) (Fig. 9). These isolated compounds were not tested for any relevant biological activity.⁹⁹

The previously mentioned cytochalasan monomer (**61**) and its previously reported 18-keto analogue aspochalasin B (**82**), together with three unusual homodimers cytochalasans derivatives previously undescribed namely bisaspochalasins A (**83**), B (**84**) and C (**85**), (Fig. 10), were obtained from the organic extract of the plant derived fungus *A. flavipes*, isolated from *Hevea*

brasiliensis steams, collected from Yunnan Province, China, in Banna Prefecture, it is worth mention that **85** might be an artifact of **84**, through a Schenckene photooxygenation. Compounds **83**–**85** were tested for their immunosuppressive effect, among them only **83** displayed an inhibition effect towards human T cell proliferation activated by anti CD3/anti-CD28 antibodies, with IC_{50} value of 15.8 μM .¹³⁶ Asporychalasin (**86**) (Fig. 10) a further cytochalasin derivative with an unprecedented 6/6/11 skeleton, was isolated from the Red Sea derived fungus *A. oryzae* isolated from the sediments collected in Saudi Arabia from Jeddah. Asporychalasin (**86**) displayed mild antiproliferative properties against three human cell lines, A549, HepG2, and MCF7 cells with IC_{50} values of 8.8, 7.4, and 8.3 $\mu\text{g mL}^{-1}$, respectively, when compared to Doxorubicin (IC_{50} values of 0.3, 0.2, and 0.4 $\mu\text{g mL}^{-1}$, respectively) as positive control, additionally compound **86**, showed no toxicity towards zebrafish embryos.¹³⁷

Further five previously unreported cytochalasan monomers namely aspermichalasines A (**87**), B (**88**), C (**89**), D (**90**), and E (**91**), aspermichalasine A (**87**), represent the first example of cytochalasan monomer possesses a 5/6/5/8 skeleton, along with three previously undiscovered cytochalasan heterotetramers namely asperflavipines C (**92**), D (**93**), and E (**94**) (Fig. 10), were obtained through the chemical examination of the EtOAc extract of the medicinal plant derived fungus *A. micronesiensis*, isolated from *Phyllanthus glaucus* roots, collected in China, Jiangxi Province, in the mountain of LuShan. Compounds **88**–**90** and **92**–**94** displayed potent cytotoxic effect against the HL60 cells with IC_{50} values ranging from 5.67 to 18.75 μM . Furthermore, **88** and **94** exhibited strong cytotoxicity against Hep3B cells with IC_{50} values of 7.99 and 5.60 μM , respectively, when compared to *Cis*-platin (IC_{50} value of 2.15 μM) as positive control. Additionally, **92** was found as potent apoptosis inducer in HL60 cells.¹³⁸ A chemical examination of the medicinal plant derived fungus *Aspergillus* sp., isolated from *Lonicera japonica* Thunb, stems and flowers, led to the isolation of eight previously unreported cytochalasan derivatives, namely aspergicytochalasans A (**95**), B (**96**), C (**97**), D (**98**), E (**99**) and F (**100**), (Fig. 11) along with the previously mentioned analogues (**1**), (**2**), (**3**), (**14**), and (**20**). Compounds **95**–**100** were examined for their antibacterial properties towards *E. coli* ATCC25922 and *S. aureus* subsp. *aureus* ATCC29213, where aspergicytochalasans C (**97**) and D (**98**) showed antibacterial activity against *S. aureus* subsp. *aureus* ATCC29213 with MIC values of 128 and 64 $\mu\text{g mL}^{-1}$, respectively. Additionally, **95**–**100** were evaluated for their anti-inflammatory effects by examining their ability to inhibit NO production in LPS-induced RAW 264.7 macrophages. Whilst

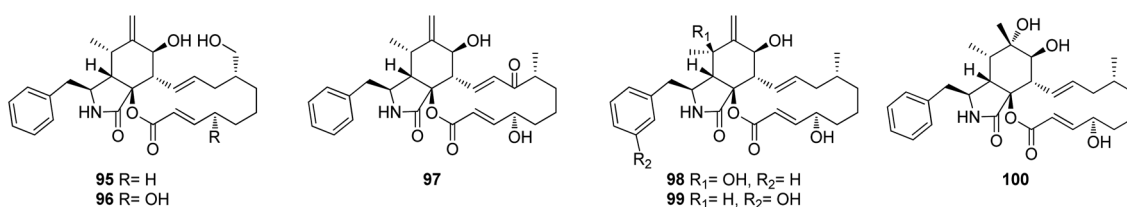


Fig. 11 Chemical structures of **95**–**100**.



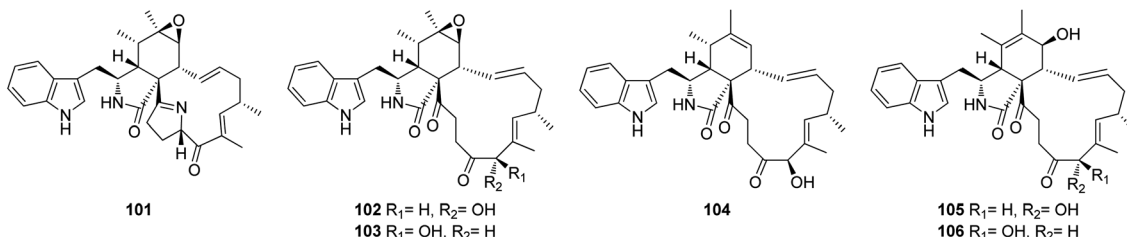


Fig. 12 Chemical structures of 101–106

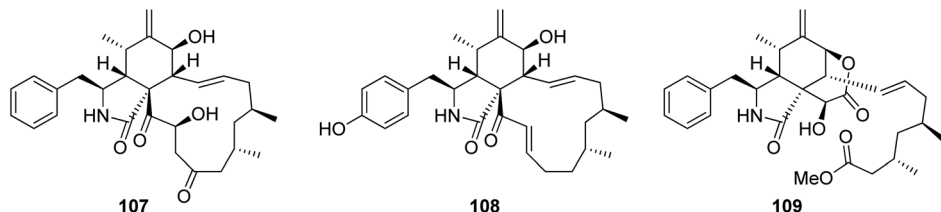


Fig. 13 Chemical structures of 107–109.

compounds **95**, **97**, **99** and **100** exhibited an inhibition effect towards the NO production with IC_{50} values of 26.8, 17.1, 31.2 and 12.7 μ M, respectively. Compounds **96** and **98** were found inactive.¹³⁹

3.3.1.1.2. Genus *Penicillium* (Mycobank ID 9257). Chemical investigation of the marine alga derived fungus *Penicillium* sp. OUPS-79, isolated from *Enteromorpha intestinalis*, led to the isolation of five previously unreported cytochalasan derivatives namely, penochalasins D (101), E (102), F (103), G (104), and H (105), along with the previously reported analogue chaetoglobosin O (106) (Fig. 12). Compounds 101–106 displayed potent cytotoxic effect towards P388 cancer cell line with ED₅₀ values of 3.2, 2.1, 1.8, 1.9, 2.8, and 2.4 $\mu\text{g mL}^{-1}$, respectively, when compared to 5-Fluorouracil as positive control (ED₅₀ value of 0.08 $\mu\text{g mL}^{-1}$).¹⁴⁰

3.3.1.1.2. Fungi of the family Trichocomaceae. 3.3.1.1.2.1.

Genus *Talaromyces* (MycoBank ID 5347). Three previously unreported cytochalasans namely talachalasins A (107), B (108) and C (109), possessing an unusual 16 β -methyl group (Fig. 13), were isolated from the marine derived fungus *Talaromyces muroi* sp. SCSIO 40439, isolated from the deep sea, sediment of the South China sea. Compounds 107–109 were examined for their cytotoxic effects towards SF-268, MCF-7, HepG2 and A549 cancer cell lines. Whilst 107 and 108, showed mild and weak effects with IC₅₀ values ranging from 3.40 to 10.02 and 17.30 to 30.58 μ M, respectively. Compound 109 displayed no activity against the examined cancer cell lines. Additionally, they were tested for their antiviral effect towards HSV-1 (herpes simplex virus) and RSV (respiratory syncytial virus). Whilst 107 and 109 showed no antiviral activity, 108 displayed moderate and potent antiviral activity with IC₅₀ values of 20.0 and 12.5 μ M when compared to Ribavirin (IC₅₀ value of 8.25 μ M) as positive control, and selectivity index 1.50 and 3.20, respectively.¹⁴¹

3.4. Fungi of the class Leotiomycetes

3.4.1. Fungi of the subclass Leotiomycetidae

3.4.1.1. Fungi of the order Helotiales

3.4.1.1.1. Fungi of the family Sclerotiniaceae. 3.4.1.1.1.1.

Genus Botryotinia (Mycobank ID 638). A chemical manipulation of the plant derived fungus *Botryotinia fuckeliana* A-S-3, isolated from the roots of *Ajuga decumbens*, collected in China, Fujian Province, led to the isolation of three previously reported cytochalasan derivatives phenochalasin B (110), 1,3-dioxacyclotridecino (111) and 12-cytochalasin (112) (Fig. 14). Compounds 110–112 were examined for their cytotoxic effects against SMMC-7721, A549, HepG2 and MCF-7 cancer cell lines. Whilst 111, displayed no cytotoxicity against the examined cancer cell lines with IC_{50} values of $>50 \mu\text{M}$, 110 and 112 showed potential anticancer effects with IC_{50} values ranging from 0.10 to 7.43 and 0.59 to 0.88 μM , respectively. Furthermore, 110 and 112 were found to induce apoptosis in HepG2 tumour cell line.¹⁴²

3.5. Fungi of the class Sordariomycetes

3.5.1. Fungi of the subclass Sordariomycetidae

3.5.1.1. Fungi of the order Diaporthales

3.5.1.1.1. Fungi of the family Cryphonectriaceae. 3.5.1.1.1.1.

Genus Endothia (MycoBank ID 1810). Chemical examination of the endophytic fungus *Endothia gyrosa* IFB-E023, isolated from the healthy leaf of *Vatica mangachapo*, collected from botanical garden in the south of China, led to the isolation of the previously undescribed cytochalasans Z10 (113) and Z11 (114) along with the previously reported epoxycytochalasin H (115) cytochalasin H (116), and cytochalasin J (117) (Fig. 15). Compounds 113–117 were examined for their anti-tumour effects against human leukaemia K562 cancer cell line using 5-Fluorouracil (IC₅₀ value of 33.0 μ M), as positive control, where they displayed cytotoxicity with IC₅₀ values of 28.3, 24.4, 24.5, 10.1 and 1.5 μ M, respectively.¹⁴³

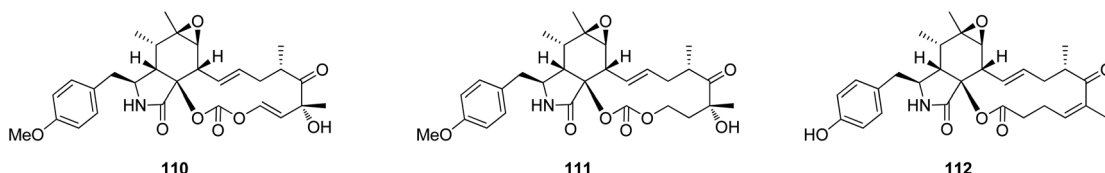


Fig. 14 Chemical structures of 110–112.

3.5.1.1.2. Genus *Cytospora* (Mycobank ID 7904). Chemical investigation of the MeOH extract of the plant derived fungus *Cytospora chrysosperma*, isolated from the aerial part of *Hippophae rhamnoides*, collected from Qinghai Province (China), resulted in the isolation of three previously undescribed cytochalasans derivatives namely cytochrysins A (118), B (119) and C (120) (Fig. 16). Compounds 118–120 were tested for their antibacterial effects towards carbapenem-resistant *Pseudomonas aeruginosa*, methicillin resistant *S. aureus*, multi-drug-resistant *Enterococcus faecalis*, multi-drug-resistant *Enterococcus faecium*, carbapenem-resistant *Acinetobacter baumannii*, multi-drug-resistant *Staphylococcus epidermidis*, carbapenem-resistant *Klebsiella pneumoniae*, and carbapenem-resistant *E. coli* using Ciprofloxacin, as positive control. Whilst 119 showed no antibacterial effects, 118 displayed significant antibacterial activity against *E. faecium* with MIC value of $25 \mu\text{g mL}^{-1}$, as well as 120 showed potent antibacterial activities against *S. aureus* with MIC value of $25 \mu\text{g mL}^{-1}$. Furthermore, they were examined for their antifungal activity against the plant pathogenic fungi *Physalospora piricola*, *Fusarium oxysporum*, *Diplodia maydis*, *Verticillium dahliae*, *Sclerotinia sclerotiorum*, *Rhizoctonia solani*, and *Aphelenchoides fragiae*, using Ketoconazole as positive control. Indeed, none of the isolated compounds displayed antifungal activity against these plant pathogenic fungi.¹⁴⁴

3.5.1.1.2. Fungi of the family Diaporthaceae. 3.5.1.1.2.1.

Genus *Diaporthe* (Mycobank ID 839358). Ten cytochalasans derivatives including the previously reported 21-O-deacetyl-L-696,474 (121), phomopsichalasin G (122), diaporthichalasins A (123), B (124) and C (125), along with the previously undescribed diaporthichalasins D (126), E (127), F (128), G (129) and H (130) (Fig. 17), were recorded from the EtOAc extract of the endophytic fungus *Diaporthe* sp. SC-J0138, obtained from fresh leaves of *Cyclosorus parasiticus*, collected in Guangdong Province, (China). Whilst diaporthichalasin G (129) displayed no cytotoxicity against A549, HeLa, HepG2 and MCF-7 cancer cell lines, diaporthichalasin H (130) was proven to be active against

these cells, with IC_{50} values ranging from 9.9 to 32.1 μM . Furthermore, all the other compounds had a demonstrable cytotoxicity against these cells, *i.e.*, 21-*O*-deacetyl-L-696,474 (**121**) displayed cytotoxicity against A549, HeLa and HepG2 cells, with IC_{50} values of 17.3, 14.7 and 26.2 μM , respectively. However, **121** displayed no cytotoxicity towards the MCF-7 cell line.

Similarly, phomopsichalasin G (122) was found to be active against HeLa and HepG2 cells with IC_{50} values of 24.5 and 11.0 μM , respectively, but no activity was reported against A549 and MCF-7 cancer cells. Diaporthichalasin A (123) only showed cytotoxicity against HepG2 cells with IC_{50} value of 10.1 μM . Whilst diaporthichalasin B (124) displayed moderate cytotoxicity against HeLa and HepG2 cells with IC_{50} values of 22.1 and 21.2 μM , respectively. Diaporthichalasin C (125) showed anti-tumour effects against A549, HeLa and HepG2, with IC_{50} values of 12.0, 15.2 and 38.1 μM , respectively. However, diaporthichalasin D (126), displayed potent cytotoxicity against A549, HeLa and HepG2 cells, with IC_{50} values of 13.7, 15.3 and 8.8 μM , respectively. Additionally, diaporthichalasin E (127) showed selective cytotoxicity towards HepG2 cell line with IC_{50} value of 30.6 μM . Furthermore, diaporthichalasin F (128) only displayed selective cytotoxicity against HeLa and HepG2 cells with IC_{50} values of 34.7 and 16.5 μM , respectively, when compared to Adriamycin (IC_{50} values ranged from 0.31 to 1.02 μM).¹⁴⁵ A chemical investigation of the organic extract of the endophytic derived fungus *D. ueckerae* SC-J0123, isolated from *Pteris vittata* L. leaves collected from Shatoujiao forestry centre, Guangdong Province, China, led to the isolation of the previously mentioned cytochalasan derivatives (116) and (117), along with the previously described cytochalasans J₁ (131), J₂ (132), J₃ (133), longichalasin B (134), RKS-1778 (135), and phomopchalasin A (136), together with the previously unreported ueckerchalasins A (137), B (138), C (139), D (140), E (141) and 4'-hydroxycytochalasin J₃ (142) (Fig. 17). It is worth mentioning that 137–139, possesses an unusual 5/6/6/7-fused heterocycle core. Compounds 116–117, and 133–142, were examined for

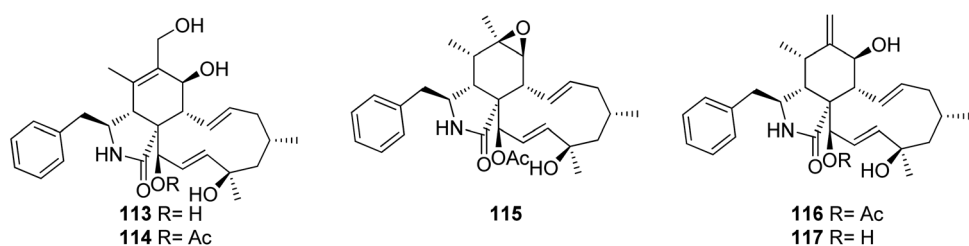


Fig. 15 Chemical structures of 113–117.

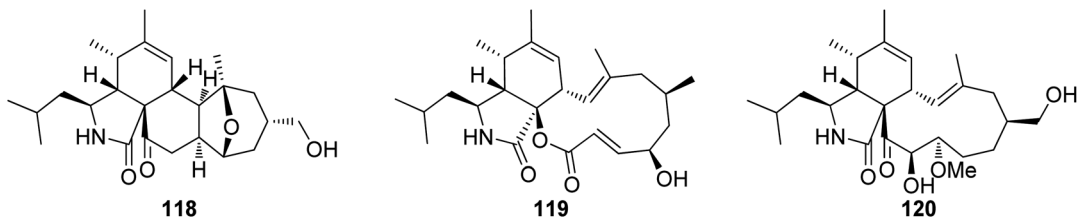


Fig. 16 Chemical structures of 118–120.

their antibacterial abilities against *Staphylococcus aureus* (SA) and methicillin-resistant *S. aureus* (MRSA) using Kanamycin and Vancomycin (MIC values of 0.625 and 1.25 $\mu\text{g mL}^{-1}$, respectively), as positive control. Only two compounds 136 and 139, displayed weak antibacterial effects against the examined bacterial strains with MIC values of (20 and 20 $\mu\text{g mL}^{-1}$) and (20 and 40 $\mu\text{g mL}^{-1}$), against SA or MRSA, respectively. Additionally, 137–142, were tested for their anti-tumour effect towards A549, MCF-7, HepG2, and HeLa cancer cells and non-cancerous Vero

cells using MTT method to quantify cell viability and Adriamycin (IC_{50} values ranged from 0.11 to 0.80 μM), as positive control. Whilst **139–141** displayed weak cytotoxicity towards HepG2 and/or HeLa cells with IC_{50} values ranging from 18.0 to 36.4 μM , **137**, **138**, and **142** showed no cytotoxicity against these cells.¹⁴⁶ Additionally, the previously mentioned cytochalasan analogues (**116**), and (**117**), were obtained from an organic extract of the endophytic derived fungus *D. cf. ueckeri*, isolated

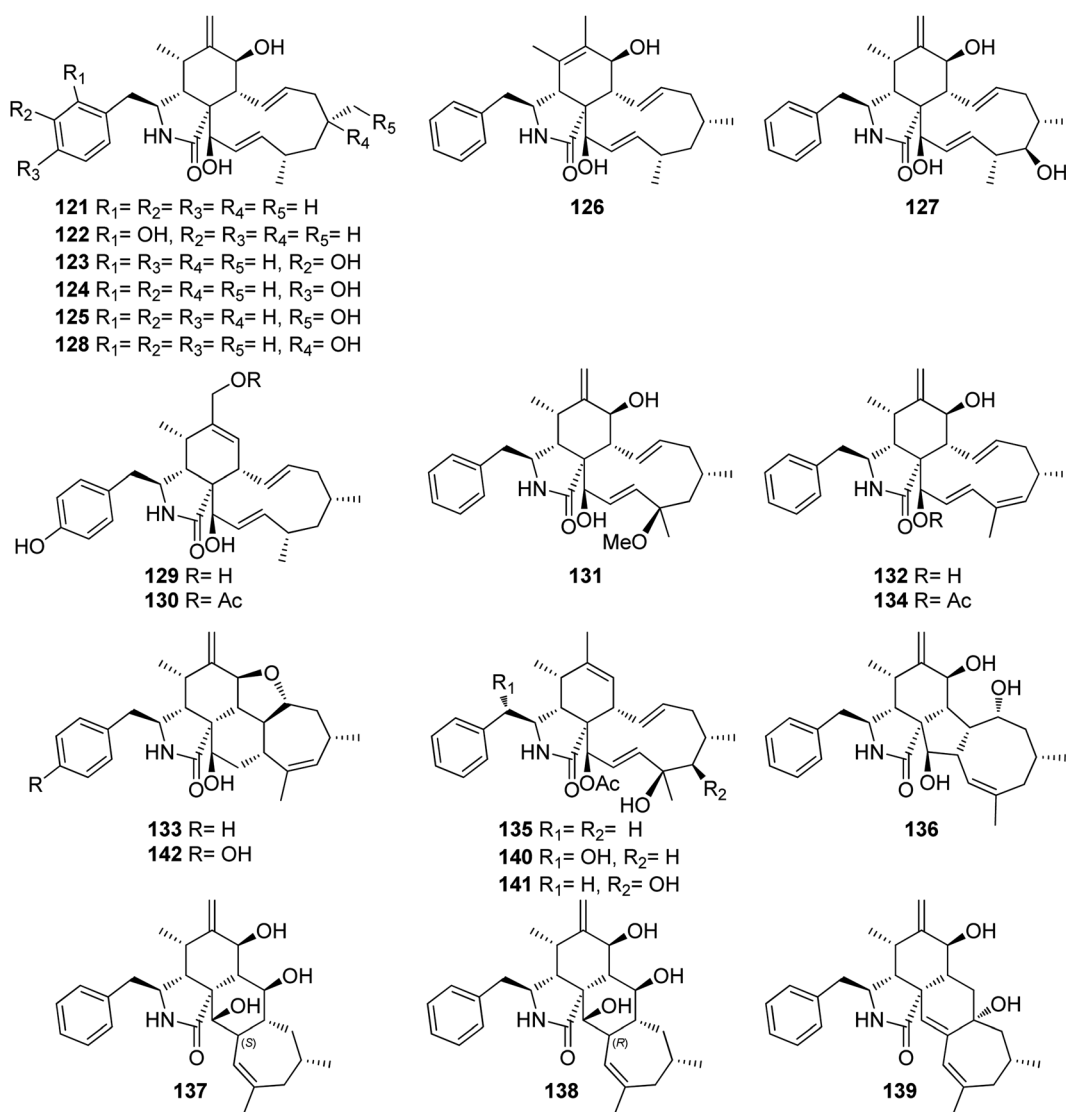


Fig. 17 Chemical structures of 121–142

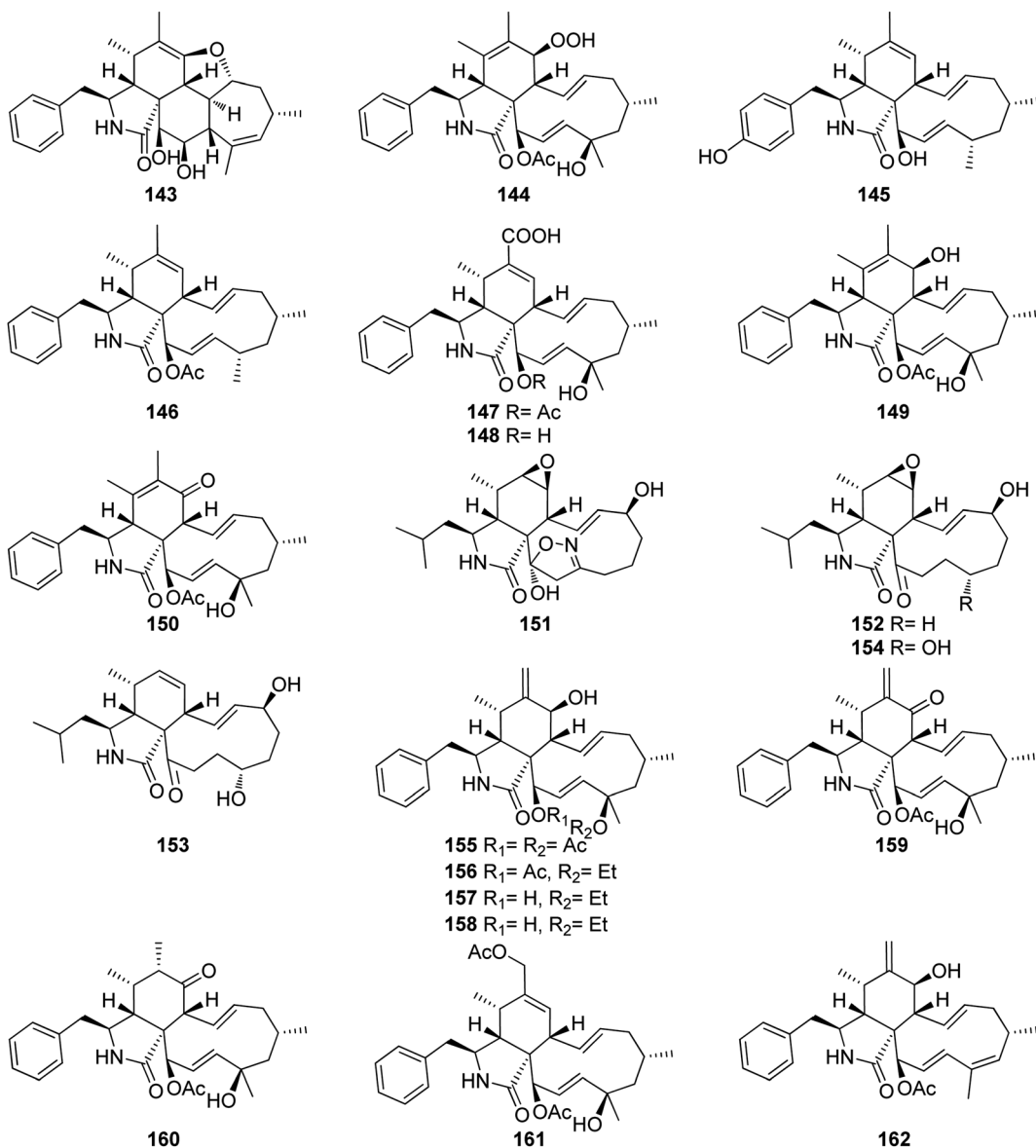


Fig. 18 Chemical structures of 143–162.

from *Pittosporum mannii*, collected from the west of Cameroon in Tonga.⁵⁵

3.5.1.2.2. Genus *Phomopsis* (Mycobank ID 9365) [taxonomically updated to *Diaporthe*]. The aforementioned cytochalasan derivatives (117) and (136), along with two previously undescribed analogues namely phomopchalasins B (143) and C (144) (Fig. 18), were identified from an organic extract of the medicinal plant derived fungus *Phomopsis* sp. shj2, isolated from *I. eriocalyx* var. *laxiflora*. It is worth mentioning that phomopchalasin A (144) possesses an unusual hydroperoxy motif in position C-7. Compounds 136, 143 and 144 were examined for their *in vitro* anti-inflammatory, cytotoxicity and antimigratory abilities using MG132, *Cis*-platin (IC_{50} values ranged from 1.1 to 12.7 μ M), and cytochalasin D (366), respectively as the positive controls. Compounds 143–144 disrupted migrations of MDA-MB-231 cells with IC_{50} values of 19.1 and

12.7 μ M, respectively. Additionally, 144 exhibited a mild cytotoxic effect towards A-549, HL-60, and SMMC-7721, cancer cells with IC_{50} values of 21.1, 14.9, and 22.7 μ M, respectively. Moreover, 144 showed a potent inhibitory activity on nitric oxide (NO) production with IC_{50} value of 11.2 μ M, when compared to MG-132 (IC_{50} value of 0.2 μ M) as positive control.¹⁴⁷ The chemical examination of the mangrove derived fungi *Phomopsis* sp. xy21 and *Phomopsis* sp. xy22, isolated from *Xylocarpus granatum* leaves, collected from Trang Province in Thailand, led to the isolation of the aforementioned derivatives (115–117) and (121–123), along with the previously unreported phomopsichalasin F (145) as well as the previously described 18-deoxy-cytochalasin H (7, L-696,474) (146) together with the previously undescribed phomopsichalasins D (147) and F (148) (Fig. 18). All the isolated compounds were examined for their cytotoxicity using the MTT method and *Cis*-platin (IC_{50} values of 8.5, 6.3,

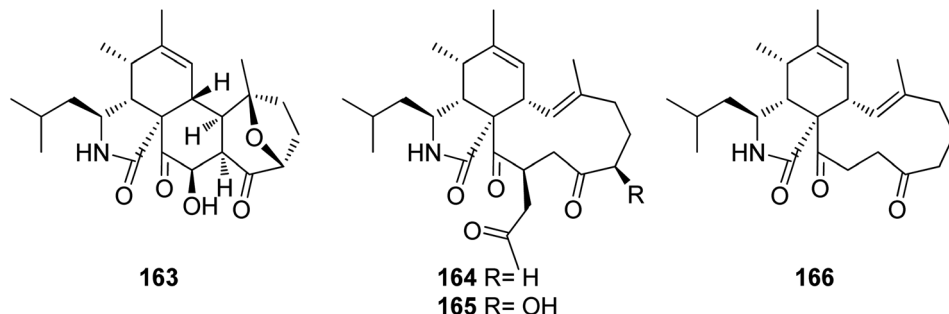


Fig. 19 Chemical structures of 163–166.

18.1, 22.0, 28.2, 12.1, 10.7, and 15.4 μ M, respectively) as positive control, against A2780, MDA-MB-231, A375, HCT-8, HCT-8/T, A549, SMMC-7721, and AGS cancer cell lines. Whilst (122) showed potent cytotoxic effect towards A2780, MDA-MB-231, A549, HCT-8, and HCT-8/T with IC_{50} values of 7.1, 3.4, 6.4, 7.5 and 8.6 μ M, respectively. Moreover, (147) displayed no cytotoxic activity against the examined tumour cell lines with IC_{50} value of >100 μ M.¹⁴⁸ The previously described cytochalasin N (149), along with the previously unreported phomocytocalasin (150) (Fig. 18), together with the previously mentioned cytochalasan derivatives (116), and (135), were isolated from the endophytic fungus *P. theicola*, isolated from *L. hypophaea* leaves, collected in Mutan, Taiwan. Compounds 116, 149 and 150 were examined for their inhibitory effect towards NO and IL-6 production using Quercetin (IC_{50} values of 36.8, and 31.3 μ M, respectively), as positive control. Among them, cytochalasin N (149) exhibited weak inhibitory ability with IC_{50} value of 77.8 μ M. Furthermore,

they were examined against the progesterone receptor (PR) antagonism using RU486 (IC_{50} values 0.000063 μ M) as positive control. Among the isolated compounds, cytochalasin H (116), displayed significant antagonism effect with the IC_{50} value of 1.42 μ M.¹⁴⁹ Three previously unreported cytochalasan derivatives namely phomopsisins A (151), B (152) and C (153), along with the previously reported once xylarisin (154) (Fig. 18), were obtained through the chemical examination of the endophytic fungus *Phomopsis* sp. sh917, isolated from *I. eriocalyx* var. *laxiflora* stems, collected in China, from Kunming botanical garden. Compounds 151–152 displayed no significant cytotoxic effect when examined for their cytotoxicity against SW480, MCF-7, SMMC-7721, A549, and HL-60 cells using the MTT method and Taxol & Cis-platin, as positive controls. Moreover, among the isolated compounds, phomopsisin C (153) showed moderate inhibition effect towards NO-production when compared with the positive control L-NMMA, with IC_{50} values of

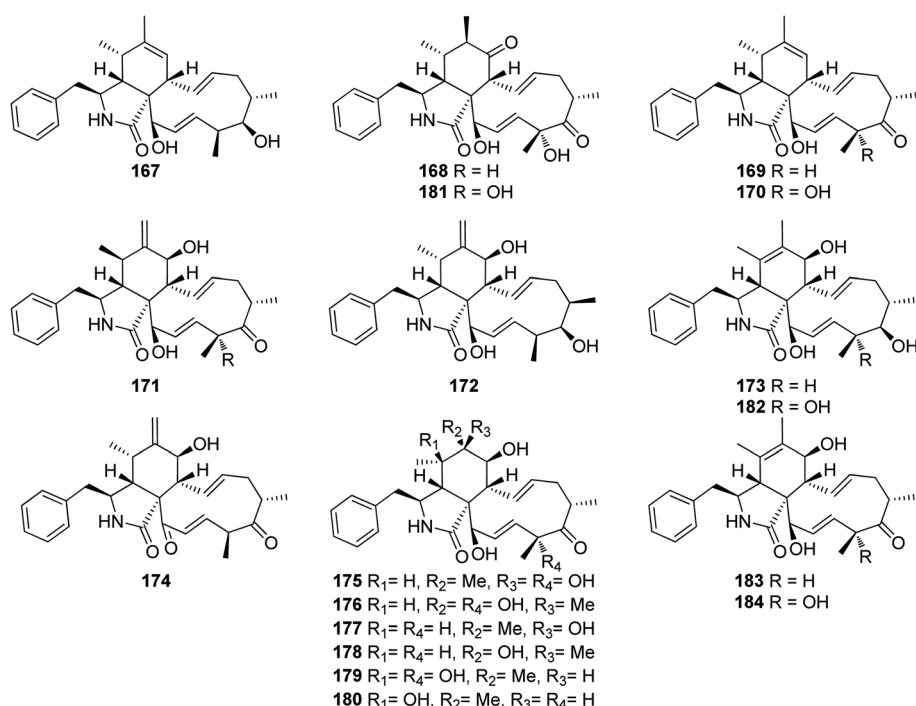


Fig. 20 Chemical structures of 167–184.



32.38 and 42.34 μM , respectively.¹⁵⁰ Chemical investigation of the endophytic fungus *Phomopsis* sp. shj2, isolated from the stems of *I. eriocalyx* var. *laxiflora*, collected in China from Kunming botanical garden; led to the isolation of the previously mentioned derivatives (116), (131), and (135) along with the previously undescribed 18-acetoxycytochalasin H (155), 18-ethoxycytochalasin H (156), 18-acetoxycytochalasin J (157), 18-ethoxycytochalasin J (158), 7-oxocytochalasin H (159), cytochalasin H₃ (160), cytochalasin H₄ (161), together with the previously reported 21-acetoxycytochalasin J₂ (162) (Fig. 18). Compounds 116, 131, 135, 155–157 and 161–162 were examined for their *in vitro* antimigratory abilities against MDA-MB-231, using cytochalasin D (366) (IC₅₀ value of 0.78 μM) as positive control. Whilst cytochalasin H₄ (161) displayed no antimigratory effect with IC₅₀ value >25 μM , the rest of the examined compounds were found to be active with IC₅₀ values ranging from 1.01–10.42 μM .¹⁵¹

3.5.2. Fungi of the subclass Hypocreomycetidae

3.5.2.1. Fungi of the order Hypocreales

3.5.2.1.1. Fungi of the family Bionectriaceae. 3.5.2.1.1.1.

Genus Clonostachys (MycoBank ID 7701) (Spicaria, MycoBank ID 22355). Four previously unreported derivatives, spicochalasin A (163), aspochalasin N (164), O (165) and Q (166) (Fig. 19), along with the previously mentioned derivatives, (61), (70), (71) and (82), were isolated from the marine derived fungus *Spicaria elegans*, isolated from the marine sediment of Jiaozhou Bay, China. All compounds were examined for their cytotoxicity against MOLT4, A549, HL-60 and BEL-7402 cell lines. Whilst 70

and 164–166 were found to be inactive with IC₅₀ values >100 μM , 61 displayed mild to potent cytotoxicity with IC₅₀ values ranging from 2.3 to 16.3 μM . Aspochalasin B (82) exhibited cytotoxicity against MOLT4, A549, and HL60 with IC₅₀ value of 13.0, 19.6, and 11.6 μM , respectively. Moreover 71 and 163 showed moderate cytotoxicity against HL-60 with IC₅₀ values of 20.0 and 19.9 μM , respectively.¹⁵²

3.5.2.1.2. Fungi of the family Clavicipitaceae. 3.5.2.1.2.1.

Genus Metarhizium (MycoBank ID 8912). Fourteen previously unreported cytochalasans derivatives namely brunnesins A (167), B (168), C (169), D (170), E (171), F (172), G (173), H (174), I (175), J (176), K (177), L (178), M (179), N (180) along with the previously reported analogues, 6,7-dihydro-7-oxo-deacetylcytochalasin C (181), zygosporin D (182), deacetylcytochalasin C (183) and 18-deshydroxyl-deacetylcytochalasin C (184), (Fig. 20) were isolated from the organic extract of the pathogenic derived fungus *Metarhizium brunneum* TBRC-BCC 79240, isolated from the dead insect (Lepidoptera), collected in Thailand from the Province of Kalasin. Compounds 167–173 and 175–184 were evaluated for their antibacterial using Isoniazid, Rifampicin, Vancomycin and Erythromycin (MIC values ranged from 0.0063 to 25.0 $\mu\text{g mL}^{-1}$) as positive controls, against *Mycobacterium tuberculosis*, *Staphylococcus aureus*, *Acinetobacter baumannii* and for their antifungal activity using Amphotericin (MIC value ranged from 0.781 to 1.56 $\mu\text{g mL}^{-1}$) as positive control, towards the phytopathogenic fungi, *Alternaria brassicicola*, *Colletotrichum acutatum*, and *Curvularia lunata*, as

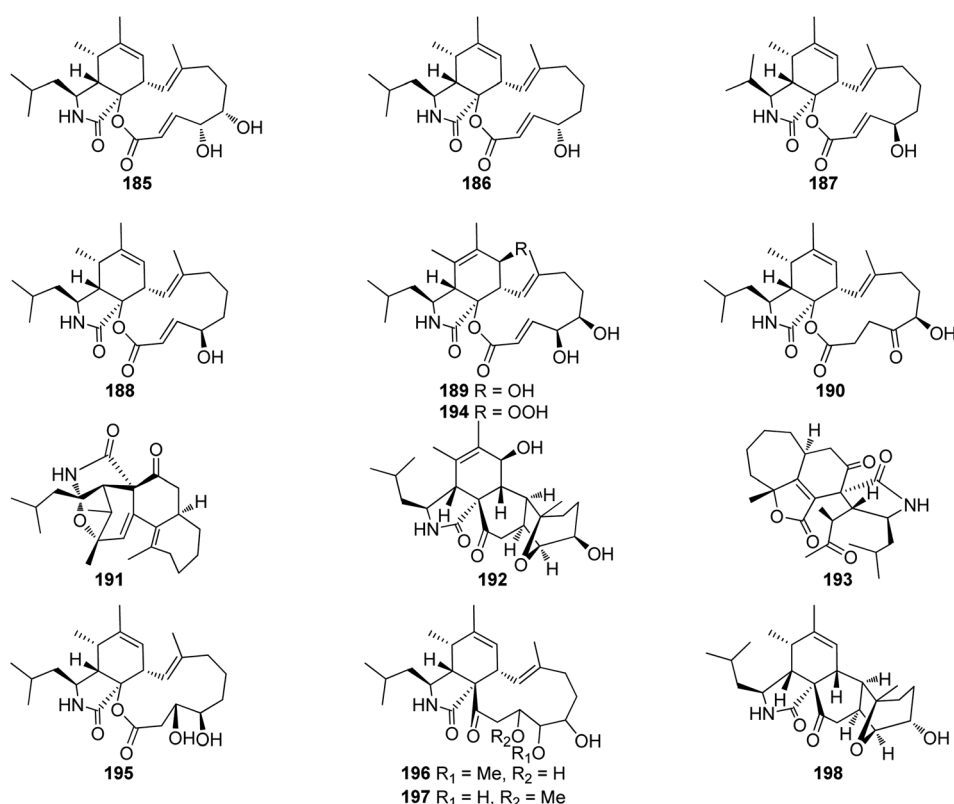


Fig. 21 Chemical structures of 185–198.



well as their cytotoxicity using Doxorubicin, Ellipticine and Tamoxifen (IC_{50} values ranged from 0.077 to 9.14 $\mu\text{g mL}^{-1}$) as positive controls, against the mammalian cells MCF-7, NCI-H187 and Vero.

Additionally, the examined compounds displayed neither antibacterial nor antifungal against (*S. aureus* and *A. baumannii*), and (*A. brassicicola*, *C. acutatum*, and *C. lunata*), with MIC values of $>50 \mu\text{g mL}^{-1}$. However, **168**, **170–173** and **181–184** displayed weak to mild anti-bacterial activity against *M. tuberculosis* with MIC values ranging from 25 to 50 $\mu\text{g mL}^{-1}$. Furthermore, whilst **167–169**, **171**, **176–177**, **181** and **183–184**, showed no cytotoxic effect against the examined cell lines with IC_{50} values of $>50 \mu\text{g mL}^{-1}$, compound **170** displayed significant cytotoxicity against all the examined cells with IC_{50} values of 16.8, 3.71 and 2.09 $\mu\text{g mL}^{-1}$, respectively.

Additionally, **172** and **182**, showed a selective remarkable effect against the Vero cell lines with IC_{50} values of 4.03 and 0.637 $\mu\text{g mL}^{-1}$, respectively. Moreover, **173** and **179–180** showed cytotoxic ability against NCI-H187 and Vero cells with IC_{50} values ranging from 3.98 to 44.81 $\mu\text{g mL}^{-1}$. Furthermore, **175** and **178** exhibited a selective activity against NCI-H187 cancer cell line with IC_{50} values of 18.59 and 18.54 $\mu\text{g mL}^{-1}$, respectively.¹⁵³

3.5.2.1.3. Fungi of the family Hypocreaceae. 3.5.2.1.3.1. Genus *Trichoderma* (MycoBank ID 10282). A chemical exploration of the medicinal plant fungus *Trichoderma gamsii*, isolated from *Panax notoginseng*, led to the isolation of the previously reported cytochalasin derivatives aspochalasins I (**185**), and J (**186**), together with two previously unreported analogues namely trichalasins A (**187**) and B (**188**) (Fig. 21). Compounds **185–188** were tested for their effect against HeLa cancer cell lines using Taxol and VP-16 as positive controls (EC_{50} value of 0.0025 and 0.0057 μM , respectively). Among them, only aspochalasin J (**186**) showed weak cytotoxic effect with IC_{50} value of 27.8 μM .⁵⁹ Further examination of the same endophytic fungus by the same group resulted in the isolation of the previously mentioned analogues (**61**), (**70**) and (**71**), together with the two previously unreported trichalasins C (**189**) and D (**190**) (Fig. 21). All the isolated compounds were examined for their cytotoxic activity towards the HeLa cancer cell line, using VP-16 and Taxol as positive controls.

Whilst aspochalasin D (**61**) exhibited cytotoxicity with EC_{50} value of 5.72 μM , all the other compounds showed no

cytotoxicity with EC_{50} values of $>40 \mu\text{M}$.¹⁵⁴ Further investigation of the same fungal strain by the same group yielded in the isolation of the previously mentioned cytochalasan derivatives (**61**), (**185**) and (**186**), along with two additional previously unreported analogues trichoderones A (**191**) and B (**192**) (Fig. 21). All isolated compounds were examined for their cytotoxicity against HeLa cell line using VP-16 and Taxol as positive controls. Whilst aspochalasins D (**61**) and J (**186**), showed cytotoxic effect with IC_{50} value of 5.72 and 27.4 μM , respectively, aspochalasin I (**185**), trichoderones A (**191**) and B (**192**) were found inactive.¹⁵⁵

Later, the same group reported the isolation of a further previously unreported trichodermone (**193**) (Fig. 21), along with (**61**), which might be considered as its possible biosynthetic precursor. Whilst trichodermone (**193**), displayed no cytotoxicity against HeLa cell line, aspochalasin D (**61**) showed mild cytotoxic effect with IC_{50} value of 5.72 μM .¹⁵⁶ Furthermore, three previously unreported analogues namely trichalasins E (**194**), F (**195**), and H (**198**), along with two previously reported derivatives namely, aspochalasin K (**196**), and trichalasin G (**197**), (Fig. 21), together with the previously mentioned analogues (**81**) and (**189**) were isolated during a re-examination of the same fungal strain by the same group.

Compounds **81**, **189**, and **194–198**, were examined for their cytotoxic effects against A549, MDA-MB-231 and PANC-1 tumour cell lines using 5-Fluorouracil (IC_{50} values of 0.47, 0.12 and 0.67 μM , respectively) as positive control. Among the reported metabolites only trichalasin G (**197**) displayed weak cytotoxicity against MDA-MB-231 with IC_{50} value of 60.6 μM .¹⁵⁷

3.5.2.1.4. Fungi of the family Nectriaceae. 3.5.2.1.4.1. Genus *Calonectria* (MycoBank ID 746). Chemical examination of the plant derived fungus *Calonectria morganii* (synonym *Cylindrocladium scoparium*), led to the detection of two previously unreported analogues namely chaetoglobosin A (**199**) and 19-O-acetylchaetoglobosin A (**200**) (Fig. 22).¹⁵⁸

3.5.2.1.5. Fungi of the family Stachybotryaceae. 3.5.2.1.5.1. Genus *Stachybotrys* (MycoBank ID 10052). Chemical examination of the mountain derived fungus *Stachybotrys charatum*, collected at height of 3600 m of Tibet isolated from an unnamed glacier, led to the isolation of seven previously unreported analogues namely alachalasins A (**201**), B (**202**), C (**203**), D (**204**), E (**205**), F (**206**), and G (**207**) (Fig. 23). Alachalasin A (**201**)

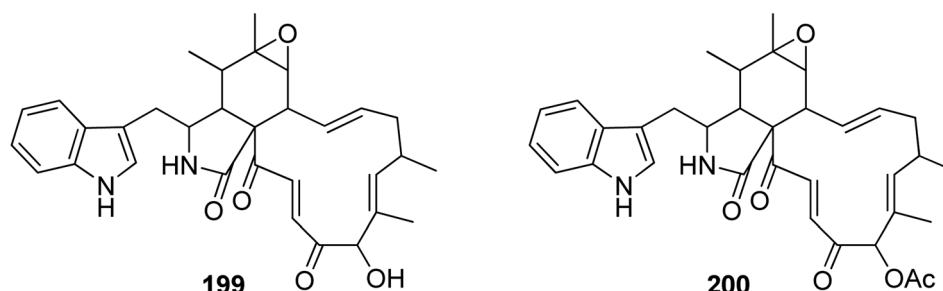


Fig. 22 Chemical structures of **199–200**.



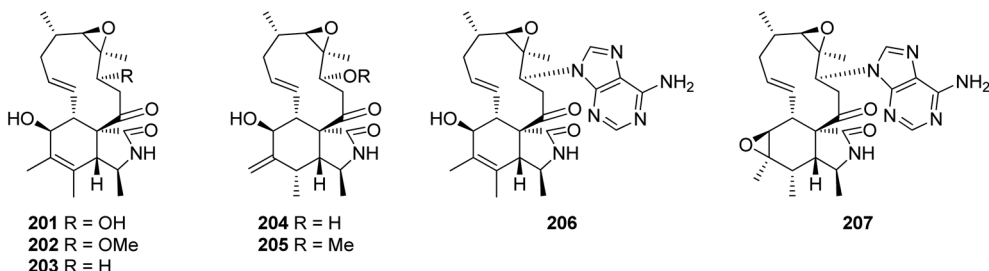


Fig. 23 Chemical structures of 201–207.

displayed anti-HIV-1 activity and *in vitro* activity against HIV-1_{LAI} in C8166 cells, with CC₅₀ and EC₅₀ values of 101.55 and 8.01 μ M, respectively, when compared to Indinavir (EC₅₀ value of 0.00818 μ M). Additionally, all the isolated compounds were tested for their antimicrobial activity against different bacterial strains including *Streptococcus mutans* (ATCC 25175), *Staphylococcus aureus* (ATCC 6538), *Enterococcus faecalis* (ATCC 19433), *Micrococcus luteus* (ATCC 9431), and *Sarcina lutea* (CMCC

B28001), as well as a panel of fungi including *Candida albicans* (ATCC 10231), *Geotrichum candidum* (AS2.498), and *Aspergillus fumigatus* (ATCC 10894), while none of them showed antimicrobial effect against *S. lutea*, *S. mutans*, *E. faecalis*, *G. candidum*, *A. fumigatus*, and *C. albicans*, at a concentration of 100 μ g per disk; alachalasin D (204) displayed activity against *S. aureus* and *M. luteus* at a concentration of 100 μ g per disk with an inhibition zones of 7 and 9 mm, respectively. Furthermore,

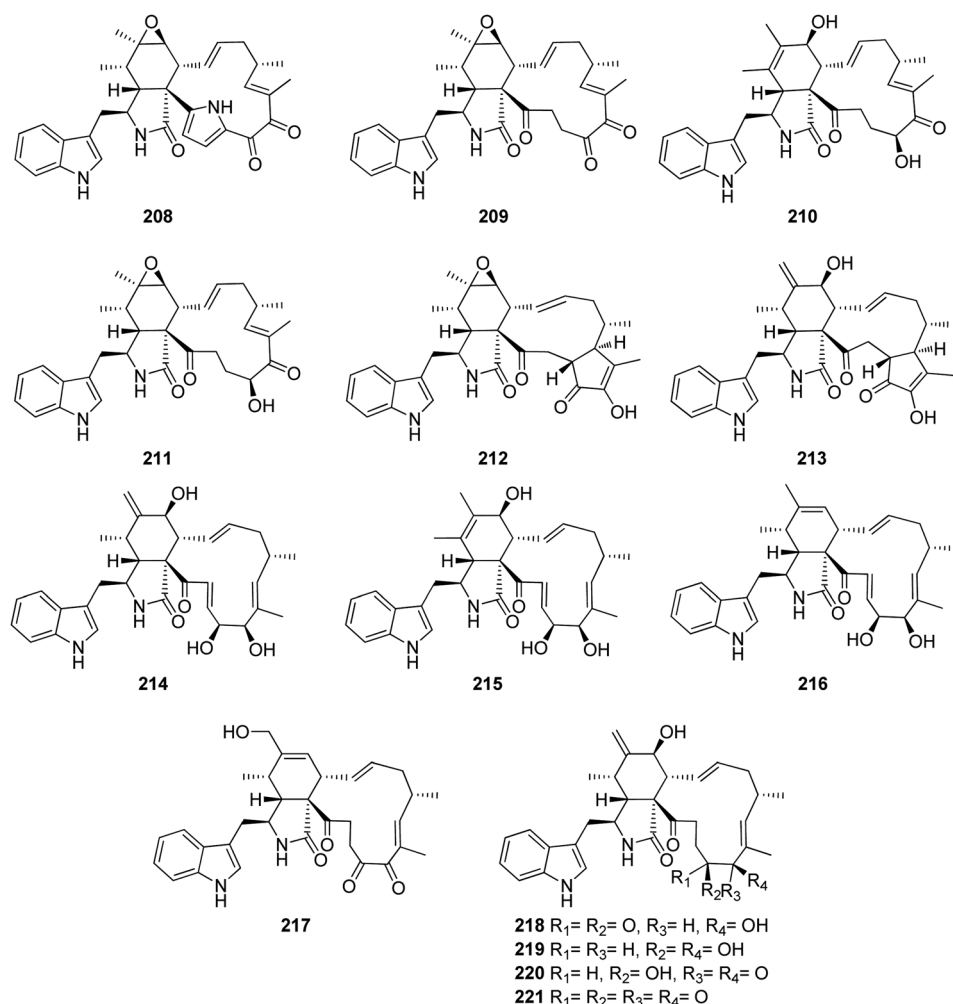


Fig. 24 Chemical structures of 208–221.



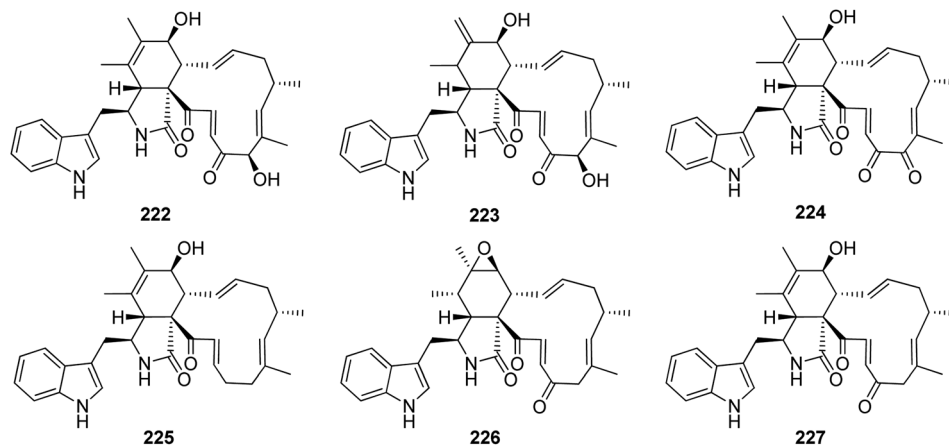


Fig. 25 Chemical structures of 222–227.

alachalasin G (207) displayed mild effect towards *S. aureus*, exhibiting an inhibition zone of 15 mm at a concentration of 100 μ g per disk as well as showed an MIC value of 99 μ M.⁶⁵

3.5.2.2. Fungi of the order Sordariales

3.5.2.2.1. Fungi of the family Chaetomiaceae. 3.5.2.2.1.1.

Genus Chaetomium (MycoBank ID 953). Five previously described cytochalasan derivatives namely penochalasin A (208), chaetoglobosins C (209), E (210), F (211) and chaetoglobosin U (212) (Fig. 24) were isolated from the plant derived fungus *Chaetomium globosum* IFB-E019, isolated from *Imperata cylindrica*, collected in China, from Yancheng seashore, from the Province of Jiangsu. Compound 212 displayed strong cytotoxic effect against KB cancer cell line with IC₅₀ value of 16.0 μ M, with almost an identical value reported for the positive control 5-Fluorouracil (*i.e.*, IC₅₀ value of 14.0 μ M). Additionally, 208–211 showed mild cytotoxicity against KB cancer cell with IC₅₀ values of 34.0, 40.0, 52.0 and 48.0 μ M, respectively.¹⁵⁹ Chemical inspection of the organic extract of the marine green alga derived fungus *C. globosum* QEN-14, isolated from *Ulva pertusifera* fresh tissue, collected in China from the coastline of Qingdao Province, led to the isolation of seven previously unreported cytochalasan derivatives namely cytoglobosins A–G (213–219), along with the previously described analogues chaetoglobosin F_{ex} (220) and isochaetoglobosin D (221) (Fig. 24). Compounds 213–217 and 219, were tested for their

cytotoxic effects against KB, A549, and P388 cell lines. Whilst 213, 214, 217, and 219, were found inactive with IC₅₀ values of >10 μ M, 215 and 216, exhibited a selective cytotoxicity against A549 with IC₅₀ values of 2.26 and 2.55 μ M, respectively.¹⁶⁰

Dou *et al.* isolated the previously mentioned analogue (220) from the marine-derived fungus *C. globosum* QEN-14. Subsequently, they investigated its biological activity and proposed that its anti-inflammatory potential might be attributed to its ability to negatively regulate phosphorylation of ERK1/2, JNK1/2, and p38, as well as inhibit NF- κ B. On the other hand, these inhibitory activities may also be attributed to the blocking of mCD14 expression.¹⁶¹ Further nine cytochalasan derivatives were reported from the soil derived fungus *C. elatum* ChE01, isolated from a soil sample collected in Thailand from the Province of Yala, including the previously mentioned derivatives (209), (211), and (221), along with the previously reported chaetoglobosins B (222), D (223), and G (224), together with three previously undescribed analogues namely chaetoglobosin V (225), prochaetoglobosin III (226), and prochaetoglobosin III_{ed} (227) (Fig. 25). Compounds 209, 211, and 221–227, exhibited potent cytotoxicity against the cholangiocarcinoma cells with IC₅₀ values ranging from 3.41 to 86.95 μ M when compared to 5-Fluorouracil (IC₅₀ value 348 μ M), as positive control. Additionally, all the examined compounds displayed cytotoxic effect against the human breast cancer with IC₅₀ values ranging from 2.54 to 21.29 μ M, when compared to Ellipticine (IC₅₀ value 1.06 μ M), as positive control.¹⁶²

Additional two previously undescribed cytochalasan derivatives exhibited unprecedented 6/6/5/5/7 pentacyclic ring system, namely chaetoconvosins A & B (228 & 229) (Fig. 26) were recorded from the plant derived fungus *C. convolutum* cib-100, isolated from the roots of wheat, collected in China, Sichuan Province. Compounds 228–229 were examined for their cytotoxicity against SMMC-7721, A549, HEPG2, PC-3, and A375 tumour cell lines using *Cis*-platin as positive control. Whilst 229 exhibited moderate cytotoxicity against the examined cells with IC₅₀ values of 43.0, 26.12, 44.60, 49.74 and 47.93 μ M, respectively, 228 was found inactive. Furthermore 216, displayed an inhibitory activity towards root elongation.¹⁶³

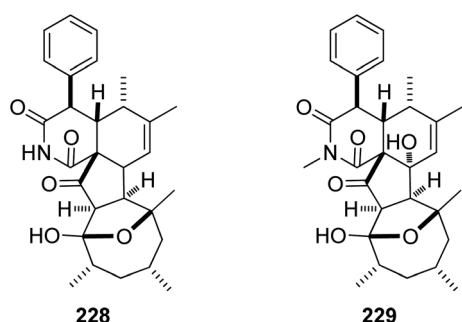


Fig. 26 Chemical structures of 228–229.



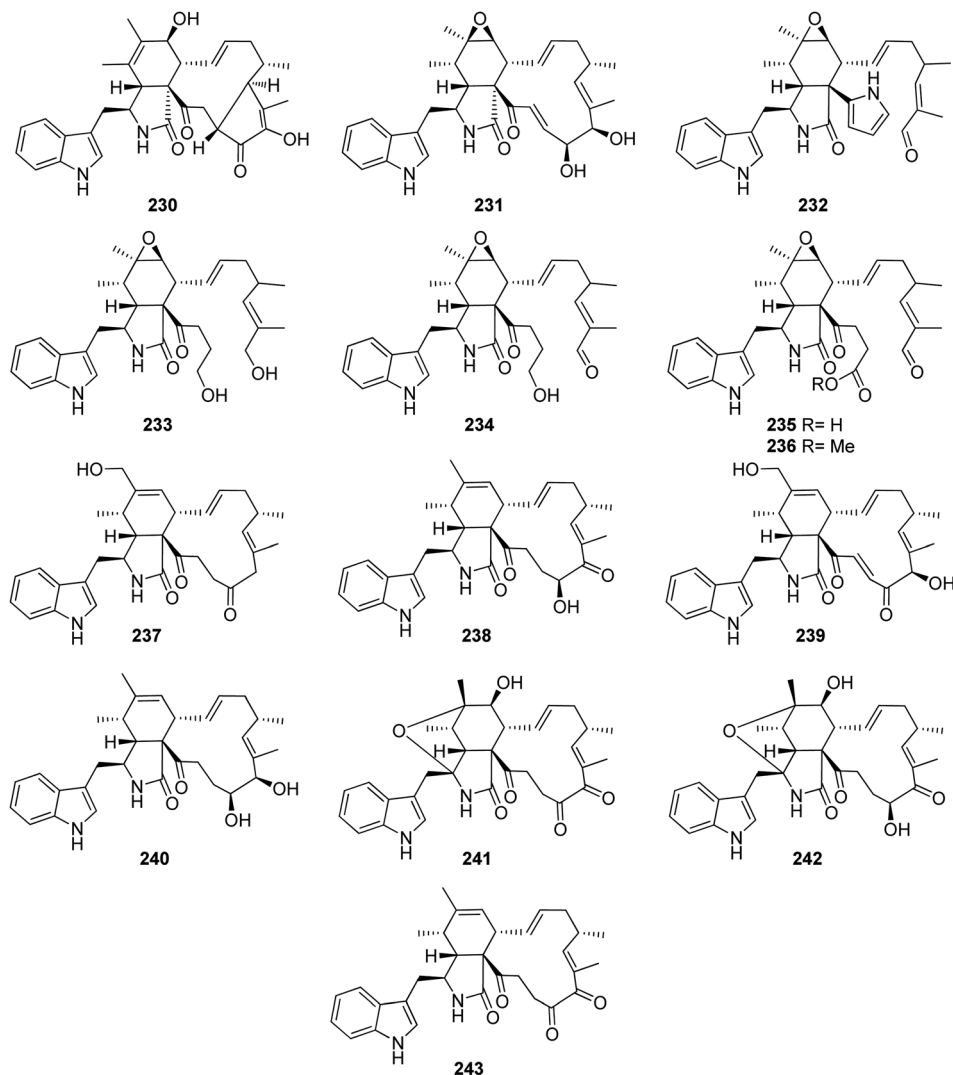


Fig. 27 Chemical structures of 230–243.

Chaetoglobosin V_b (230) (Fig. 27), a previously undescribed cytochalasan derivative along with the previously mentioned analogue (224), were reported from the plant derived fungus *C. globosum*, isolated from *G. biloba* leaves. Compounds 224 and 230 were tested for their antibacterial properties towards *E. coli*, *S. aureus*, *B. cereus*, *B. subtilis* and *P. aeruginosa*, using Ampicillin as positive control. Whilst 230 showed no activity against all the examined bacterial strains with MIC values of $>100 \mu\text{g mL}^{-1}$. Compound 224 exhibited weak antibacterial ability against *S. aureus*, *B. cereus*, and *P. aeruginosa* with MIC values of $50 \mu\text{g mL}^{-1}$. Additionally, both compounds were checked for their activity against selected phytopathogens, using Carbendazim and Hymexazol as positive controls. Whilst 224 showed weak antifungal activity against *F. graminearum*, *A. solani*, and *A. alternate*, with MIC values of 50, 25, and $25 \mu\text{g mL}^{-1}$, respectively. Additionally, 230 was found inactive against all the examined phytopathogens with MIC values of $>100 \mu\text{g mL}^{-1}$.¹⁶⁴ The chemical inspection of the medicinal plant derived fungus *C. globosum*, isolated from *G. biloba* leaves, collected in

Shandong Province, China afforded the isolation of five previously reported derivatives including 20-dihydrochaetoglobosin A (231) (Fig. 27) along with the previously mentioned analogues (209), (210), (211), and (220). Compounds 209–211 and 220, displayed phytotoxic effect towards radish seedlings when compared to Glyphosate as positive control. Additionally, 210, 211, 220 and 231 were examined for their antitumour activity against the HCT116 tumour cell line using Etoposide ($\text{IC}_{50} 2.13 \mu\text{M}$) as positive control. Compound 210 was found inactive with IC_{50} value of $>100 \mu\text{M}$, however 211, 220, and 231 displayed mild to strong activity with IC_{50} values of 17.8, 4.43, and $8.44 \mu\text{M}$, respectively. These findings reflect crucial role of the epoxide ring as well as the double bond at C-6(12), which enhance the cytotoxicity.¹⁶⁵ A chemical exploration of the methanolic extract of the arthropods derived fungus *C. globosum* TW1-1, isolated from pillbug (*Armadillidium vulgare*), collected in China Hubei Province, yielded ten previously undescribed cytochalasan analogues namely armochaetoglobins A–J (232–241), along with the previously reported chaetoglobosin W (242) and



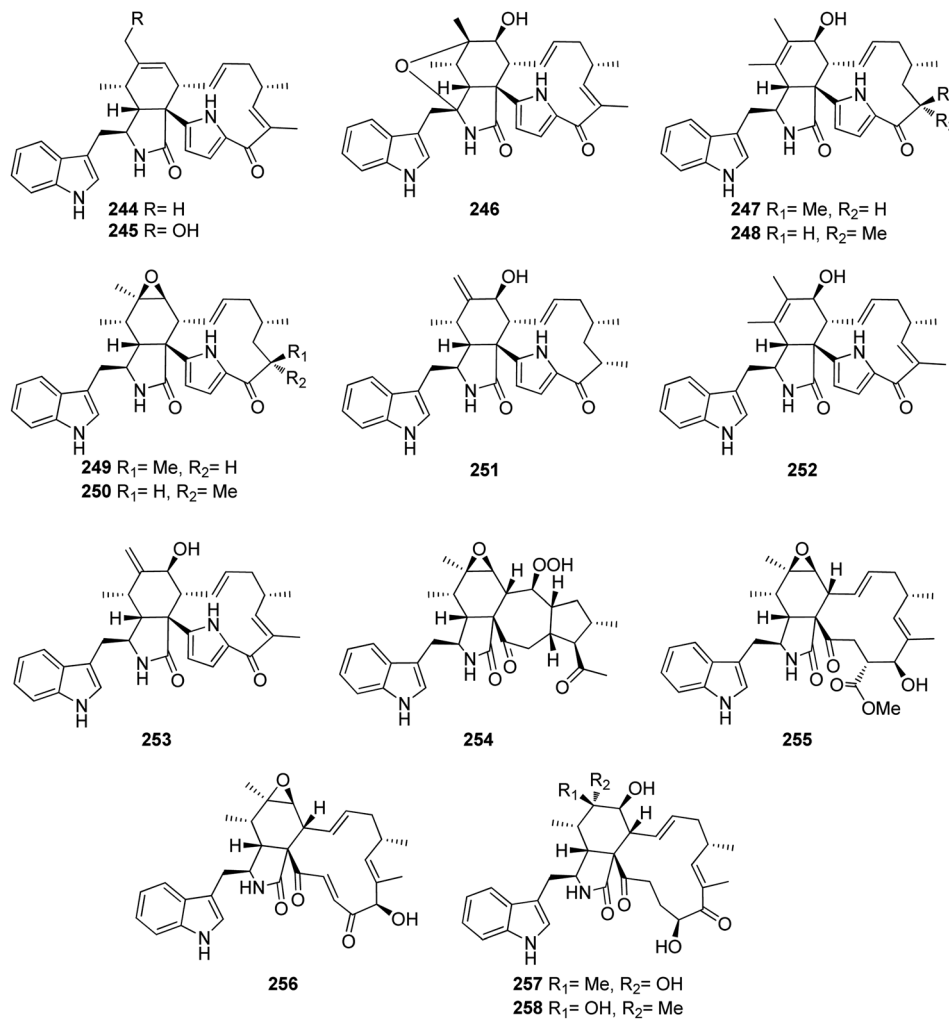


Fig. 28 Chemical structures of 244–258.

isochaetoglobosin J (243) (Fig. 27) together with the previously mentioned cytoglobosin derivatives (215) and (217). Compounds 233–241 were examined for their cytotoxicity against HL-60, SMMC-7721, A549, MCF-7, and SW480, tumour cell lines using Paclitaxel and *Cis*-platin as positive controls (IC_{50} values between <0.0008 –0.58 and 1.33–13.3 μM , respectively). Compounds 237 and 240 were found inactive with IC_{50} values of >40 μM , however 236, 238, 239 and 241, exhibited strong to weak cytotoxicity with IC_{50} values ranging from (10.84–38.17 μM), (12.58–20.55 μM), (3.31–9.83 μM), and (17.43–35.28 μM), respectively. Furthermore, 233 and 234 displayed a selective moderate cytotoxicity against HL-60, SMMC-7721, and A549 cancer cell lines with IC_{50} values ranging from (16.47–30.88 μM), and (10.62–16.32 μM), respectively. Additionally, 235 showed a selective cytotoxicity against SMMC-7721 cell line with IC_{50} value of 24.99 μM .¹⁶⁶

Further examination of the same fungal strain by the same group, resulted in the isolation armochaetoglobins K–R (244–251), additional eight previously undescribed derivatives resembled the unusual pyrrole-based cytochalasans, along with the previously described analogues penochalasins B–C (252–

253) (Fig. 28), together with the previously mentioned analogue (208). All the isolated compounds were examined for their antiviral activity against the HIV using the cytopathic effect and p24 assays, and AZT (EC_{50} 0.012 μM), as positive control. Among them, 245–247 and 250–252 displayed strong anti-HIV activity with EC_{50} values of 0.48, 0.55, 0.25, 0.31, 0.34 and 0.11 μM , respectively and with a selectivity index ranging from 12.33 to 75.42, however 208, 244, 248, 249, and 253, were found to be less potent with EC_{50} values of 6.12, 1.23, 0.61, 0.68, and 4.92 μM , respectively.¹⁶⁷ Further investigation by the same groups for the same fungal strain led to the isolation of three previously undescribed analogues namely armochaeglobines A–C (254–256) (Fig. 28), along with the previously mentioned derivatives (199) and (212). Compounds 254–256 were examined for their cytotoxicity against SW480, HL-60, MCF-7, SMMC-7721, and A549 cancer cell lines, using MTS method and *Cis*-platin (IC_{50} values of 10.1, 2.2, 12.2, 10.2, and 7.3 μM , respectively), as positive control. Among them, 255 displayed a mild cytotoxicity with IC_{50} values ranging from 3.4 and 14.7 μM , against the examined cancer cell lines.¹⁶⁸ The previously mentioned cytochalasan derivatives (199) and C (209), were reported from the



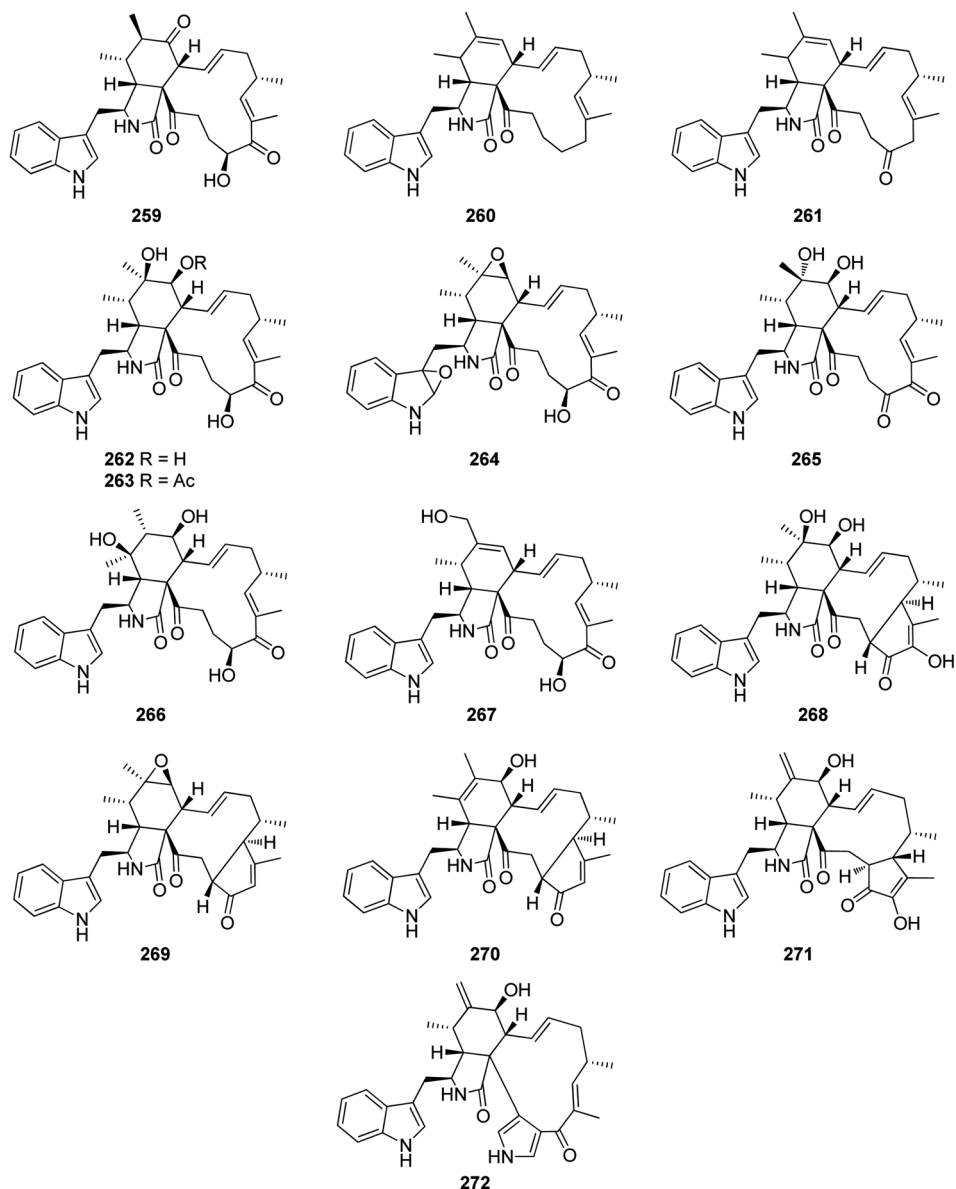


Fig. 29 Chemical structures of 259–272.

ethyl acetate extract of the aquatic plant derived fungus *C. globosum*, obtained from *Nymphaea nouchali*, collected in Sri Lanka from the Province of Gampaha. Both compounds were examined for their antimicrobial abilities against the Gram-positive bacteria, methicillin-resistant *S. aureus* (MRSA, ATCC 33591), *S. aureus* (ATCC 43300) and *B. subtilis* (UBC 344). Whilst **199** displayed moderate antibacterial activity against the examined Gram-positive bacteria with MIC values of 32, 32 and 16 μ g mL $^{-1}$, respectively. Compound **209** was found to be inactive.¹⁶⁹ A chemical inspection of the marine derived fungus *C. globosum* MCCC 3A00607, isolated from the sediments collected from the Indian Ocean led to the isolation of the previously mentioned analogues **210–211**, **214–215**, and **220–222**, along with two previously undescribed analogues namely cytoglobosins H-I (**257–258**) (Fig. 28). All the isolated compounds were evaluated for their cytotoxicity against MDA-MB-231, LNCaP, and B16F10

cancer cell lines using *Cis*-platin (IC₅₀ values of 2.48, 1.04 and 2.80 μ M, respectively), as positive control. None of them showed cytotoxicity towards MDA-MB-231B. Furthermore, **258** was found inactive against LNCaP, and B16F10 cancer cell lines as well. Interestingly, **210** displayed the highest cytotoxicity against B16F10 and LNCaP tumour cell line with IC₅₀ values of 2.78 and 0.63 μ M, respectively.¹⁷⁰

A chemical exploration of the pillbug derived fungus *C. globosum* TW1-1, isolated from *R. vulgare*, collected from Hubei Province, China, afforded the isolation of the previously mentioned derivatives **211–213**, **225**, and **231**, along with the previously described chaetoglobosin Y (**259**), prochaetoglobosins I-II (**260–261**), together with nine previously undescribed polyoxygenated cytochalasan derivatives namely armochae-toglobosin S (**262**), 7-O-acetylarmochae-toglobosin S (**263**), armochae-toglobosins T-Z (**264–270**) (Fig. 29). Compounds **262–270** were

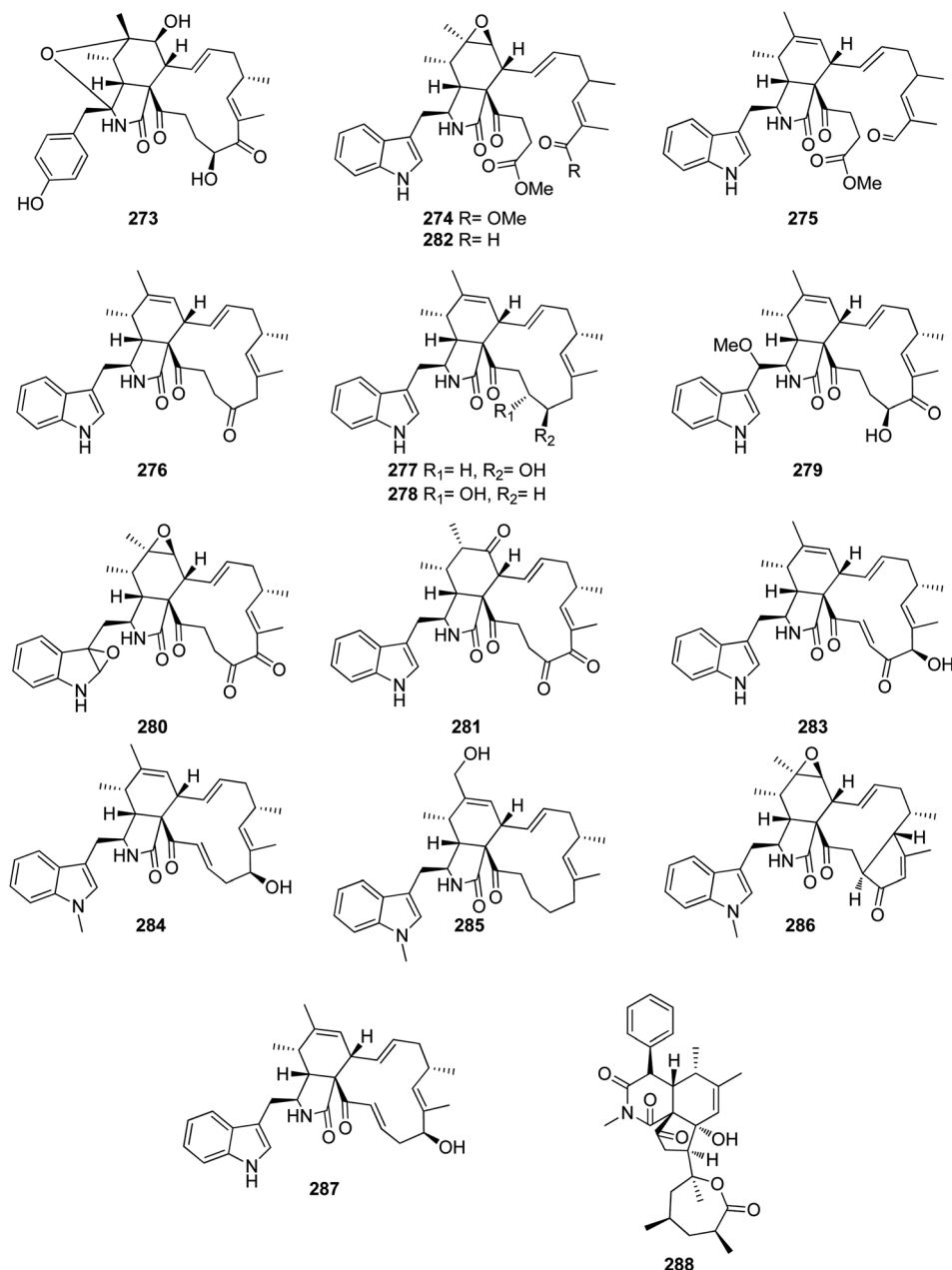


Fig. 30 Chemical structures of 273–288.

examined for their cytotoxicity against the cancer cell lines SMMC-7721, HL-60, A549, SW480, MCF-7, and BEAS-2B using *Cis*-platin (IC₅₀ values of 10.21, 1.93, 6.59, 12.16, 8.20, and 9.07 μM , respectively) as positive control. Whilst 262–268 exhibited no cytotoxicity, 269 displayed moderated activity against all the examined cell lines except MCF-7 line with IC₅₀ values ranging from 14.13 to 30.42 μM . Moreover, 270 displayed a selective cytotoxic effect against HL-60, A549, and BEAS-2B cells with IC₅₀ values of 10.45, 23.11 and 10.45 μM , respectively.¹⁷¹ The previously mentioned analogues 209–211, 213–215, 220, 224, 221, and 230 along with two previously unreported analogues namely cytoglobosin A_b (271) and isochaetoglobosin D_b (272) (Fig. 29) were reported from the organic extract of the fungus *C.*

globosum SNSHI-5. Compounds 271–272 were tested for their cytotoxic activity against H292 cells, where 271 displayed no cytotoxic effect, 272 displayed promising cytotoxicity with IC₅₀ value of 3.5 μM .^{172,173}

A chemical inspection of an organic extract of the arthropod *A. vulgare* derived fungus *C. globosum* TW1-1, grown in a L-tyrosine rich media, afforded the isolation of nine previously undescribed cytochalasans namely armochaetoglasins A–I (273–281), along with the previously described derivatives armochaetoglobin E (282) and chaetoglobosin J (283) (Fig. 30) together with the previously mentioned analogue 225. Compounds 225 and 273–283 were tested for their cytotoxicity against SW480, HT1080, SW1990, MM231, HL60, U87MG,



HEP3B and A549 cells, and NCM460 (normal colonic epithelial cell), using the MTS method and *Cis*-platin (IC_{50} values of 1.42, 2.47, 3.75, 4.62, 1.63, 2.13, 2.96 2.79 and 0.85 μ M, respectively) as positive control. Compounds 273, and 275–282 were found inactive with IC_{50} values of >40 μ M. On the other hand, 225, 274 and 283, displayed weak selective cytotoxicity with IC_{50} values ranging from 19.5 and 34.72 μ M. Additionally, all the isolated compounds were found inactive against the drug-resistant microbial pathogens, *K. pneumonia*, *E. coli*, and *S. aureus*.¹⁷⁴ Further re-examination by the same group on the same fungal strain grown in a cultural medium rich in 1-methyl-L-tryptophan (1-MT) instead of L-tyrosine, resulted in the isolation of three previously unreported cytochalasans namely armochaetoglobosins A–C (284–286), along with the previously undescribed chaetoglobosin T (287) (Fig. 30), together with the previously mentioned derivatives 209, 230, and 269. All compounds were examined for their antibacterial activity against five drug-resistant bacterial strains methicillin-resistant *S. aureus* ATCC 43300; ESBL-producing *E. coli* ATCC 35218; *E. faecalis* ATCC 29212; NDM-1-producing *K. pneumoniae* ATCC BAA2146; and *P. aeruginosa* ATCC 15542. Compound 209 was found inactive. On the other hand, 286 displayed potent antibacterial effect against *K. pneumoniae* when compared to the positive control

Meropenem with MIC values of 4 and 8 μ g mL⁻¹, respectively.¹⁷⁵ Chamiside A (288) (Fig. 30), a previously undescribed cytochalasans analogue possessing an unusual 6/6/5-Fluorouracilised tricyclic ring system, bearing the rare lactone seven membered and a benzene ring was recorded from the medicinal plant derived fungus *C. nigricolor* F5, isolated from *Mahonia fortunei* roots, collected from Qingdao Province, China. Compound 288 showed moderate antibacterial effect towards *S. aureus* (ATCC 6538), with MIC value of 25 μ g mL⁻¹.¹⁷⁶

A chemical examination of the soil derived fungus *C. madrasense* 375, isolated from a soil sample of Sinkiang Province desert, China, afforded the isolation of the previously undescribed chaetomadrasins A–B (289–290) (Fig. 31), along with the previously mentioned derivatives 213, 221, 224, 230, 265, and 271. Compounds 289–290 were evaluated for their cytotoxicity towards HepG2 tumour cell line, where they displayed mild activity when compared to the positive control *Cis*-platin, with IC_{50} values of 8.7, 19.4 and 3.14 μ M, respectively.¹⁷⁷ The HPLC-DAD-guided separation of the soft coral derived *C. globosum* C2F17, led to the isolation of the previously mentioned derivatives 104, 199, 209–211, 220–222, 223–224, 230, 238 and 259, along with the previously reported aurochaeglobosin B (291) and the previously unreported 6-O-

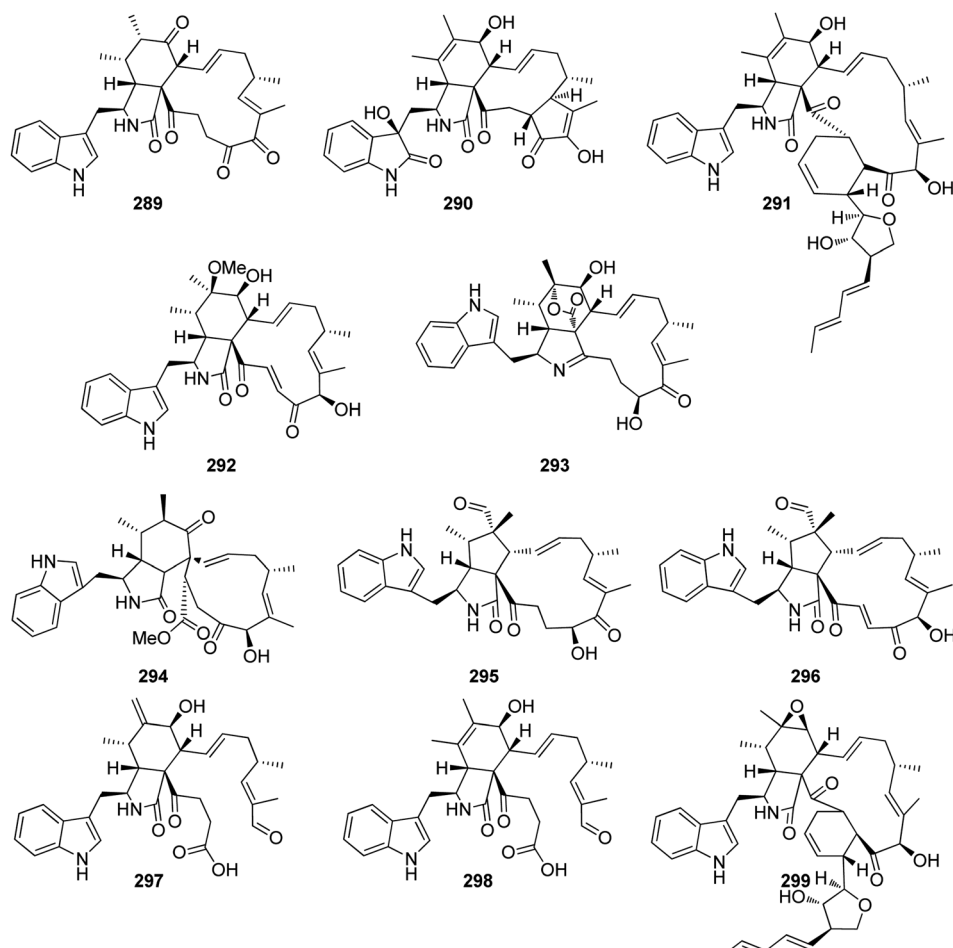


Fig. 31 Chemical structures of 289–299.



methyl-chaetoglobosin Q (292) (Fig. 31). Compounds **104**, **209**–**211**, **220**–**224**, **230**, **238**, **259**, and **291**, were tested for their cytotoxicity against U937, H1975, K562, MOLT-4, BGC823, MCF-7, HeLa, A549, Huh-7 and HL60 tumour cell lines. Compounds **104**, **209**, **211**, **221**–**224**, **230**, **238**, **259**, and **291**, were found inactive with IC_{50} values >10 μ M, but **210** displayed significant activity against all the examined cancer cells with IC_{50} values ranging from 1.4 to 9.2 μ M. Furthermore, **220** exhibited a selective cytotoxicity against MOLT-4, Huh7, U937, and MCF-7 cells, with IC_{50} values of ranging from 2.9 to 7.5 μ M, respectively. Moreover, **104**, **209**–**211**, **220**–**224**, **230**, **238**, **259**, and **291**, were found inactive when tested for their anti-tuberculosis activity.¹⁷⁸ Additionally, four previously unreported cytochalasans derivatives namely pchaeglobolactone A (293), spirochaeglobosin A (294), pchaeglobosals A–B (295–296) (Fig. 31), were reported from the endophytic derived fungus *C. globosum* P2-2-2, isolated from a *Ptychomitrion* plant, collected in China from Hubei Province. Compound **296** exhibited potent cytotoxicity against A549, HepG2, MCF-7, CT26, and HT29 with IC_{50} values ranging from 1.04 to 9.90 μ M, when compared to Doxorubicin hydrochloride (IC_{50} values ranging from 0.48 to 1.37 μ M) as positive control. Furthermore, it displayed apoptosis-inducing and cell cycle arrest activities in HT26 and

CT29 cells.¹⁷⁹ The aforementioned cytochalasan derivatives **210**, **222** and **252**, were recorded from the endophytic derived fungus *C. globosum* TY1, isolated from the medicinal plant *Ginkgo biloba* fresh bark. Compounds **210**, **222** and **252**, haven't been examined for any relevant biological activity.¹⁸⁰

Two previously unreported 19,20-seco-chaetoglobosins namely salchaetoglobosins A–B (297–298) (Fig. 31), along with the previously mentioned analogues **210**, **220**, and **230**, were reported from the plant derived fungus *C. globosum* D38. All the isolated compounds were examined for their cytotoxicity against HCT-116 and PC-3 cells. Only **297** exhibited a mild cytotoxicity against PC-3 tumour cells with IC_{50} value of 62.21 μ M. Additionally, the isolated compounds were examined for the anti-inflammatory activity. None of them was active.¹⁸¹ The previously mentioned cytochalasan derivatives **199**, **209**, **210**, **212**, **215**, **230**, **240**, **260** and II **261**, along with the previously undescribed aureochaeglobosin A (299) (Fig. 31), were documented from the plant derived fungus *C. globosum*, collected in China, Yunnan Province. All the isolated compounds were examined for their antibacterial activity against *B. subtilis*, *S. typhimurium*, and *S. aureus* and for their antifungal activity toward *Fusarium graminearum* and *Gibberella saubinetii*, using Vancomycin and Nystatin as positive controls respectively. All

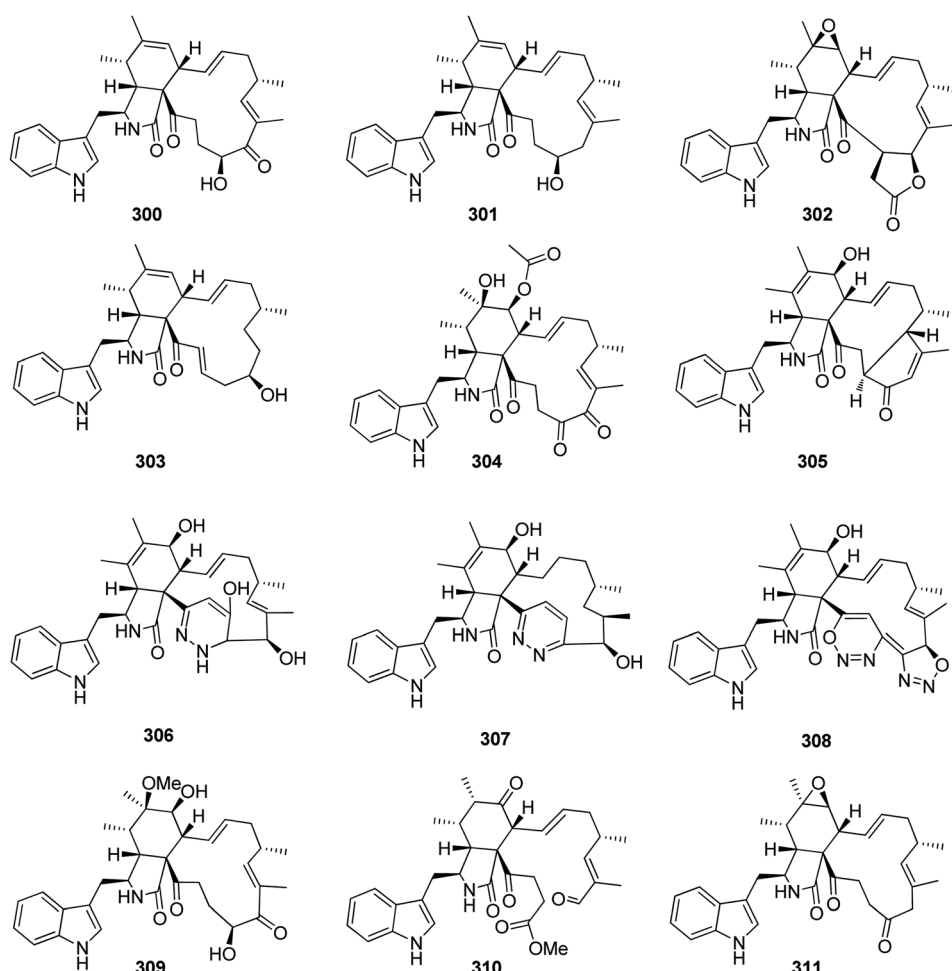


Fig. 32 Chemical structures of **300**–**311**.



the isolated compounds displayed weak to potent antimicrobial effect against all the examined microbial strains with MIC values ranging from 4 and 512 μM .¹⁸²

A chemical investigation of the mangrove derived fungus *C. globosum* kz-19, isolated from *Ceriops tagal* twigs, collected in China from Hainan Province, afforded the isolation of the previously mentioned cytochalasan analogues **104**, **209**, **210**, **220**, **221**, **223**, **224**, **225**, **227**, and **283**, along with the previously described armochaetoglobosin G (**300**) penochalasin J (**301**), together with four previously undescribed cytochalasans namely phychaetoglobins A-D (**302**-**305**) (Fig. 32). They were examined for their cytotoxicity against HeLa and A549 tumour cell lines using the MTT methods and Adriamycin (IC_{50} values of 0.8 and 2.9 μM , respectively), as positive control. Whilst phychaetoglobin A (**302**) was found inactive against HeLa cell line with IC_{50} value of >40 μM , all the other compounds displayed notable cytotoxicity with IC_{50} values ranging from 3.7

and 39.1 μM . Additionally, **302**-**303** were found inactive against A549 tumour cells with IC_{50} values of >40 μM , however all other compounds displayed weak to moderate cytotoxicity with IC_{50} values ranging from 7.3 and 32.3 μM .¹⁸³ A chemical inspection of the genetically engineered soil derived fungus *C. madrasense* **375**, isolated from a soil sample collected from the desert of Xinjiang Province, China, afforded the isolation of the previously mentioned derivatives **210**, **213**, **222** and **223**, along with three previously undescribed analogues namely chaetoglobosins B₁-B₃ (**306**-**308**) (Fig. 32). The isolated compounds were tested for their cytotoxicity against A549, HCC827, SW620, and MDA-MB-231 tumour cell lines. Compounds **307** and **308** were found inactive with IC_{50} values of >20 μM , however, **210** displayed potent cytotoxicity with IC_{50} values of 2.0, 1.7, 2.9, and 9.9 μM , respectively when compared to the positive control *Cis*-platin with IC_{50} values of 6.4, 4.5, 4.2 and 47.7 μM , respectively. Additionally, **210** showed strong cytotoxicity against two drug-

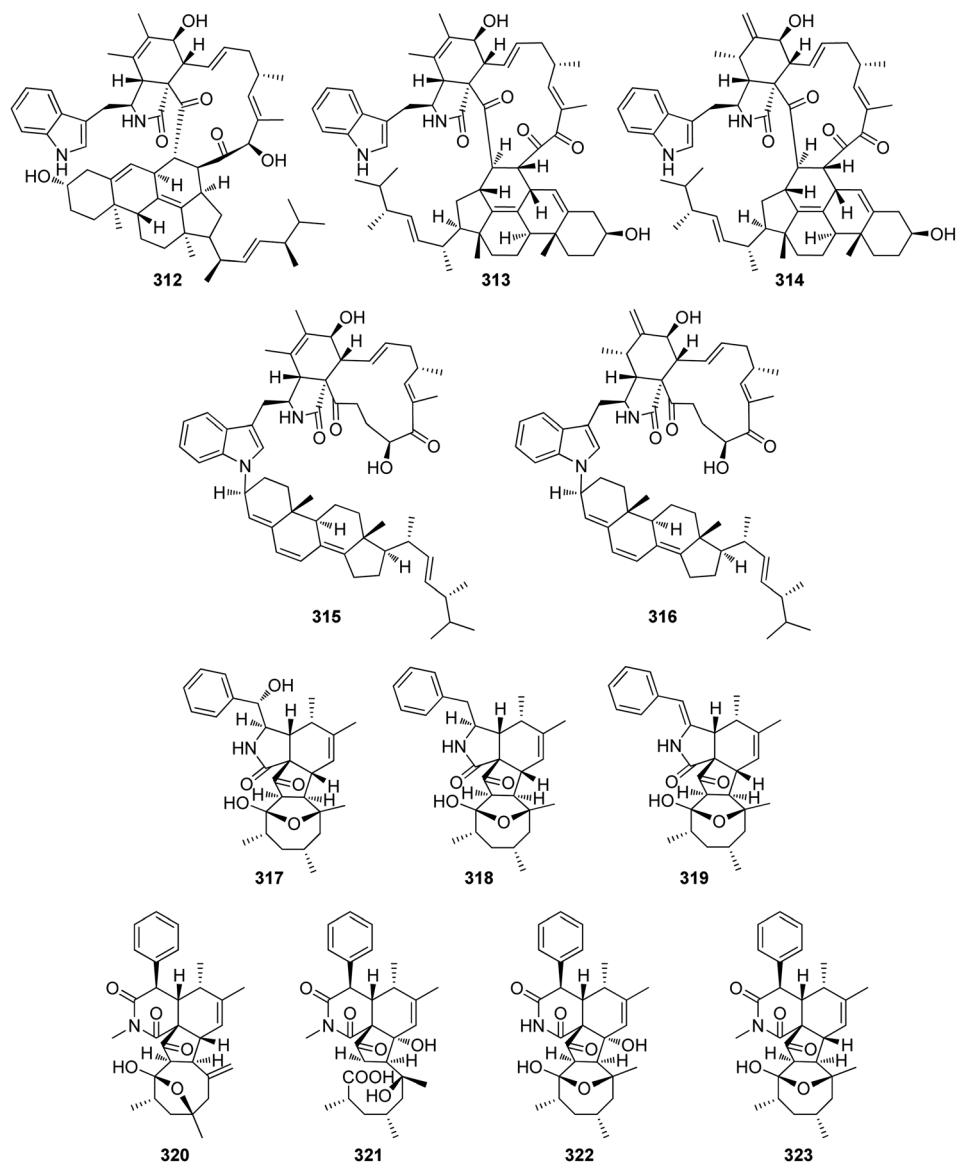


Fig. 33 Chemical structures of **312**–**323**.



resistant HCC827 cells (Osimertinib-resistant, Gefitinib-resistant) with IC_{50} values of 2.8 and 5.1 μM , respectively.¹⁸⁴ The chemical investigation of the plant derived fungus *C. tecifimetii* S104, isolated from *Rubia podantha* roots collected from Kunming Province China, led to the isolation of the previously mentioned analogues 210, 220–224, 230, 259, and 281 along with a previously unreported rubichaetoglobin A (309) (Fig. 32). They were tested for their cytotoxicity against MDA-MB-231, HCT116, and HepG2 using *Cis*-platin (IC_{50} values of 27.89, 10.31, and 12.75 μM , against the tested cells respectively), as positive control. Compounds 210 and 221 displayed mild cytotoxicity against MDA-MB-231 cell line with IC_{50} values of 10.27 and 11.43 μM , respectively. Additionally, none of them exhibited antibacterial activity against *S. aureus*, *B. subtilis*, and *E. faecalis*. Moreover, all the compounds showed no anti-

inflammatory activity.¹⁸⁵ Armochaetoglasins L (310) and M (311) (Fig. 32), two previously undescribed cytochalasans analogues were reported from the arthropod derived fungus *C. globosum*, isolated from *Armadillidium vulgare*, collected in China Hubei Province. Both compounds showed moderate inhibitory activity against NO production when compared to the positive control Indomethacin with IC_{50} values of 7.06, 9.97, and 3.15 $\mu\text{g mL}^{-1}$, respectively. Additionally, none of the obtained compounds displayed antibacterial effect against *K. pneumoniae*, *E. coli* and *S. aureus* with MIC values of $\geq 100 \mu\text{g mL}^{-1}$.¹⁸⁶

Five unusual heterodimers cytochalasan derivatives namely ergochaeglobosins A–E (312–316) (Fig. 33), were reported from the plant derived fungus *C. globosum* P2-2-2, isolated from *Ptychomitrium* plant, collected in China, from Hubei Province.

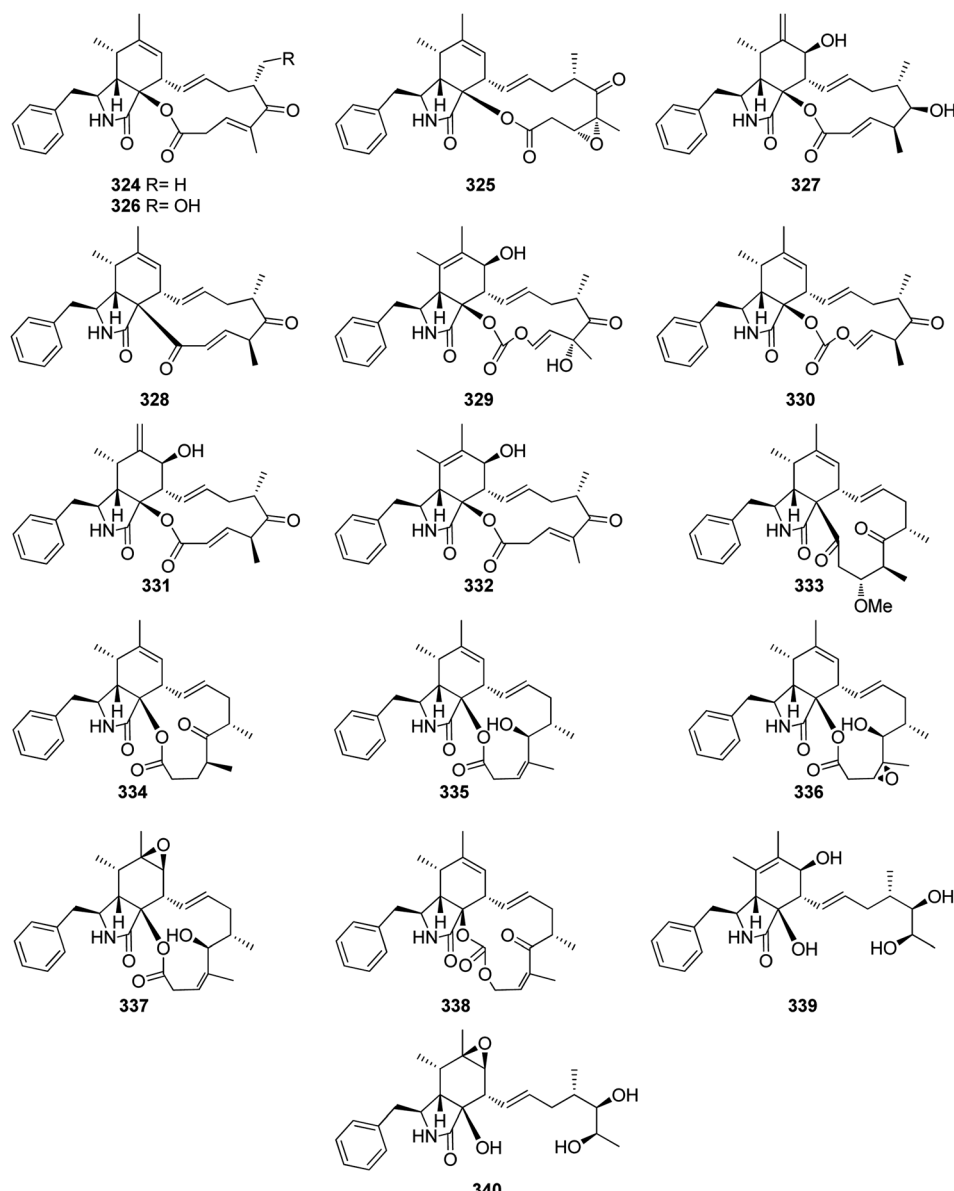


Fig. 34 Chemical structures of 324–340.



Whilst **312–316** displayed mild immunosuppressive effect towards LPS-induced B cells with IC_{50} ranging from 14.10 to 32.10 $\mu\text{mol L}^{-1}$ when compared to Mycophenolate mofetil (MMF, IC_{50} value 0.01 $\mu\text{mol L}^{-1}$), as positive control, only **312–314** showed an inhibitory activity against ConA-induced T cells, with IC_{50} ranging from 19.20 and 47.81 $\mu\text{mol L}^{-1}$ when compared to Cyclosporin A (CsA, IC_{50} value 0.01 $\mu\text{mol L}^{-1}$), as positive control. Furthermore, only **312** showed weak cytotoxic effect against CT26 tumour cell lines with IC_{50} value of 39.1 $\mu\text{mol L}^{-1}$, when compared to Doxorubicin hydrochloride (IC_{50} value 1.01 $\mu\text{mol L}^{-1}$), as positive control. Additionally, **314** displayed significant TRAIL-resistance-over-coming activity.¹⁸⁷ A chemical manipulation of the medicinal plant derived fungus *C. nigricolor* F5, isolated from *Mahonia fortunei* roots, afforded the isolation of five previously undescribed cytochalasans derivatives namely chamisides B–F (**317–321**) along with two previously reported analogues chaetoconvosins C–D (**322–323**) (Fig. 33). All the isolated compounds were found inactive when examine for their antibacterial and anticandidal abilities. Additionally, the crude extract, along with pure **317** and **321** were examine for their ability to inhibit *A. thaliana* root elongation. Only **317**, displayed a mild inhibition effect. Furthermore, all the isolated compounds as well as the previously mentioned analogue (**288**) were evaluated for their interaction with cholesterol transporter protein Niemann-Pick C1-like 1 (NPC1L1), using molecular docking calculations. Compound **321** showed the highest binding affinity to NPC1L1.⁵¹

3.5.3. Fungi of the subclass Xylariomycetidae

3.5.3.1. Fungi of the order Xylariales

3.5.3.1.1. Fungi of the family Apicomplexidae

genus *Arthrinium* (MycoBank ID 7214). A chemical investiga-

Genus Arthrinium (MycoBank ID 7214). A chemical investigation of the marine sponge *P. fusca*, derived fungus *Arthrinium arundinis* ZSDS1-F3, collected from the Island of Xisha (China) afforded the isolation of the previously mentioned analogue 68, along with five previously undescribed analogues namely

arthriniumnins A-D (324–327) and ketocytochalasin (328), together with the previously described cytochalasin K (329), Cytochalasin Z₁₆ (330), 10-phenyl-[12]-cytochalasin Z₁₆ (331), and cytotochalasin Z₁₇ (332) (Fig. 34). Compounds 68, 324, 325, and 327–332 were examined for their cytotoxicity against K562, A549, Huh-7, H1975, MCF-7, U937, BGC823, HL60, HeLa, and MOLT-4 cancer cell lines using CCK8 (DojinDo) and Trichostatin A as the positive controls. Whilst 68, 324, 325, 327, 328, 330, and 332, displayed no cytotoxicity against all the examined cells, 329 displayed weak cytotoxicity against K562, A549, Huh-7, H1975, HL60, HeLa, and MOLT-4 with IC₅₀ values ranging from 10.5 to 47.4 μ M, respectively.

Furthermore, 331 displayed a mild cytotoxic effect against all the examined cells except of Huh-7 cell, with IC_{50} values ranging from 1.1 and 18.8 μ M. Additionally, none of these compounds exhibited antituberculosis activity.¹⁸⁸

A chemical inspection of the plant derived fungus *A. arundinis* DJ-13, isolated from *Aconitum brevicalcaratum*, roots collected from the mountain of Dongjia, Yunnan Province (China), afforded the isolation of the previously mentioned analogues **68**, and **324–327**, along with six previously unreported analogues namely arundisins A–F (**333–338**), together with two previously described derivatives namely cytochalasin Z12 (**339**) and cytochalasin Z21 (**340**) (Fig. 34).

Compounds 333–336 and 338 were examined for their cytotoxic effects against HL-60, A549, SMMC-7721, MCF-7, and SW480 tumour cell lines using *Cis*-platin (IC_{50} values ranged from 2.256 to 23.96 μ M), and Taxol (IC_{50} values ranged from <0.008 to 0.196 μ M), as positive controls. Whilst 336 and 338, displayed no cytotoxicity against all the examined cells, the rest of compounds exhibited weak to potent cytotoxicity with IC_{50} values ranging from 9.59 to 30.31 μ M.

Additionally the antimicrobial activity of these compounds was evaluated against *E. coli* and *C. albicans* using Kanamycin (MIC 2.0 $\mu\text{g mL}^{-1}$), and Nystatin (MIC 1.0 $\mu\text{g mL}^{-1}$), as positive

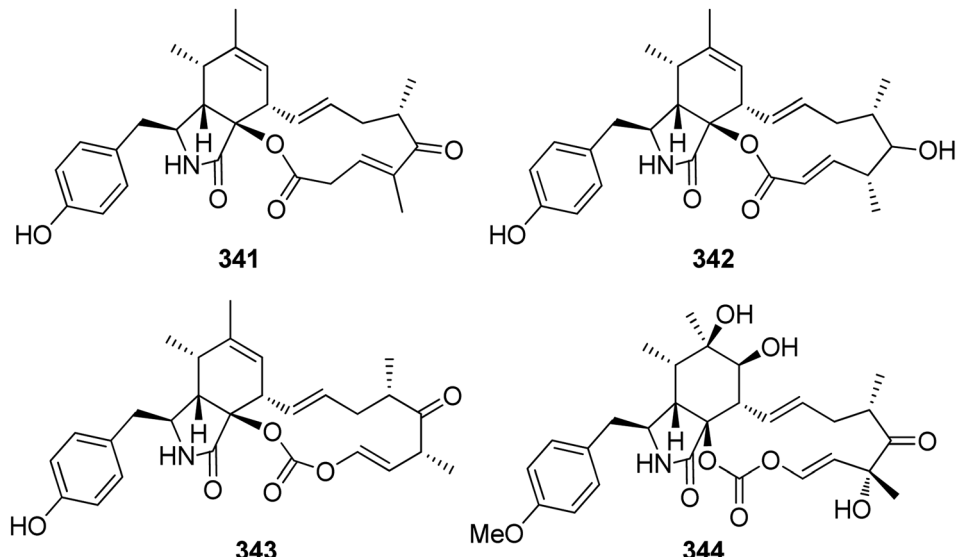


Fig. 35 Chemical structures of 341–344

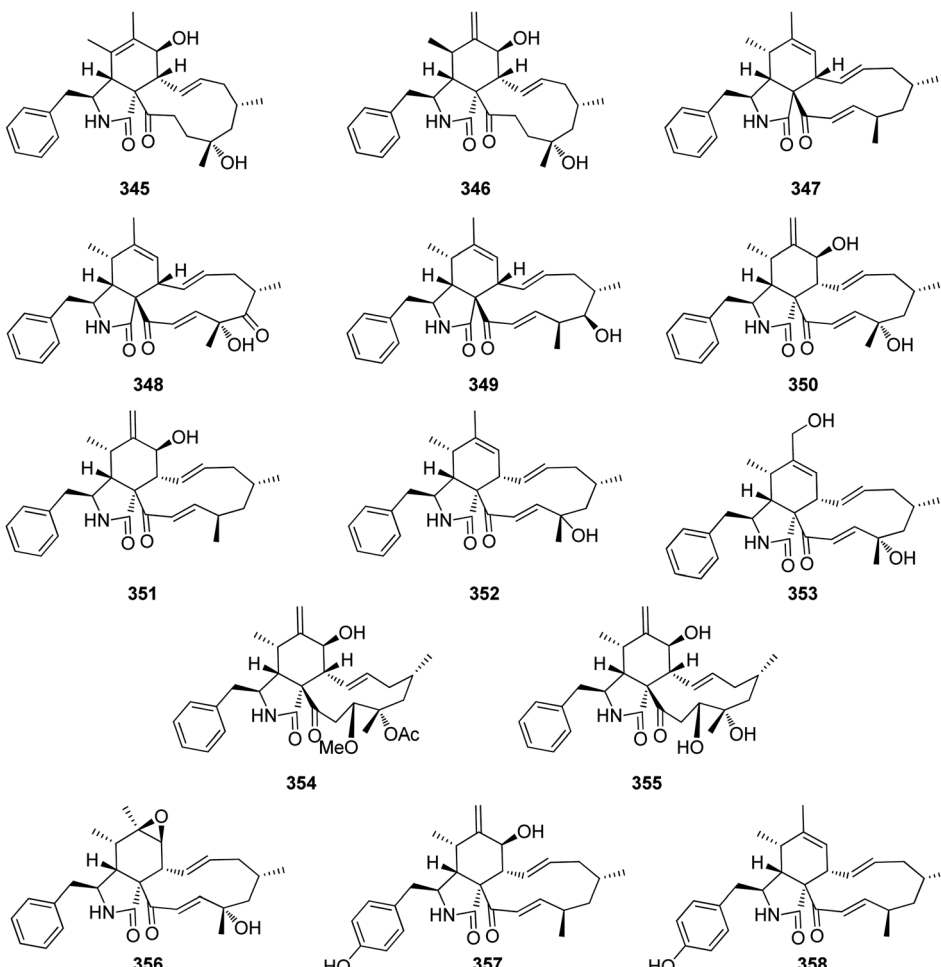


Fig. 36 Chemical structures of 345–358.

controls, respectively. Only, 336 and 338, displayed weak antimicrobial activity against *E. coli* and *C. albicans* with MIC values of 8 and 32 $\mu\text{g mL}^{-1}$, respectively.¹⁸⁹

3.5.3.1.2. Fungi of the family Diatrypaceae. **3.5.3.1.2.1. Genus *Eutypella* (MycoBank ID 1951).** Chemical investigation of the soil derived fungus *Eutypella* sp. D-1, isolated from the soil sample collected from the District of Alesund, Arctic, led to the isolation of three previously undescribed cytochalasans derivatives namely, cytochalasans Z24 (341), Z25 (342) and Z26 (343), along with the previously described analogue scoparasin B (344) (Fig. 35). When they tested for their cytotoxicity against U251, SW-1990, SG7901, MCF-7, Huh-7, HeLa, and H460 cells. Indeed, 343 was found inactive with IC_{50} value of $>100 \mu\text{M}$, 341 exhibited weak to mild cytotoxicity against the examined cells with IC_{50} values ranging from 9.33 and 73.21 μM , respectively. Regarding 342, it displayed weak selective cytotoxicity against SW-1990 and SG7901 cells with IC_{50} values of 50.1 and 50.87 μM respectively. For 344, it was found inactive only against H460 cells with IC_{50} value of 3.9 μM .^{190,191}

3.5.3.1.3. Fungi of the family Hypoxylaceae. **3.5.3.1.3.1. Genus *Daldinia* (MycoBank ID 1408).** Chemical inspection of

the EtOAc extract obtained from *Daldinia concentrica* fruit bodies, isolated from *Fraxinus excelsior* trunks collected in North Rhine Westphalia, Germany, in the Neandertal near Haan-Gruiten, resulted in the isolation of the previously mentioned analogue 110.¹⁹²

Chemical examination of the South China Sea derived fungus *D. eschscholtzii* HJ001, isolated from the mangrove *Brguiera sexangula* var.*rhynchopetala*, led to the isolation of one previously unreported cytochalasan analogue namely [11]-cytochalasa-5(6),13-diene-1,21-dione-7,18-dihydroxy-16,18-dimethyl-10-phenyl-(7S*,13E,16S*,18R*) (345), along with its previously reported analogue [11]-cytochalasa-6(12),13-diene-1,21-dione-7,18-dihydroxy-16,18-dimethyl-10-phenyl-(7S*,13E,16S*,18R*) (346), (Fig. 36). Both 345–346 were examined for their cytotoxic effects against HepG2, A549, and HeLa tumour cell lines using MTT method and Epirubicin as positive control, both compounds displayed no cytotoxicity towards the tested cell lines. Furthermore, both compounds were tested for their antibacterial effect against the pathogenic bacterial strains *B. cereus* (ATCC 11778), *E. coli* (ATCC 25922), *S. aureus* (ATCC 25923), Methicillin-resistant *S. aureus* MRSA (ATCC 33591), *V. alginolyticus* (ATCC 17749), and *V. parahaemolyticus* (ATCC

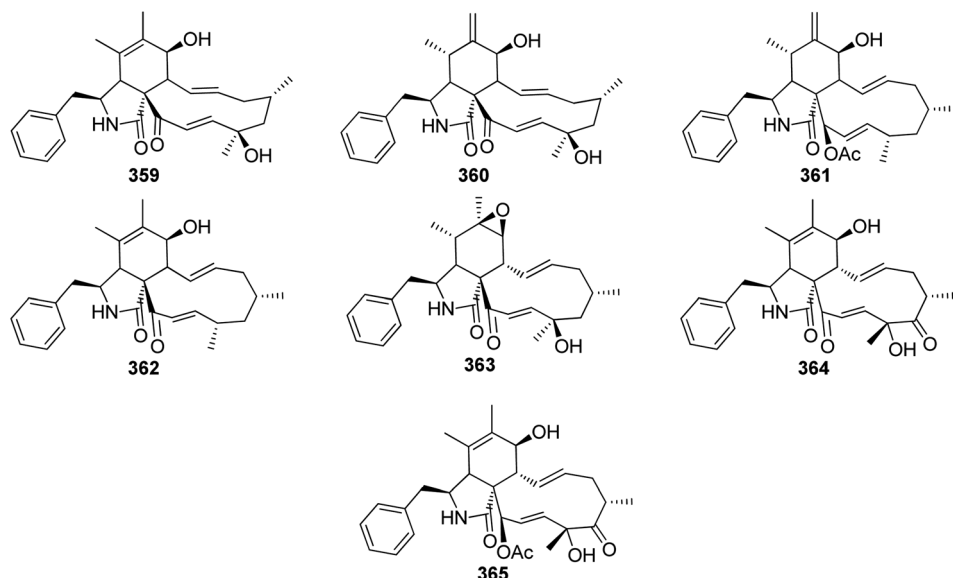


Fig. 37 Chemical structures of 359–365.

17802), using Ciprofloxacin as positive control, among them 345, displayed weak antibacterial effect against *B. cereus*, *E. coli*, *S. aureus*, *V. alginolyticus* and *V. parahaemolyticus* with MIC values of $50 \mu\text{g mL}^{-1}$.¹⁹³

Chemical investigation of the stomata of the sugarcane derived fungus *D. sacchari*, led to the isolation of two novel cytochalasans analogues namely saccalasins A (347) and B (348), along with the previously described (16S,17R,18S)-16,18-dimethyl-17-hydroxy-10-phenyl[11]cytochalasa-6,13,19-triene 1,21-dione (349) (Fig. 36), together with the previously mentioned analogue 328. Compounds 328, and 347–349, were tested for their antimicrobial effect against several bacterial and fungal strains. Whilst 347 was found to be inactive against all the examined microorganisms, the rest of the compounds displayed antimicrobial effect against *Mucor hiemalis* DSM2656 using Nystatin (MIC $16.66 \mu\text{g mL}^{-1}$) as positive control, *Bacillus subtilis* DSM10, *Staphylococcus aureus* DSM346 using Oxytetracycline (MIC values of 8.33 and $0.41 \mu\text{g mL}^{-1}$, respectively) as positive control, with MIC value ranged from 16.66 to $66.66 \mu\text{g mL}^{-1}$. Additionally, 328 and 349 displayed mild to potent antimicrobial ability against *Schizosaccharomyces pombe* DSM70572, when compared to Nystatin as positive control with MIC values of 33.33 , 16.66 and $16.66 \mu\text{g mL}^{-1}$, respectively.

Moreover, only 349 showed weak antibacterial effect against *Micrococcus luteus* DSM1790, when compared to the positive control Oxytetracycline with MIC values of 66.66 and $0.41 \mu\text{g mL}^{-1}$, respectively. Furthermore, the isolated compounds were tested for their cytotoxic effects towards A431, A549, KB3.1, L929, MCF-7, PC-3 and SKOV-3 tumour cell lines using the positive control Epothilon B (IC_{50} values of 0.0001 , 0.002 , 0.00006 , 0.0008 , 0.00004 , 0.0011 , and $0.00012 \mu\text{g mL}^{-1}$, respectively), where all the isolated compounds displayed moderate to strong cytotoxic effect against all the examined cells with IC_{50} values ranged from 0.14 to $6.1 \mu\text{g mL}^{-1}$.¹⁹⁴

The previously mentioned 349, along with four previously reported analogues (350–353) (Fig. 36), were isolated from the stomata of *D. eschscholtzii* BBH42278. The isolated compounds along with previously mentioned 347, were examined for their antibacterial effect against *Staphylococcus aureus*, as well as to check their ability to inhibit the biofilm formation. Despite they displayed weak antibacterial effect with MIC values of $>256 \mu\text{g mL}^{-1}$, 351 showed no effect against the biofilm formation, 347 and 349 showed mild effect toward the biofilm formation with 20–40% inhibition effect, and interestingly 350, 352 and 353, showed strong inhibition effect against the biofilm formation with potency effect of 70–90%.¹⁹⁵

Daldinin (354), a previously undescribed cytochalasin analogue, along with the previously described [11]-cytochalasa-6(12),13-diene-1,21-dione-7,18,19-trihydroxy-16,18-dimethyl-10-phenyl-(7S*,13E,16S*,18S*,19R*) (355) and the previously mentioned (346) (Fig. 36), were isolated from the organic extract of *D. concentrica* fruiting bodies, collected in Vietnam from the Pumat National Park of Nghe, compounds 346, 354 and 355, were tested for their cytotoxic effects against SK-LU-1, HepG2, Hep3B, SW480, and MCF7 cancer cell lines using Ellipticine (IC_{50} values of 0.4 , 0.4 , 0.4 , 0.5 , and $0.4 \mu\text{M}$, respectively) as positive control, all of them displayed weak to mild cytotoxic effect against the tested cells with IC_{50} values ranged from 11.4 to $58.2 \mu\text{M}$.¹⁹⁶

Kretz *et al.*,¹²⁴ 2019, examined the previously mentioned analogues 347, 349, and 350–353, along with (7S,13E,16S,18S,19E)16,18-dimethyl-6,7-epoxy-18-hydroxy-10-phenyl-[11]-cytochalasa-13,19-diene-1,21-dione (356), isolated from *D. eschscholtzii*, as well as phenochalasins C (357) and D (358) (Fig. 36), obtained from *D. kretzschmarioides*, which originally described as *Hypoxyylon kretzschmarioides*,¹⁹⁷ based on the taxonomic study by Wongkanoun *et al.*¹⁹⁷ While 352–353, and 356 showed the ability to disrupt the F-actin network incompletely at a concentration of $5 \mu\text{g mL}^{-1}$, 351 and 357 caused



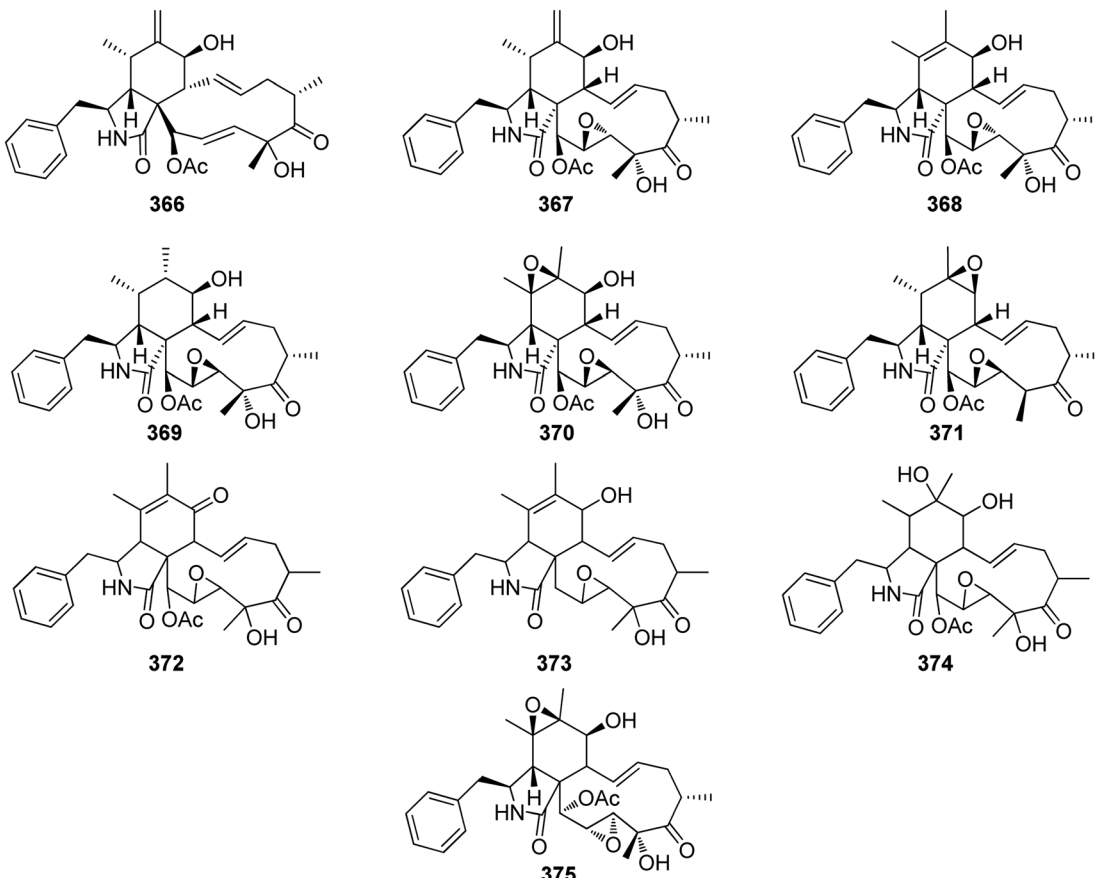


Fig. 38 Chemical structures of 366–375.

complete disruption at $5 \mu\text{g mL}^{-1}$, and 350 caused complete disruption at $1 \mu\text{g mL}^{-1}$.¹²⁴

3.5.3.1.3.2. Genus Hypoxylon (MycoBank ID 2456). Chemical investigation of the fungus *Hypoxylon fragiforme*, led to the isolation of the previously mentioned derivative 116, along with two previously undescribed analogues namely fragiformins A (359) and B (360) (Fig. 37). The discovered compounds along with the previously mentioned derivatives 2, 14, 110, 117, 199, 346, 350 and 355–365, were tested for their nematocidal effect against *Caenorhabditis elegans*. All compounds displayed anti-nematode effect with LD₅₀ and LD₉₀ of ranged from 10 to >100. Additionally, the above-mentioned compounds were examined for their antimicrobial effect against *B. subtilis*, *Y. lipolytica*, *M. hiemalis*, *P. griseofulvum*, *S. chartarum*, *T. atroviride*, and *T. harzianum* where all of them showed weak to potent effect with MIC values ranged from 1 to $50 \mu\text{g mL}^{-1}$.¹⁹⁸

The previously mentioned analogues 116, 359 and 360, were isolated from *H. howeanum*, where these compounds were evaluated for their antibacterial effect against *B. subtilis*, using Penicillin G (inhibition zone of 23 mm) as positive control, where they showed antibacterial effect with an inhibition zone of 15, 16 and 18 mm, respectively. Additionally, they were tested for their antifungal effect against *Y. lipolytica* using Actinomycin D (inhibition zone of 17 mm), as positive control where they showed effect with an inhibition zone of 18, 19 and 21 mm,

respectively; interestingly, all of them were found to be inactive when they were undergone for MIC evaluation against *B. subtilis*, *T. atroviride*, and *Y. lipolytica*. Furthermore, none of the obtained compounds showed nematocidal effect against *Caenorhabditis elegans*.¹⁹⁹

Chemical investigation of the fungus *H. fragiforme*, collected from Harz Mountains, led to the isolation of the previously mentioned analogues 116, and 123, along with the previously described L-696,474 (361), as well as the previously mentioned 357 and 358, that were isolated from *H. cf. kretzschmariooides* BBH42276. The isolated compounds were examined for their antibacterial effect against *Staphylococcus aureus*, as well as to check their ability to inhibit the biofilm formation, even though they displayed weak antibacterial effect with MIC values of >256 $\mu\text{g mL}^{-1}$, while compound 116 displayed no effect toward biofilm formation, the rest of the compounds displayed mild effect toward the biofilm formation with potency of 20–70%.¹⁹⁵ Fragiformins C (362) and D (363), (Fig. 37), along with the previously mentioned 346, were obtained through the chemical investigation of *H. fragiforme*, isolated from *Fagus sylvatica*. While 362 caused a partial reversible and incomplete actin disruption at $5 \mu\text{g mL}^{-1}$, 363 caused a complete irreversible disruption at $1 \mu\text{g mL}^{-1}$.¹²⁴ Chemical examination of *H. fuscum* complex, led to the isolation of pseudofuscochalasin A (364), a structurally related analogue to cytochalasin C (365) (Fig. 37).



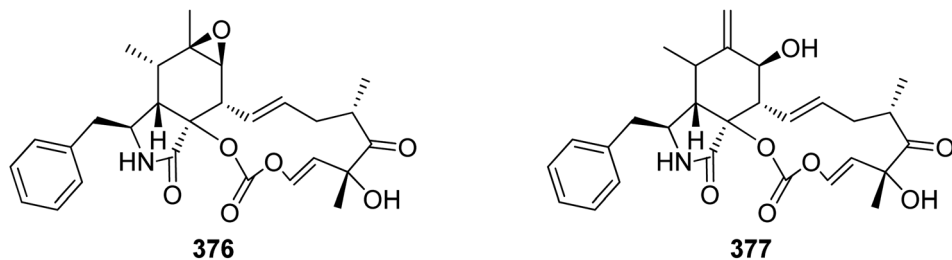


Fig. 39 Chemical structures of 376–377.

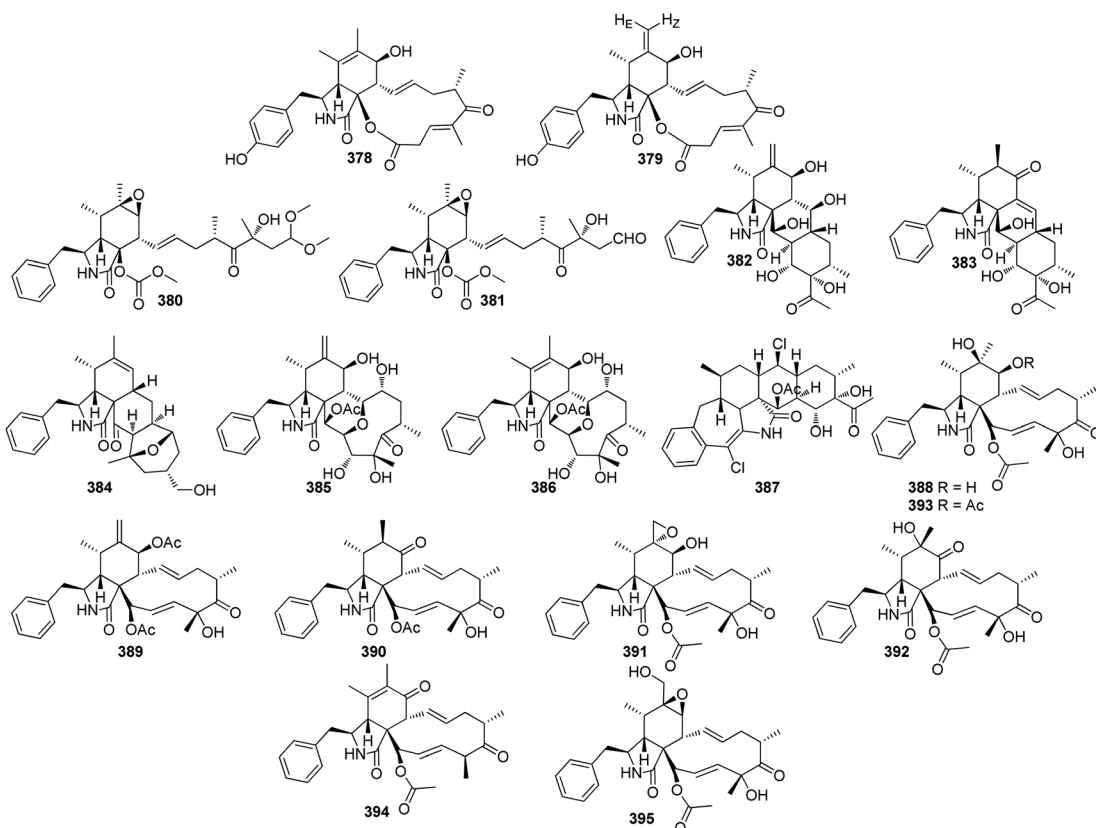


Fig. 40 Chemical structures of 378–395.

Compound **364**, when compared to cytochalasin C (**365**) in an actin disruption assay using fluorescence microscopy of human osteosarcoma U2OS cells, demonstrated comparable activity towards F-actin, but its effect was irreversible, in contrast to cytochalasin C (**365**).²⁰⁰

3.5.3.1.4. *Fungi of the family Xylariaceae.* 3.5.3.1.4.1. *Genus Rosellinia (MycoBank ID 4785).* The previously mentioned analogue 365, along with three previously reported analogues namely cytochalasin D (366), 19,20-epoxycytochalasin D (367), and 19,20-epoxycytochalasin C (368), together with the previously unreported jammosporin A (369) (Fig. 38), were isolated from the medicinal plant derived fungus *Rosellinia sanctae-cruciana*, isolated from *Albizia lebbeck* leaves, collected in India, Jammu. All the compounds as well as the crude extract were examined for their cytotoxicity against MOLT-4, A549, MIAPaCa-

2, and MDAMB-231 cancer cell lines, all of them displayed selective cytotoxicity against MOLT-4 tumour cell line with IC_{50} values of 6, 25, 10, 8, and 20 $\mu\text{mol L}^{-1}$, respectively and 10 $\mu\text{g mL}^{-1}$ for the crude extract, when compared to Flavopiridol (0.5 $\mu\text{mol L}^{-1}$).²⁰¹

The previously mentioned cytochalasin analogues **367** and **368**, along with two previously reported derivatives namely 19,20-epoxycytochalasin N (**370**) and 18-deoxy-19,20-epoxycytochalasin Q (**371**) (Fig. 38) were isolated from the culture of *R. rickii*. Compounds **367**–**368** and **370**–**371** were examined for their antibacterial effect against *Staphylococcus aureus*, as well as to check their ability to inhibit the biofilm formation. All of them displayed weak antibacterial effect with MIC values of $>256 \mu\text{g mL}^{-1}$, and only **368**, showed a mild effect toward the biofilm formation with potency of 40–70%.¹⁹⁵

Through semipreparative HPLC, seven cytochalasans were isolated from the crude extract of *R. sanctae-cruciana*, including the previously mentioned 365, 366, 367, and 368 along with other three analogues *i.e.*, oxidized 19,20-epoxycytochalasin C (372), deacetyl 19,20-epoxycytochalasin C (373), and cytochalasin P1 (374) (Fig. 38). The isolated compounds were examined for their antitumour activity against FR-2, A549, PC3, HCT-116, MCF-7, HT-29, and SW-620 tumour cell lines, where all of them showed cytotoxicity against the different tested cells with IC_{50} values ranged from 0.658 to >100 μ M, respectively.

Additionally, 368, were tested *in vivo* against colon induced cancer, where it was found to be an effective agent with IC_{50} value of 866 nM, when compared to Flavopiridol (IC_{50} ; 290 nM), as positive control.²⁰² Further examination of the same fungus by the same group led to the successful isolation of the previously undescribed optical isomer of compound 370, namely 19,20-epoxycytochalasin N1 (375) (Fig. 38). Compound 375 displayed weak to potent cytotoxicity against FR-2, A549, PC3, HCT-116, MCF-7, HT-29, and SW-620 tumour cell lines with IC_{50}

values ranged from 1.34 to 36.85 μ M, when compared to Paclitaxel ($IC_{50} < 0.01$ –0.140 μ M) and 5-Fluorouracil (IC_{50} 14.76–82.49 μ M) as positive controls.²⁰³

3.5.3.1.4.2. Genus *Dematophora* (*Mycobank ID 216282*).

Chemical examination of *Dematophora necatrix* (MUCL 57709), led to the isolation of cytochalasin E (376) and its related analogue $\Delta^{6,12}$ -cytochalasin E (377) (Fig. 39), along with their previously mentioned analogue 329. Compounds 329 and 376–377 were examined for their antimicrobial effect against a wide panel of microorganisms, among them only compound 376, showed an inhibition effect against *Saccharomyces pombe*, with MIC value of 16.8 μ M. Additionally, the obtained compounds were tested for their cytotoxic effects towards L929, KB3.1, PC-3, MCF-7, SKOV-3, A431 and A549, where all of them displayed moderate effect against all the examined cells, with IC_{50} values ranged from 0.026 and 14.5 μ M. Furthermore, they were examined for their F-actin network disruptors, where compound 376 and 377 caused collapse of the F-actin network, totally at a concentration of >0.3 μ g mL^{-1} , while compound 329,

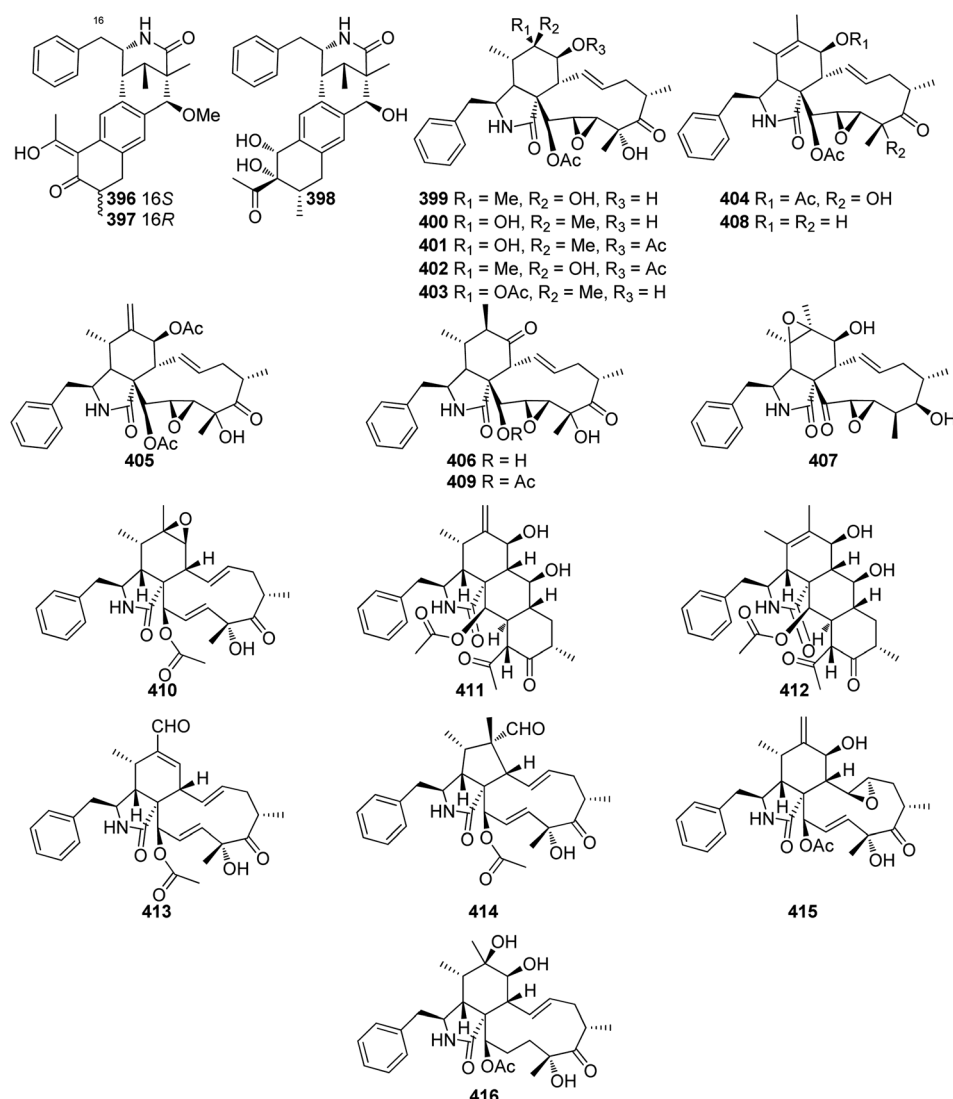


Fig. 41 Chemical structures of 396–416.



showed its effect only at a higher concentration of $10 \mu\text{g mL}^{-1}$.²⁰⁴

3.5.3.1.4.3. Genus Xylaria (MycoBank ID 5832). Cytochalasans Z₂₇ (378), and Z₂₈ (379), two previously undescribed analogues along with two previously reported analogues namely cytochalasin Z₁₈ (380), and seco-cytochalasin E (381) (Fig. 40), together with the previously mentioned analogue 376, were isolated from the EtOAc extract of endophytic fungus *Xylaria* sp. XC16 isolated from *Toona sinensis* healthy leaves, collected in China from Shaanxi Province. All the obtained compounds were tested for their toxicity against the brine shrimp, where all compounds displayed very weak toxic effect with lethality below 10%. Apart from 376, it showed strong toxic effect with lethality of 100%, at a concentration of $50 \mu\text{M}$, in a concentration dependent manner when compared to Toosendanin as positive control.

Additionally, the abovementioned compounds were examined for their phytotoxicity towards *Lactuca sativa* and *Raphanus sativus*, seedling growth. While 378–381, were inactive at a concentration of $100 \mu\text{M}$, 376, showed strong phytotoxicity even was higher than that of the positive control Glyphosate. Furthermore, they were examined for their activity against four different pathogens, including *Gibberella saubinetti*, *Fusarium solani*, *Alternaria solani* and *Botrytis cinerea*, where they showed weak to mild effect with MIC values ranged from 12.5 to $>100 \mu\text{M}$, when compared to Carbendazim (MIC 3.13–6.25 μM) and Hymexazol (MIC 12.5–50 μM), as positive controls.²⁰⁵

Curtachalasins A–B (382–383) (Fig. 40), two previously undescribed cytochalasans, possessing an unusual pyrrolidine/perhydroanthracene tetracyclic ring system, were reported from the potato derived fungus *X. curta* E10, isolated from the stem tissues collected in China, Dali Province. Both compounds displayed weak antifungal activity against *Microsporum gypseum*, with inhibition percentage of 70.3 and 68.4%, respectively.²⁰⁶

A chemical examination of the plant derived fungus *X. striata*, isolated from *Sophora japonica* trunk base, collected from Sichuan Province, (China) afforded the isolation of a previously unreported xylastriasan A (384) (Fig. 40), a cytochalasin featuring an unusual pentacyclic ring system. Compound 384 displayed weak cytotoxicity against HEPG2, A549, and B16 cells with IC₅₀ values of 93.61, 91.58 and 85.61 μM , respectively when compared to Paclitaxel as positive control.²⁰⁷ Two previously undescribed cytochalasan derivatives namely, cytochalasans D1 (385) and C1 (386) (Fig. 40), were reported from the potato derived fungus *X. cf. curta*, isolated from *Solanum tuberosum* stem tissue. Both 385–386 displayed mild cytotoxicity against HL-60 cancer cells with IC₅₀ values of 12.7 and 22.3 μM , respectively. Additionally, only 385 showed a weak cytotoxicity against SMMC-7721 with IC₅₀ value of 37.2 μM ,²⁰⁸ when compared to *Cis*-platin (IC₅₀ values of 4.86 and 25.61 μM , respectively) as positive control.

Further examination of the same fungal strain by the same group, afforded isolation of a previously unreported halogenated hexacyclic cytochalasan, namely xylarichalasin A (387) (Fig. 40). It showed moderate to potent cytotoxicity against HL-60, A549, SMMC-7721, MCF-7, and SW480 cells with IC₅₀ values of 17.3, 11.8, 8.6, 6.3 and 13.2 μM , respectively,²⁰⁹ when compared to *Cis*-platin (IC₅₀ values of 2.0, 13.2, 12.7, 23.3 and 18.0 μM , respectively) as positive control. The previously mentioned analogues 181, 182, 365, and 366 along with the previously described cytochalasans P (388), 7-O-acetylcyclotrichalasin D (389), and cytochalasin C (390), together with five previously undescribed analogues namely 6,12-epoxy-cytochalasin D (391), 6-*epi*-cytochalasin P (392), 7-O-acetylcyclotrichalasin P (393), 7-oxo-cytochalasin C (394) and 12-hydroxycytochalasin Q (395) (Fig. 40), were reported from mountain derived fungus *X. longipes*, isolated from a sample collected from the mountain of Ailao, China. The abovementioned compounds were examined for their cytotoxicity

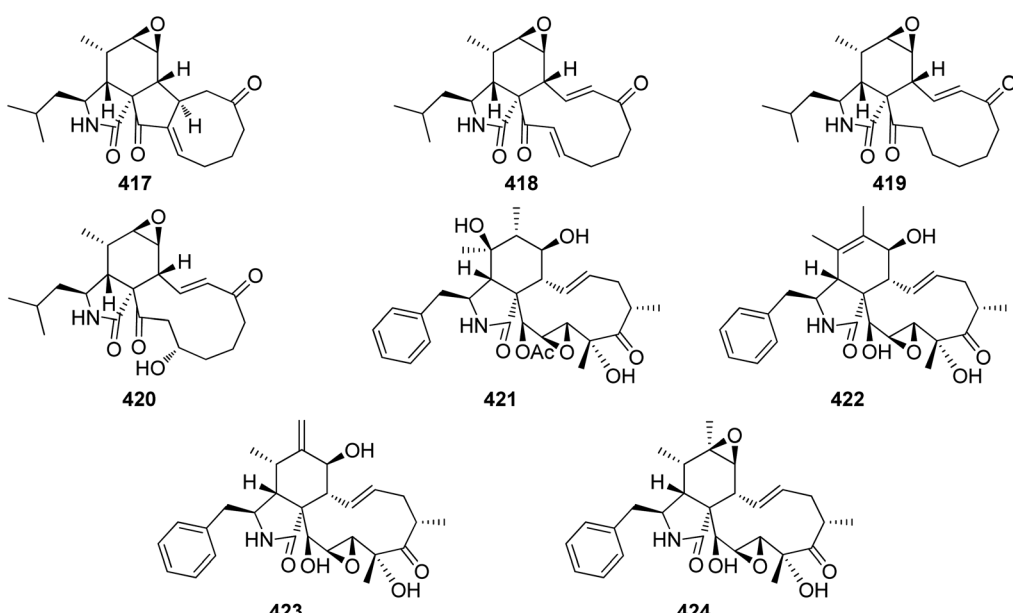


Fig. 42 Chemical structures of 417–424.



against HL-60, A549 SMMC-7721, MCF-7, and SW480 cells (IC_{50} values of 4.86, 25.61, 21.13, 23.59 and 27.7 μM , respectively) using *Cis*-platin as positive control. Potentially, **181**, **182**, **366**, **388** and **390** displayed selective cytotoxicity with IC_{50} values 4.17–37.18 μM .²¹⁰

A chemical inspection of the plant derived fungus *X. cf. curta* E10, isolated from *Solanum tuberosum* stem tissues, collected from Yunnan Province (China), afforded the isolation of three previously undescribed cytochalasan analogue, featuring an unusual bridged 6/6/6 ring fused system, namely curtachalasins C–E (**396**–**398**) (Fig. 41). Compounds **396** and **398**, were examined for their antifungal effect against fluconazole-resistant *C. albicans*, whereas **396** displayed significant improvement when compared to Fluconazole as positive control. On the contrary, **398** exhibited weak antifungal effect.²¹¹ Chemical inspection of the potato derived fungus *X. cf. curta*, isolated from *Solanum tuberosum* steam tissue, resulted in the isolation of nine previously undescribed cytochalasans namely 19-*epi*-cytochalasin P1 (**399**), 6-*epi*-19,20-epoxycytochalasin P (**400**), 7-O-acetyl-6-*epi*-19,20-epoxycytochalasin P (**401**), 7-O-acetyl 19-*epi*-cytochalasin P1 (**402**), 6-O-acetyl-6-*epi*-19,20-epoxycytochalasin P (**403**), 7-O-acetyl-19,20-epoxycytochalasin C (**404**), 7-O-acetyl 19,20-epoxycytochalasin C (exomethylene analogue) (**405**), deacetyl-5,6-dihydro-7-oxo-19,20-epoxycytochalasin C (**406**), and 18-deoxy-21-oxo-deacetyl-19,20-epoxycytochalasin N (**407**) along with two previously described analogues namely 18-desoxy-19,20 epoxycytochalasin C (**408**) and 5,6-dihydro-7-oxo-19,20-epoxycytochalasin C (**409**), (Fig. 41) together with the previously mentioned derivatives **367** and **368**. All the above-mentioned compounds were tested for their cytotoxicity against five cancer cell lines HL-60, A549, SMM-7721 MCF-7 and SW480 using (IC_{50} values of 4.86, 25.61, 21.13, 23.59, and 27.70 μM , respectively) *Cis*-platin as positive control. Among them, **368**, **399**, **401**, **405**, and **409** displayed cytotoxic effect against HL-60 tumour cells with IC_{50} values of 1.11, 13.31, 37.16, 25.83, and 10.04 μM , respectively. Additionally, **401** and **405** showed weak cytotoxicity towards MCF-7 cell lines with IC_{50} values of 26.64, and 34.03 μM , respectively.²¹² da Silva *et al.*, examined the crude extract of the endophytic fungus *Xylaria* sp, isolated from *Turnera ulmifolia* flowers collected Manaus, Brazil, that resulted in the isolation of the previously described cytochalasin Q (**410**) (Fig. 41), along with the previously mentioned analogues **2**, **252**, and **367**.²¹³ Four previously unreported cytochalasans namely arbuschalasins A–D (**411**–**414**), along with the previously 13,14-epoxid-cytochalasin D (**415**), and cytochalasin O (**416**), and (Fig. 41), together with the previously mentioned **181**, **182**, **183**, **355**, **365**, **366**, **367**, **368**, **388**, **390**, **395**, were reported from the mangrove derived fungus *X. arbuscula* GZS74, isolated from *Bruguiera gymnorhiza* fruits, collected from Guangzhou Province, China. All the isolated compounds were examined for their cytotoxicity against HCT-15 cells. Whilst **411**–**414**, displayed weak cytotoxic effect with 50% inhibition rate at concentration of 100 μM , **181**, **183**, **365**–**368**, **388**, **390**, **410** and **415**–**416**, displayed moderate cytotoxicity with IC_{50} values ranging from 50 and 100 μM . Moreover, **182** and **395**, exhibited potent cytotoxicity with IC_{50} values of 13.5 and 13.4 μM ,

respectively when compared with the positive control 5-Fluorouracil (IC_{50} 103.1 μM).²¹⁴

A chemical investigation of the plant derived fungus *Xylaria* sp. WH2D4, isolated from *Palicourea elata* leaves collected in Costa Rica, afforded the isolation of four previously undescribed cytochalasans analogues namely lagambasines A–D (**417**–**420**) (Fig. 42). It is worth noting that **418**–**419** were obtained as an inseparable mixture. None of them exhibited antifungal ability against *Trichoderma longibrachiatum* UAMH 7956 and *T. reesei* QM6a, when compared to Hygromycin B as positive control.²¹⁵

The previously undescribed karyochalasin (**421**), along with three previously reported analogues namely deacetyl 19,20-epoxycytochalasin C (**422**), engleromycin (**423**), and 19,20-epoxycytochalasin Q (**424**) (Fig. 42), together with the previously mentioned derivatives **367**, **368**, **370**, **374**, **400** and **409**, were isolated from the culture of *X. karyophthora* NRRL 66613. These compounds were tested for their antimicrobial ability against a several microorganisms, among them only compounds **367**–**368** displayed weak effect towards *S. pombe* (MIC values of 127 and 64 μM , respectively), while **367** showed weak effect against *B. subtilis* (MIC value of 127 μM) and **368** showed weak effect against *C. albicans* (MIC value of 127 μM).²¹⁶

Additionally, the authors studied and evaluated the ability of these compounds to inhibit biofilm formation and disperse preformed biofilms produced by *S. aureus* and *C. albicans*. Compounds **367**–**368**, **409**, and **424** were effective in inhibiting and dispersing biofilms of both organisms at varying concentrations, with no lethal effects observed, as their concentrations were below the toxicity levels determined in the MIC assay. Compound **421** showed activity only in dispersing preformed biofilms of *C. albicans*, while **400** was inactive in both biofilm inhibition and dispersal. None of the compounds exhibited significant activity against *P. aeruginosa* biofilms.²¹⁶

Furthermore, the authors evaluated the cytotoxic effects of all compounds against a panel of murine (fibroblast) and human cancer cell lines. The bioactivity showed variability, with **370**, **374**, **400**, and **421** displaying no or weak cytotoxicity against L929 fibroblasts ($>25 \mu\text{M}$). Cytotoxicity against other human cell lines was weak (2, 20.3 μM against KB3.1 cells) or moderately reduced compared to other cytochalasans (1 and 3 vs. 5 and 10, 3.5 and 3.4 μM vs. 0.1 and 0.5 μM against KB3.1 cells). Interestingly, **367**–**368** and **422**–**424** exhibited the strongest overall cytotoxicity.²¹⁶

Moreover, these compounds showed induced changes to the F-actin network, with the severity of these changes correlating with their cytotoxicity in the MTT assay (except for **370** and **421**). At low doses, **367**–**368**, **409**, and **424** caused the loss of lamellipodia and the formation of F-actin-rich aggregates in the cell body. High-dose treatments led to complete collapse of the F-actin network, characterized by the reduction of stress fibers, retraction of the cell periphery, and the formation of knot-like aggregates resembling a tree root network. Indeed, cytochalasans **400**, **409**, and **421** had less pronounced effects, even at high doses, with **400** and **421** showing no visible difference compared to the DMSO control. In contrast, **367** exhibited a high-dose-like effect even at low doses. Compound **423** showed a stronger



impact on F-actin organization than **368**, **370**, **409**, **422**, and **424**, even at lower concentrations, causing the loss of visible stress fibers and F-actin aggregation. Finally, recovery experiments demonstrated that all compounds tested **367–368**, **370**, **409** and **422–424** fully reversed the F-actin network disruption after high-dose treatment for 1 hour, with a recovery time of 1 hour.²¹⁶

4. Pharmacokinetics and ADMET of cytochalasans derived from fungi

Overall, a list of **424** cytochalasans were characterized from **27** fungal genera. These include ten major genera, namely *Arthrinium*, *Aspergillus*, *Chaetomium*, *Daldinia*, *Endothia*, *Metarhizium*, *Phoma*, *Phomopsis*, *Trichoderma*, and *Xylaria*. In addition to these ten genera, another class called “Others” was created,

comprising the remaining **17** minority genera, namely *Boeremia*, *Botryotinia*, *Calonectria*, *Cytospora*, *Dematophora*, *Eutypella*, *Hypoxylon*, *Penicillium*, *Perenniporia*, *Periconia*, *Pyrenophora*, *Rosellinia*, *Sparticola*, *Spicaria*, *Stachybotrys*, *Talaromyces*, and *Westerdykella*. The identified fungal-derived cytochalasans had comprised diverse biological and pharmacological properties including anticancer, antiviral, antimicrobial, antioxidant, and anti-inflammatory activity. However, the biological activity of approximately **17%** of reported cytochalasan derivatives has not been assessed. To assess the pharmacokinetics and ADMET (absorption, distribution, metabolism, excretion, and toxicity) properties of these **424** cytochalasans, two free online tools were used, SwissADME (<http://www.swissadme.ch/>) and pkCSM (<https://biosig.lab.uq.edu.au/pkcs/>).^{217,218} Of these **424** cytochalasans, it was only possible to predict these properties for **410** cytochalasan derivatives, the remaining **14** derivatives gave errors in both tools (Table

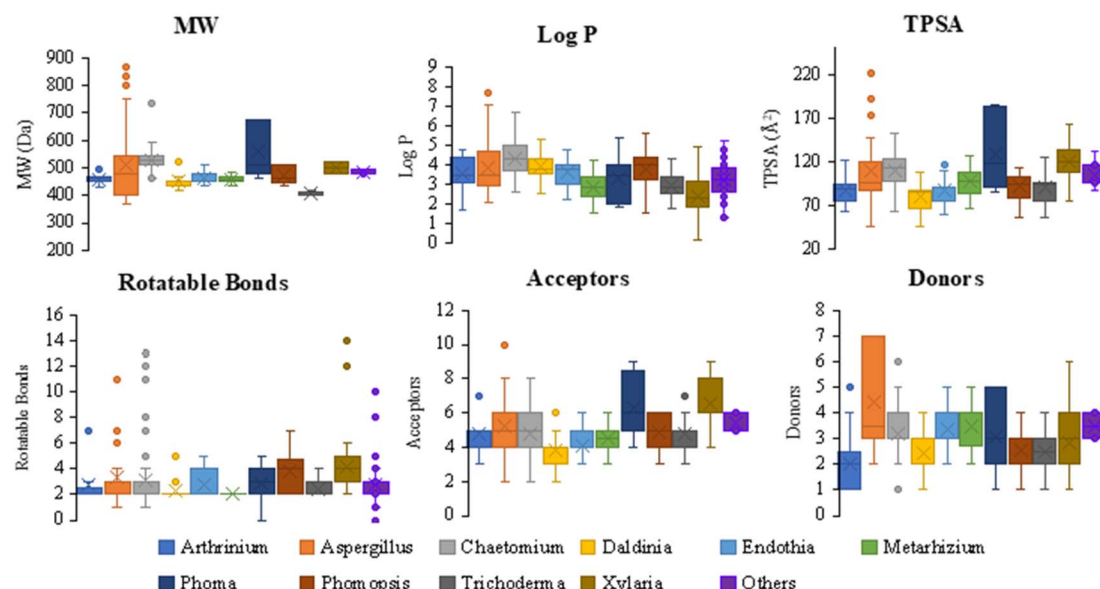


Fig. 43 Distribution of molecular weight (MW), octanol–water partition coefficient (log P), number of rotatable bonds, topological polar surface area (TPSA), number of acceptor groups (acceptors), and number of donor groups (donors) by fungal genera, *Arthrinium*, *Aspergillus*, *Chaetomium*, *Daldinia*, *Endothia*, *Metarhizium*, *Phoma*, *Phomopsis*, *Trichoderma*, *Xylaria*, and Others.

	Lipinski #violations	Ghose #violations	Veber #violations	Egan #violations	Muegge #violations
<i>Arthrinium</i>	0.00	1.00	0.00	0.00	0.06
<i>Aspergillus</i>	0.41	1.63	0.27	0.24	0.51
<i>Chaetomium</i>	0.91	2.95	0.14	0.14	0.11
<i>Daldinia</i>	0.29	1.21	0.00	0.00	0.29
<i>Endothia</i>	0.04	1.56	0.00	0.00	0.00
<i>Metarhizium</i>	0.00	1.50	0.00	0.00	0.00
<i>Phoma</i>	0.77	2.46	0.31	0.31	0.77
<i>Phomopsis</i>	0.30	2.00	0.00	0.00	0.10
<i>Trichoderma</i>	0.00	0.00	0.00	0.00	0.00
<i>Xylaria</i>	0.65	2.41	0.22	0.27	0.12
Others	0.27	1.56	0.06	0.10	0.04

Fig. 44 Heatmap of the compliance with five rules of drug-likeness, Lipinski, Ghose, Veber, Egan, and Muegg by fungal genera, *Arthrinium*, *Aspergillus*, *Chaetomium*, *Daldinia*, *Endothia*, *Metarhizium*, *Phoma*, *Phomopsis*, *Trichoderma*, *Xylaria*, and Others.

S1 in the ESI[†]). Here, we intended to highlight their potential as drug candidates by exploiting their drug-likeness using several molecular descriptors, including five drug-likeness rules such as Muegge, Ghose, Veber, Egan, and Lipinski (Fig. 43, 44 and Table S1[†]). Its pharmacokinetic properties and ADMET will also be explored with greater focus on predicting its toxicity (Table S1[†]). Its pharmacokinetic properties and ADMET will also be explored with greater focus on predicting its toxicity (Table S1[†]). There were 69 cytochalasans that satisfied all the parameters of the five tested drug-likeness rules (2, 17, 1, 4, 14, 4, and 27 cytochalasans from *Arthrinium*, *Aspergillus*, *Endothia*, *Phomopsis*, *Trichoderma*, *Xylaria*, and Others, respectively). On the other hand, there were 22 cytochalasans that violated the five tested drug-likeness rules (2–4 and 6–7 cytochalasans from *Aspergillus*, *Chaetomium*, *Phoma*, *Xylaria*, and Others, respectively), see (Fig. 43 and 44). In each of the five tested drug-likeness rules, ranges were established for each of the physicochemical properties established in each of the drug-likeness rules, for example topological polar surface area (TPSA) which is the sum of the surfaces of all the polar atoms present in a molecule, appears in three of the five tested drug-likeness rules namely Muegge, Veber and Egan. TPSA appears to be related to the potential of a compound to penetrate cell membranes and the blood–brain barrier. Egan, Veber and Muegge rules highlighted that those compounds with TPSA less than or equal to 130 Å², 140 Å² and 150 Å², respectively, tend to be well absorbed and able to reach their molecular target within cells. All cytochalasans from *Arthrinium*, *Daldinia*, *Endothia*, *Metarhizium*, *Phomopsis* and *Trichoderma* complied the Egan, Veber and Muegge drug-likeness rules in terms of TPSA and therefore had TPSA less than or equal to 130 Å² (Fig. 43).

Conversely, 12%, 31% and 10% of cytochalasans derived from *Aspergillus*, *Phoma* and *Xylaria*, respectively, fail to satisfy the Egan, Veber and Muegge drug-likeness rules with respect to TPSA (Fig. 43). Octanol–water partition coefficient ($\log P$), another measure, is related to the drug lipophilicity, which is a key property for solubility, absorption, membrane penetration, plasma protein binding, distribution, and tissue penetration. $\log P$ appears in four of the five tested drug-likeness rules namely Muegge, Ghose, Egan and Lipinski. All cytochalasans from *Arthrinium*, *Endothia*, *Metarhizium*, *Trichoderma*, and *Xylaria* complied with the Muegge, Ghose, Egan and Lipinski drug-likeness rules in terms of $\log P$, which is not greater than 5 (Fig. 43). Some cytochalasan derivatives from *Aspergillus*, *Chaetomium*, *Daldinia*, *Phoma*, *Phomopsis* and Others do not comply with the drug-likeness rules of Muegge, Ghose, Egan and Lipinski in terms of $\log P$ (Fig. 43), e.g. seven [aspochalamins A–D (57–60)] and [bisaspochalasin A–C (83–85)], twenty six some examples, [armochaetoglobins A (232)], [isochaetoglobosin J (243)], [armochaetoglobins N–R (247–251)], penochalasin B (252), [prochaetoglobosins I–II (260–261)], armochaetoglobulin C (275), [armochaetoglobosins A–C (284–285)], [chaetoglobosin T (287)], one [saccalasin A (347)], one [thiocytchalasin A (27)], one [18-deoxycytchalasin H (7, L-696,474) (146)], and one cytochalasin Z1 (41) cytochalasan derivatives violate Lipinski's drug-likeness rule in terms of $\log P$, respectively (Fig. 43). The

oral bioavailability, bioavailability score (BS), is another parameter that indicates the possibility of a compound to be more than 10% bioavailable in the absorption assays. Molecules complying with the Lipinski's drug-likeness rule and with a BS of 0.55 are considered orally bioavailable. There are 222 cytochalasan derivatives (17, 31, 10, 10, 26, 18, 6, 13, 14, 16, and 61), which showed a BS of 0.55 and with no Lipinski's drug-likeness rule violation from *Arthrinium*, *Aspergillus*, *Chaetomium*, *Daldinia*, *Endothia*, *Metarhizium*, *Phoma*, *Phomopsis*, *Trichoderma*, *Xylaria*, and Others, respectively. All *Arthrinium*, *Metarhizium* and *Trichoderma* derived cytochalasans showed a BS of 0.55 and no Lipinski's rule failure. Three cytochalasan derivatives, phomopsichalasin F (148) and curtachalasins C–D (396–397) from *Phomopsis* and *Xylaria*, respectively, are of special interest as they showed a good BS of 0.56 and no Lipinski's rule failure. The curtachalasins C–D (396–397) are particularly interesting as they exhibit the unusual bridged 6/6/6/6 ring fused system (Fig. 41). The water solubility, $\log S$, is another essential measure for drug bioavailability. Although all cytochalasans were predicted to have adequate water solubility characteristics, there were different solubility orders as *Chaetomium* derived cytochalasans were the most soluble (mean value of –3.82), followed by *Endothia* (mean value of –3.94), but *Arthrinium* were the most poorly soluble (mean value of –4.95) (Table S1[†]). Intestinal absorption (human), blood–brain barrier (BBB) permeability, P-glycoprotein (P-gp) substrate and P-gp I and II inhibition potential were also surveyed to draw insights into the pharmacokinetic behaviour of the reviewed cytochalasans. Only twenty cytochalasans from *Aspergillus* (1), *Chaetomium* (2), *Daldinia* (1), *Endothia* (2), *Phomopsis* (1), *Trichoderma* (2), *Xylaria* (4) and Others (7) showed high intestinal absorption, passively crossed BBB and no potential for P-gp inhibition (Table S1[†]), with *Xylaria* lagambasines A–C (417–419) emerging as particularly noteworthy. Some toxicological properties were also evaluated, such as AMES toxicity (related to mutagenicity), hepatotoxicity, hERG I and II inhibition (related to cardio toxicity), and skin sensitisation. A total of 106 cytochalasan derivatives were predicted without any toxicity alert for the parameters evaluated, 4, 11, 9, 4, 8, 2, 3, 6, 12, 19, and 28 cytochalasans from *Arthrinium*, *Aspergillus*, *Chaetomium*, *Daldinia*, *Endothia*, *Metarhizium*, *Phoma*, *Phomopsis*, *Trichoderma*, *Xylaria*, and Others, respectively (Table S1[†]). Surprisingly, the three cytochalasans, lagambasines A–C (417–419), obeyed all the surveyed parameters (five drug-likeness rules, $\log S$, intestinal absorption, BBB, Pgp, AMES toxicity, hepatotoxicity, hERG I and II inhibition, and skin sensitisation).

5. Applications of cytochalasans in imaging and drug discovery

In the vast realm of biomedical research, cytochalasans, a distinctive group of natural compounds derived from fungi have shown significant potential in various applications, including imaging and drug discovery. Renowned for their diverse biological activities and unique chemical structures, cytochalasans have not only demonstrated their efficacy as



antitumor and antimicrobial agents but have also opened new horizons in the realms of imaging and drug discovery. Herein we summarize whenever applicable the application of different members of cytochalasans in imaging, drug discovery and biomedical applications.

5.1. Cytochalasans as illuminating probes

Indeed, within advances in the intricate world of cellular and molecular imaging, cytochalasans have emerged as captivating tools, owing to their inherent fluorescent and structural properties. Their unique molecular characteristics enable them to serve as remarkable imaging probes, shedding light on various biological processes. In imaging, cytochalasans have been utilized as fluorescent probes due to their ability to selectively label specific cellular structures or proteins, enabling the visualization and tracking of biological processes. Their unique chemical structures and diverse modes of action make cytochalasans valuable naturally occurring molecules for the development of novel therapeutic agents.^{63,219–224}

5.1.1. Illuminating the cellular landscape. Cytochalasin H (116) and cytochalasin B (2), are two representative cytochalasans, which have been widely utilized as a cellular imaging probe. With their abilities to disrupt actin filaments, it enables the visualization of cytoskeletal dynamics and cellular morphology. By conjugating these cytochalasans with fluorophores, researchers can track cellular events and elucidate the intricacies of cellular processes.^{73,75,225–229}

5.1.2. Journeying into the molecular landscape. Interestingly, cytochalasin D (366), another member of the cytochalasan family, has demonstrated its potential in molecular imaging. By selectively binding to actin filaments within cells, it can be conjugated with imaging moieties such as radionuclides or nanoparticles. This fusion allows for targeted imaging of

disease markers, providing valuable insights into molecular processes and aiding in precise diagnostics.^{75,230–233}

5.2. The epic quest in drug discovery

Driven by their captivating chemical structures and diverse biological activities, cytochalasans have become protagonists in the epic quest for novel therapeutics. Their potential stretches beyond their direct use as therapeutic agents, serving as treasured lead compounds and scaffolds in the pursuit of groundbreaking drugs.^{63,234–236}

5.2.1. Targeted therapy. Indeed, cytochalasin A (14) exhibits multiple effects, by inhibiting platelet-mediated tumour cell adhesion to the endothelial matrix, inhibiting Kv1.5 K⁺ channels, and preventing phagocytosis in macrophages by disrupting actin polymerization. These diverse actions highlight its potential anticancer benefits and broader impact on cellular processes.^{237,238} Moreover, cytochalasin E (376), a derivative has shown promise as a targeted therapy agent. By selectively inhibiting the microfilament network within cancer cells, it disrupts cell division and induces apoptosis. Furthermore, synthetic modifications to the cytochalasin E (376) structure have led to the development of analogues with enhanced potency and selectivity against specific cancer types.^{239–243}

5.2.2. Navigating the seas of drug delivery systems. Cytochalasans have ventured into unexplored territories, pushing the boundaries of scientific exploration deeply within the realm of drug delivery systems. For example, cytochalasin H (116), with its ability to self-assemble into nanostructures, has been explored as a drug delivery vehicle. By encapsulating therapeutic agents within its nanostructures, it facilitates controlled release and targeted delivery, improving drug efficacy and reducing side effects.^{244–249} Collectively, the captivating tale of

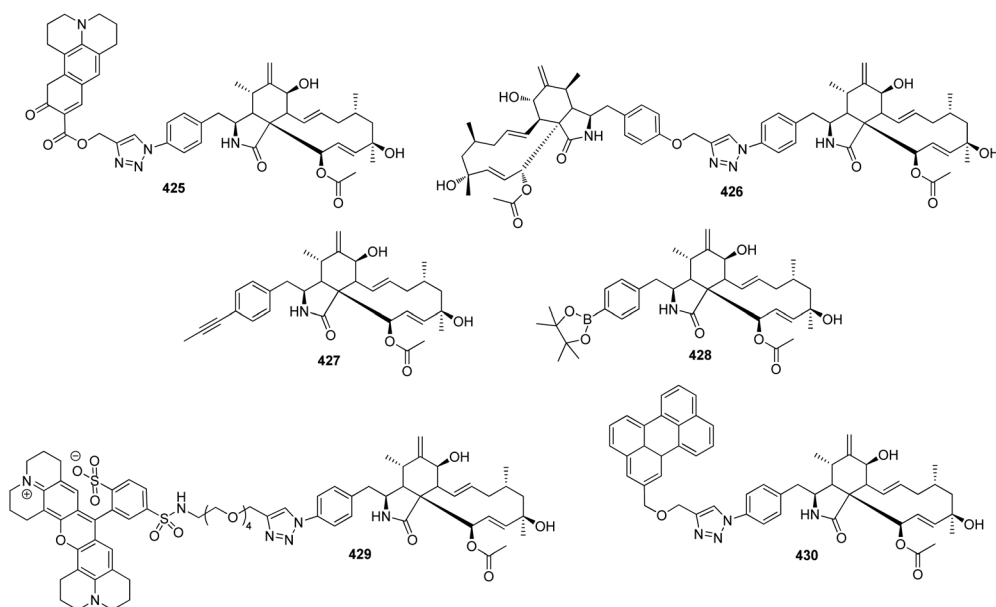


Fig. 45 Cytochalasin H (116) containing synthetic analogues/probes (425–430).



cytochalasans in imaging and drug discovery unfolds and reveals a world of boundless possibilities. Their fluorescent properties illuminate the cellular landscape, enabling us to witness the intricate choreography of life within cells. Through examples such as cytochalasin B (2) and cytochalasin D (366), we see their power as imaging probes, unravelling the secrets of cellular and molecular processes. Their unique chemical structures and selective interactions empower us on the noble quest for novel therapeutics, exemplified by compounds like cytochalasin E (376), a powerful antitumor agent. Recently, Wang *et al.*, reported on the synthesis of diverse functionalised cytochalasans through mutasynthesis and semi-synthesis strategies. Indeed, cytochalasin H (116) was employed as a key starting material for accessing a number of structurally modified cytochalasin containing probes (425–430) (Fig. 45).⁷³

These compounds were further investigated for their antifungal towards *Schizosaccharomyces pombe*, *Pichia anomala*, *Mucor hiemalis*, *Candida albicans*, and *Rhodotorula glutinis*, cytotoxicity against mouse (L929) and human (KB3.1,PC3, A549, MCF-7, A431 and SKOV-3) cell lines, and actin disruption properties *in vivo* using osteosarcoma U2OS cells. Concerning the antifungal activity, most of the compounds were inactive as antifungal, however the coumarin-based 425 exhibited remarkable activity with IC_{50} of approximately 5 mM against the opportunistic pathogen *C. albicans*. However, it showed only moderate or weak activity against the other organisms. With respect to the cytotoxicity, most of the compounds were inactive, however the dimeric analogues exhibited cytotoxicity that surpassed expectations, such as 426 with IC_{50} of 120 nM against KB3.1 cells. Acetylene 427 and borate 428 also demonstrated relatively good potency, with examples like 428 showing an IC_{50} of 300 nM against KB3.1 cells. However, the red dyed 429 displayed the most potent cytotoxicity of all, with remarkably low IC_{50} values as low as 20 nM against the KB3.1 cell line.

Regarding the actin disruption activity, the fluorescence analysis using the coumarin channel indicated that of 425 prominently co-localized with actin aggregates induced at different concentrations. In contrast, the perylene-linked 430 showed a more diffuse localization within cells and less prominent co-localization with F-actin. This difference in localization may be attributed to the increased hydrophobicity of the perylene unit, leading to stronger association with membranes. The specific association of certain actin-inhibitory compounds with actin aggregates during or after cell treatment, as well as their co-localization with phalloidin, suggests that these derivatives could serve as simple staining tools for fixed, non-treated cells. For example, staining with the hydrophilic Texas-red-linked 429 revealed selective binding to F-actin, highlighting key structures of the actin cytoskeleton at sub-micrometre resolution.

Surprisingly, staining with 429 also revealed prominent sub-compartments of the actin cytoskeleton, such as microspikes, stress fibres, and lamellipodia, with staining patterns consistent with those obtained using phalloidin. These findings indicate the continuous distribution of actin filament barbed ends within these structures composed of filaments with variable lengths, assuming the barbed end specificity of actin filament binding by this novel compound.

5.3. Current stage of clinical development of cytochalasans

As of today, the clinical application of cytochalasans is still in its infancy, with most advancements confined to preclinical and early-phase studies. However, the following points summarize the broader clinical development of cytochalasans in different biomedical applications.

5.3.1. Cardiovascular applications. Lehmann *et al.*, highlight the foundation for the use the first FDA-approved randomized trial of cytochalasin B (2) in vascular remodelling, demonstrating its safety and feasibility. However, further studies are necessary to confirm its efficacy in reducing restenosis and to optimize drug delivery systems. In this context, local delivery techniques, such as microporous infusion balloons, are being refined to enhance drug targeting and minimize systemic toxicity, potentially improving treatment.²⁵⁰

5.3.2. Oncology and cancer therapy. Cytochalasans, particularly B (2), D (366) and E (367) remain primarily in preclinical stages for cancer therapy, with their ability to disrupt actin polymerization and inhibit metastasis making them attractive candidates for further investigation, particularly in combination therapies. However, challenges such as off-target effects and cytotoxicity must be addressed before advancing to large-scale clinical trials.^{63,251–253}

5.3.3. Inflammatory and autoimmune diseases. Cytochalasans are being explored for their ability to modulate immune responses, with preclinical studies suggesting potential applications in chronic inflammatory and autoimmune diseases. However, clinical evidence is currently lacking, and further research is needed to validate these findings.^{220,254,255}

5.3.4. Infectious diseases. Anti-microbial applications of cytochalasans are promising but remain underexplored in clinical settings. Advances in drug delivery and formulation may help overcome current limitations, as cytochalasans have shown effectiveness against bacteria, viruses, parasites, and fungi. For instance, cytochalasin A (14) exhibits antibacterial and antifungal activity, while cytochalasin D (366) also has antifungal properties.²⁵⁶ Additionally, cytochalasans can inhibit biofilm formation,⁷⁵ HIV proteases, and other HIV-related pathways, as well as slightly inhibit the macropinocytosis of SARS-CoV.⁷⁵ However, before cytochalasans can be developed for broad-spectrum biotechnological applications, it is essential to understand comprehensively their complex activities is, given that they are actin cytoskeletal inhibitors, which could potentially impact various essential cell biological processes.⁷⁵

5.3.5. Modulators of stem cell differentiation. Cytochalasans are being studied as tools in cell biology and regenerative medicine due to their ability to manipulate cytoskeletal dynamics. For example, they are used *in vivo* studies to induce cell fusion, which may have applications in vaccine development and cellular therapies.^{220,222}

6. Conclusion, future directions opportunities and challenges

Fungal natural products have played a significant role in the development of therapeutic agents. Many well-known drugs,



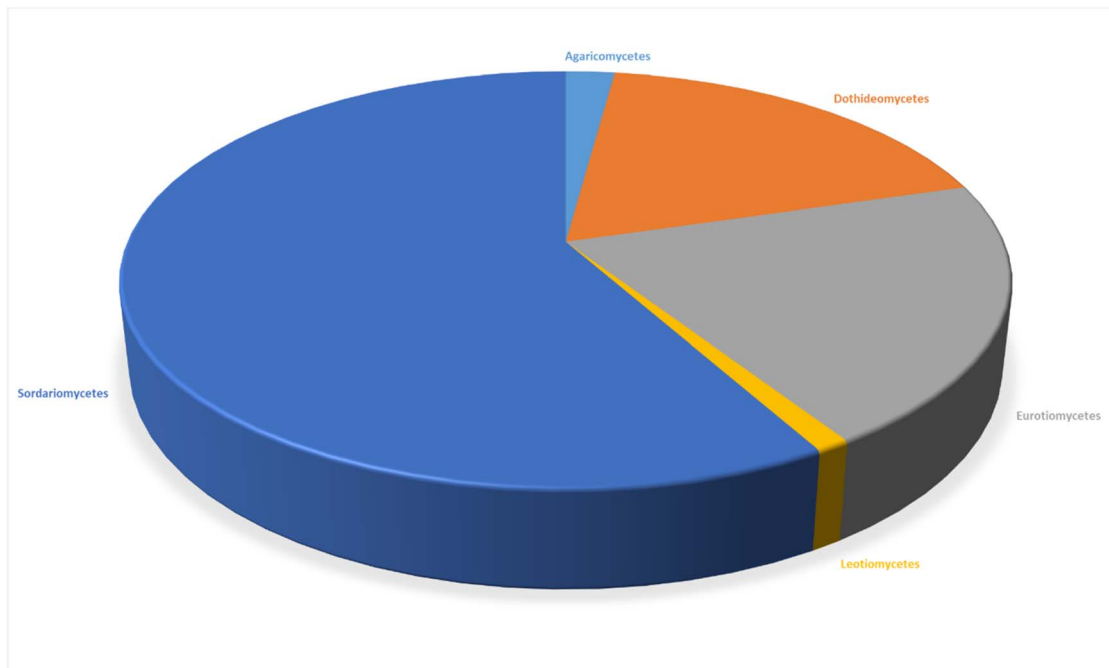


Fig. 46 Contribution of cytochalasans by different fungal classes.

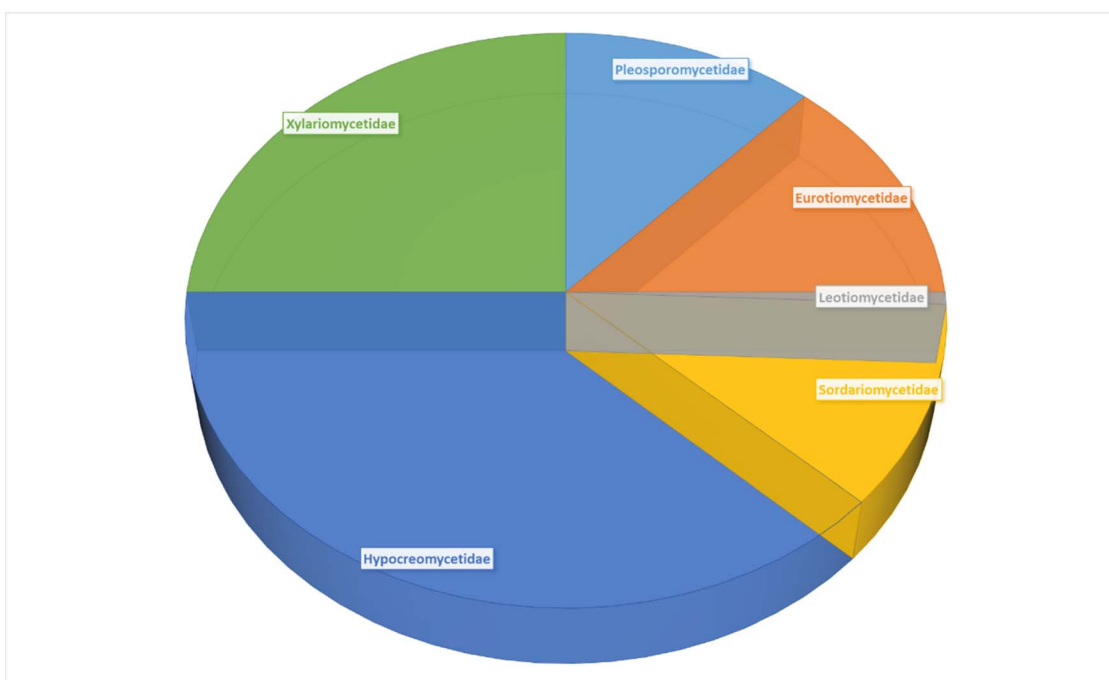


Fig. 47 Contribution of cytochalasans by different fungal sub-classes.

such as antibiotics, immunosuppressants, anticancers, anti-inflammation, and cholesterol-lowering agents, owe their origins to fungal sources. These compounds have revolutionized medicine and have been instrumental in combating various diseases. Among the extraordinary classes of secondary metabolites are cytochalasans.

Cytochalasans are a class of fungal metabolites displaying unique tricyclic core structure consisting of a polyketide-derived 11, 13 or 14-membered macrocyclic ring fused to various aromatic or heteroaromatic rings (e.g. an isoindolone moiety), where they are biosynthesized through polyketide synthase–nonribosomal peptide synthetase (PKS–NRPS) hybrid pathways. These pathways play a pivotal role in constructing the intricate



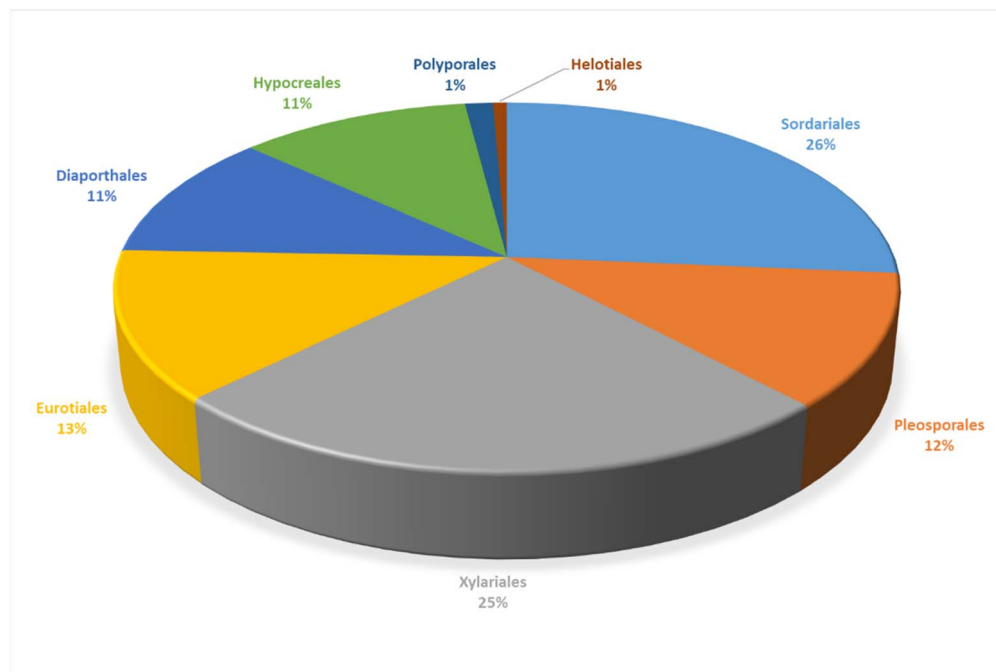


Fig. 48 Contribution of cytochalasans by different fungal orders.

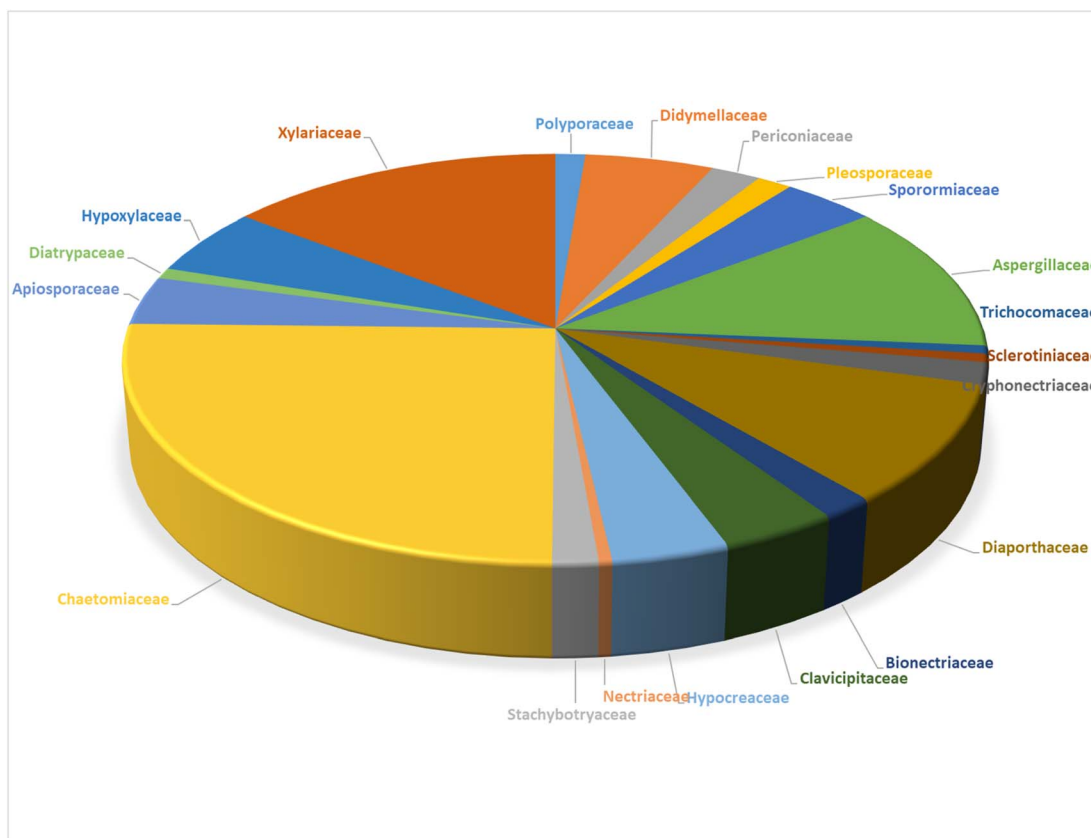


Fig. 49 Contribution of cytochalasans by various fungal families.

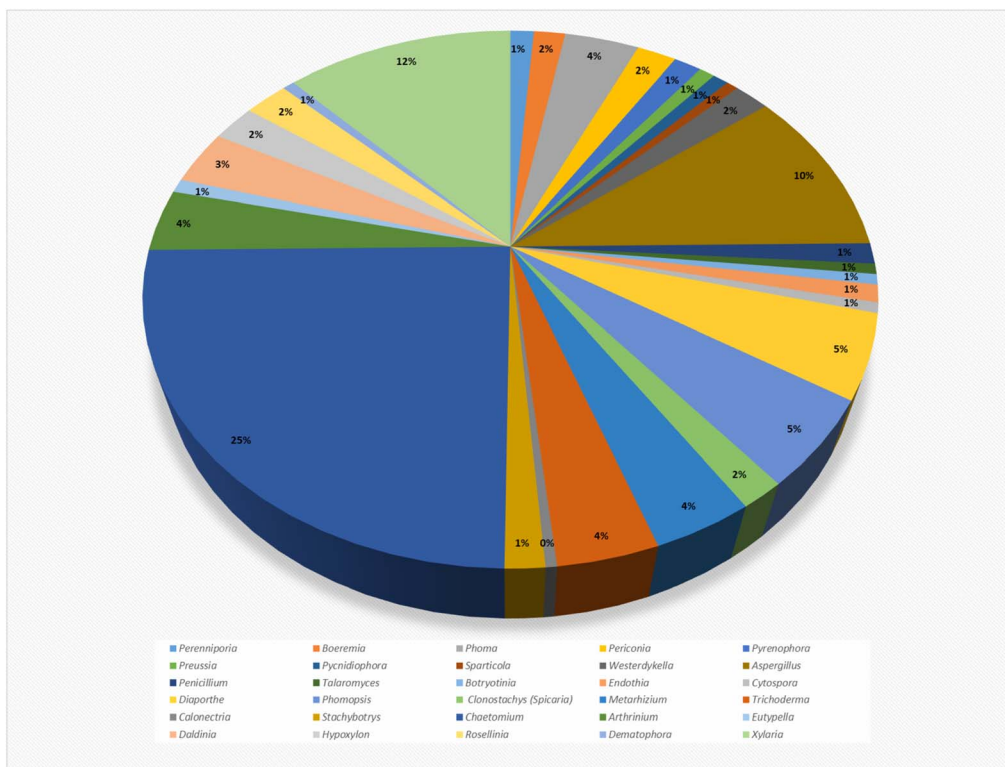


Fig. 50 Contribution of cytochalasans by different fungal genera.

molecular architecture of these metabolites. Indeed, cytochalasans were found to be a powerful natural product to serve not only as a cytotoxic agent but also as antimicrobial, antiviral, anti-inflammatory and immunosuppressive agents. Within this documentation, we tried to present a comprehensive-up-to-date literature review focused on the chemistry of 424 cytochalasans isolated over the period 2000–2023 from different fungal natural sources, along with shedding light on their biosynthetic pathways, pharmacokinetics and ADMET properties, and their application in drug discovery.

Collectively, 424 fungal derived cytochalasans were listed thoroughly by fungal class, subclass, order, family, genera and their different assigned therapeutic activities. Through the statistical analysis of the collected data, it can be concluded that the fungal class (Sordariomycetes) with 165 different cytochalasans analogues considered to be the main source of cytochalasans compounds followed by Eurotiomycetes and Dothideomycetes (Fig. 46). While according to the subclass level, Hypocreomycetidae and Xylariomycetidae represent the richest source of the targeted metabolites followed by Eurotiomycetidae, Pleosporomycetidae and Sordariomycetidae with 167, 110, 58, 52, and 50 different cytochalasan derivatives, respectively (Fig. 47).

Based on the order level fungal orders (Sordariales) and (Xylariales) with 118 and 110 different isolated cytochalasans, respectively, emerges as the richest source of cytochalasan representing 26 and 25%, respectively of the total reported cytochalasans. Furthermore, the fungal orders Diaporthales, Eurotiales, Hypocreales, and Pleosporales, were almost

identical in their contribution to the cytochalasans chemistry (Fig. 48).

Based on the family level, the family (Chaetomiaceae) represents the primary source of cytochalasans with 118 different derivatives being isolated comprising 28% of the total reported cytochalasans, followed by (Xylariaceae), (Aspergillaceae), and (Diaporthaceae) with contribution of 16%, 13% and 10% of the recorded cytochalasans, respectively (Fig. 49). The fungal species *Chaetomium* is emerging as the prevailing source of the reported compounds (Fig. 50), where a total of 118 different cytochalasans were solely isolated from this fungal species representing 25% out of the reported cytochalasans over the specified 23 years-period of the review. Regarding the therapeutic potentials of the discovered cytochalasans, a broad array of multiple biological activities was reported.

These were primarily concerned with cytotoxicity, but they also had antibacterial, antifungal, antiviral, phytotoxic, anti-inflammatory, antimigratory, enzyme inhibitory, immunosuppressive, antagonistic, F-actin network disruptors, nematocidal, and antibiofilm activities. Moreover, it is worthy to emphasise that the cytotoxicity activity was the most profoundly studied biological assay followed by the antibacterial, antifungal and phytotoxic assays.

In total 194 cytochalasans were tested for their cytotoxicity against different tumour cell lines, and a total number of 60, 23, 15, and 14 cytochalasans were evaluated for their antibacterial and antifungal, antiviral, and phytotoxic activities, respectively (Fig. 51). Furthermore, 424 cytochalasan derivatives were extensively investigated for their pharmacokinetics and ADMET



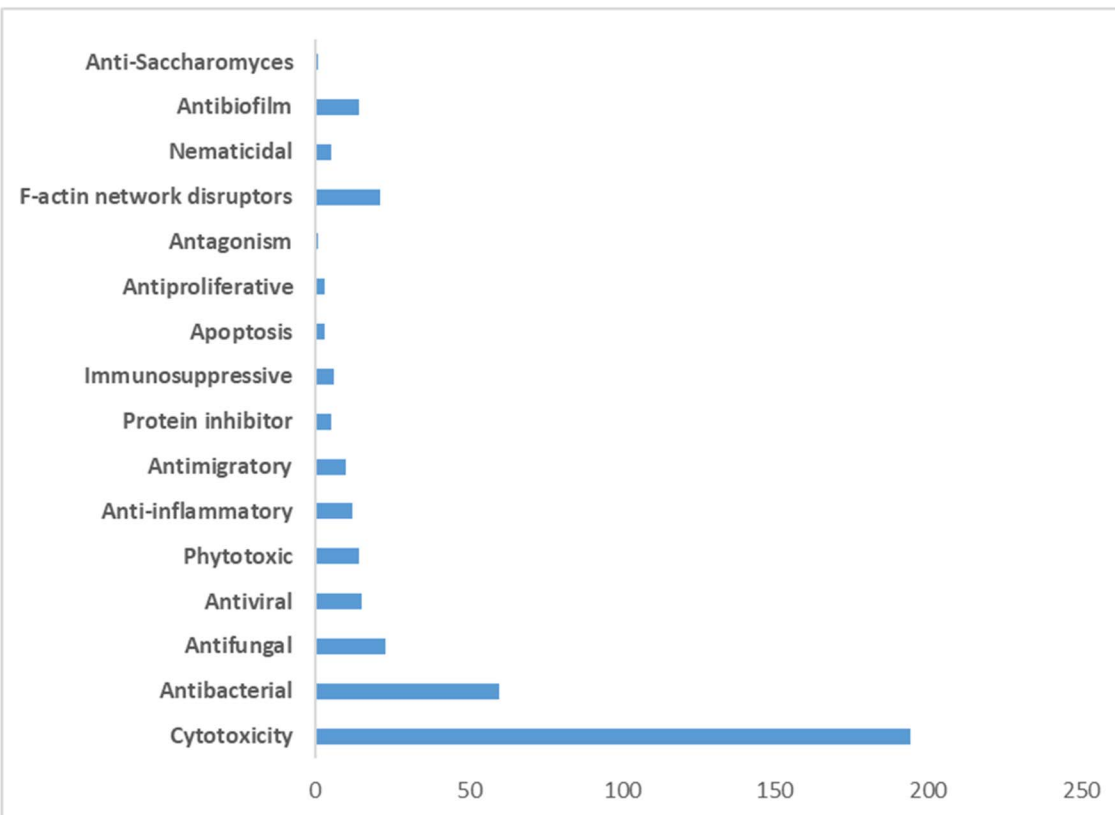


Fig. 51 Therapeutic activities of different cytochalasans obtained from various fungal species.

using two online platforms, SwissADME and pkCSM, respectively.

Among these, three derivatives, phomopsischalasin F (148) (Fig. 18) and curtachalasins C-D (396–397) (Fig. 41) from Phomopsis and Xylaria, respectively, caught our attention. They boasted a promising bioavailability score of 0.56 and no Lipinski's rule failure (see Table S1†). The curtachalasins C-D (396–397), were particularly interesting, showcasing an uncommon bridged 6/6/6 ring fused system (Fig. 41).

Remarkably, lagambasines B (418) and C (419) (Fig. 42) complied with all the assessed parameters. These parameters encompassed five drug-likeness rules, $\log S$ values, intestinal absorption, BBB permeability, Pgp interactions, AMES toxicity, hepatotoxicity, hERG I and II inhibition, and skin sensitisation (Table S1†).

Appealingly, as we shown before that cytochalasans offer promising potential in cancer therapy, immune modulation, and antimicrobial treatments. Their ability to disrupt actin polymerization and inhibit metastasis makes them valuable candidates for combination cancer therapies. Additionally, their antimicrobial properties against bacteria, fungi, and viruses, along with their ability to inhibit biofilm formation and HIV-related pathways, highlight their broad-spectrum potential. Advances in targeted drug delivery systems may further enhance their therapeutic efficacy while reducing side effects. As we continue to unravel the mysteries of cytochalasans, optimizing their structures, elucidating their mechanisms, and refining

their formulations, scaling up their production through the transient expression of their biosynthetic routes, we set sail toward a future where these remarkable compounds could transform clinical applications, offering new hope to those in need.

However, despite their biomedical potential, cytochalasans current research faces several challenges, including their off-target effects and cytotoxicity as actin inhibitors, can disrupt essential cellular processes. The complexity of their mechanisms complicates understanding and clinical application. Moreover, the transition from preclinical models to human use is hindered by insufficient clinical data and safety profiles. Regulatory hurdles and the need for extensive clinical trials further delay their development for widespread therapeutic use. Nonetheless, with continued research and refinement, cytochalasans could revolutionize medicine, addressing diseases that are currently difficult to treat.^{235,257–263}

7. Abbreviations

A2780	Human ovarian cell line
A375	Human melanoma cell line
A431	Squamous cell carcinoma
A549	Human lung cell line
ADMET	Absorption, distribution, metabolism, excretion, and toxicity



Asp0A	This is an enzyme name – an FMO from the aspergillin PZ pathway	OMeT	<i>O</i> -methyltransferase
Asp0D	This is an enzyme name – an SDR from the aspergillin PZ pathway	OXR	Oxidoreductases
B16F10	Mouse melanoma cells	P388	Lymphocytic leukaemia
BBB	Blood–brain barrier	P450	Cytochrome P450 monooxygenases
BEL-7402	Human liver cancer cell line	PANC-1	Human pancreatic cancer cell line
BGC-823	Human gastric cell line	PC-3	Human prostate cancer
BGCs	Biosynthetic gene clusters	P-gp	P-glycoprotein
BS	Bioavailability score	PKS	Polyketide synthase
BVMO	Baeyer–Villiger monooxygenases	PKS–NRPS	Polyketide synthase–nonribosomal peptide synthetase
CcsB	This is an enzyme name – a BVMO from the cytochalasin E/K pathway	PyiH	This is an enzyme name – an SDR from the pyrichalasin H pathway
CHGG_01242-1	This is an enzyme name – an FMO from the chaetoglobosin A pathway	PyiS	This is an enzyme name – the PKS–NRPS from the pyrichalasin H pathway
CT26	Murine colon carcinoma	RSV	Respiratory syncytial virus
DA	Diels–Alder	SDR	Short-chain dehydrogenase
EC ₅₀	Half-maximal effective concentration	SF-268	Human glioblastoma cell line
EtOAc	Ethyl acetate	SGC-7901	Human gastric cancer cell
FAD	Flavin adenine dinucleotide	SKOV-3	Ovarian carcinoma
FMO	Flavin-dependent monooxygenase	SMMC-7721	Human hepatocarcinoma
FNPs	Fungal-derived natural products	SW480	Colon cancer
H292	Human lung mucoepidermoid carcinoma cells	TF	Transcription factors
HCT-8	Human colorectal adenocarcinoma cell line	TNF- α	Tumour necrosis factor-alpha
HCT-8/T	Hematocrit	TPSA	Topological polar surface area
HeLa	Human cervical cell line	trans-ER	trans-acting enoylreductase
Hep3B	Human hepatoma cell line	U87MG	Human glioblastoma cell line
HepG2	Human hepatocellular cell line	α , β -HYD	α , β -hydrolase
HepG2	Hepatocellular carcinoma		
hERG	Human ether-a-go-go-related gene		
HIV	Human immunodeficiency viruses		
HL-60	Human promyelocytic leukemia cells		
HMO2	Gastric adenocarcinoma		
HSV-1	Herpes simplex virus		
HT-29	Human colon carcinoma		
Huh7	Hepatocellular carcinoma		
HUVEC	Human umbilical vein epithelial cell		
IC ₅₀	Inhibitory concentration that causes a 50% reduction in cell viability		
K562	Myelogenous leukaemia		
KB	Human nasopharyngeal epidermoid tumor		
KO	Knock-out		
L929	Mouse fibroblast		
LNCaP	Human prostate cancer cells		
L-NMMA	NG-Monomethyl-L-arginine acetate		
log <i>P</i>	Octanol–water partition coefficient		
log <i>S</i>	Water solubility		
MCF-7	Human breast cells		
MDA-MB-231	Melanoma cell line		
MeOH	Methanol		
MFS	Major facilitator superfamily		
MOLT4	T lymphoblast cell line		
MTT assay	Colorimetric assay for assessing cell metabolic activity		
MW	Molecular weight		
NADPH	Nicotinamide adenine dinucleotide phosphate		
NCI-H187	Small cell lung cancer		
NO	LPS-induced nitric oxide		
NRPS	Nonribosomal peptide synthetase		



8. Data availability

This is a review article, and no new data were generated or analyzed in this study. All data discussed are based on published literature cited within the manuscript.

9. Author contributions

Conceptualization: Amr El-Demerdash. Validation: Amr El-Demerdash. Formal analysis: Mohamed A. Tammam, Florbela Pereira, Elizabeth Skellam and Amr El-Demerdash. Investigation: Mohamed A. Tammam, Florbela Pereira, Elizabeth Skellam, A. Ganesan and Amr El-Demerdash. Resources: Mohamed A. Tammam, Florbela Pereira, Elizabeth Skellam and Amr El-Demerdash. Data curation: Mohamed A. Tammam and Amr El-Demerdash. Writing – original draft: Mohamed A. Tammam, Florbela Pereira, Elizabeth Skellam, Stefan Bidula, A. Ganesan and Amr El-Demerdash. Writing – review & editing: Mohamed A. Tammam, Florbela Pereira, Elizabeth Skellam, Stefan Bidula, A. Ganesan and Amr El-Demerdash.

10 Conflicts of interest

There are no conflicts to declare.

11 Acknowledgements

Amr El-Demerdash is thankful to his home universities, University of East Anglia (UK) and Mansoura University (Egypt)

for the unlimited support, inside and outside. Elizabeth Skellam is thankful for the National Science Foundation (NSF) for a financial support (Grant number 2048347). Mohamed A. Tammam is humbly dedicating this work to the soul of his sister Dr Mai A. Tammam who passed away on 19 March 2022, was always a kind supporter in all aspects of his life.

12. References

- 1 A. S. Abdel-Razek, M. E. El-Naggar, A. Allam, O. M. Morsy and S. I. Othman, *Processes*, 2020, **8**, 470.
- 2 H. Bansal, R. K. Singla, S. Behzad, H. Chopra, A. S. Grewal and B. Shen, *Curr. Top. Med. Chem.*, 2021, **21**, 2374–2396.
- 3 I. A. Stringlis, H. Zhang, C. M. J. Pieterse, M. D. Bolton and R. De Jonge, *Nat. Prod. Rep.*, 2018, **35**, 410–433.
- 4 D. J. Kenny and E. P. Balskus, *Chem. Soc. Rev.*, 2018, **47**, 1705–1729.
- 5 P. J. Rutledge and G. L. Challis, *Nat. Rev. Microbiol.*, 2015, **13**, 509–523.
- 6 J. W. H. Li and J. C. Vederas, *Science*, 2009, **325**, 161–165.
- 7 G. L. Challis, *J. Med. Chem.*, 2008, **51**, 2618–2628.
- 8 *Fungal Biomolecules: sources, applications and recent developments*, ed. V. K. Gupta, R. L. Mach and S. Sreenivasaprasad, 2015, 978-1-118-95829-2.
- 9 P. Spitteler, *Nat. Prod. Rep.*, 2015, **32**, 971–993.
- 10 A. H. Aly, A. Debbab and P. Proksch, *Fungal Divers.*, 2011, **50**, 3–19.
- 11 J. J. Zhong and J. H. Xiao, *Adv. Biochem. Eng. Biotechnol.*, 2009, **113**, 79–150.
- 12 *Drug Design: Novel Advances in the Omics Field and Applications*, ed. A. A. Parikesit and A. A. Parikesit, 2021, 118-95829-2.
- 13 J. Correia, A. Borges, M. Simões and L. C. Simões, *Antibiotics*, 2023, **12**, 1250.
- 14 E. Martinez-Klimova, K. Rodríguez-Peña and S. Sánchez, *Biochem. Pharmacol.*, 2017, **134**, 1–17.
- 15 N. Suwannarach, J. Kumla, K. Sujarit, T. Pattananandecha, C. Saenjum and S. Lumyong, *Molecules*, 2020, **25**, 1800.
- 16 A. Ganjoo, N. Sharma, H. Shafeeq, N. A. Bhat, K. K. Dubey and V. Babu, *Biotechnol. Bioeng.*, 2022, **119**, 3339–3369.
- 17 S. Chandra, *Appl. Microbiol. Biotechnol.*, 2012, **95**, 47–59.
- 18 S. K. Deshmukh, V. Prakash and N. Ranjan, *Front. Microbiol.*, 2018, **8**, 2536.
- 19 E. A. Elsayed, H. El Enshasy, M. A. M. Wadaan and R. Aziz, *Mediators Inflammation*, 2014, **2014**, 805841.
- 20 J. Xu, M. Yi, L. Ding, S. He, L. Dak, S. Yip, Y. Chin and K. Li, *Mar. Drugs*, 2019, **17**, 636.
- 21 M. Manzoni and M. Rollini, *Appl. Microbiol. Biotechnol.*, 2002, **58**, 555–564.
- 22 V. V. Pandey, V. K. Varshney and A. Pandey, *J. Biol. Act. Prod. Nat.*, 2019, **9**, 162–178.
- 23 N. P. Keller, *Nat. Rev. Microbiol.*, 2018, **17**, 167–180.
- 24 C. Greco, N. P. Keller and A. Rokas, *Curr. Opin. Microbiol.*, 2019, **51**, 22–29.
- 25 A. Singh, D. K. Singh, R. N. Kharwar, J. F. White, S. K. Gond, A. Singh, D. K. Singh, R. N. Kharwar, J. F. White and S. K. Gond, *Microorganisms*, 2021, **9**, 197.
- 26 A. Schueffler and T. Anke, *Nat. Prod. Rep.*, 2014, **31**, 1425–1448.
- 27 Y. M. Chianga, K. H. Lee, J. F. Sanchez, N. P. Keller and C. C. C. Wang, *Nat. Prod. Commun.*, 2009, **4**, 1510.
- 28 Y. Matsuda and I. Abe, *Nat. Prod. Rep.*, 2015, **33**, 26–53.
- 29 C. Schmidt-Dannert, *Adv. Biochem. Eng. Biotechnol.*, 2015, **148**, 19–61.
- 30 E. Skellam, *Trends Biotechnol.*, 2019, **37**, 916.
- 31 R. Linnakoski, D. Reshamwala, P. Veteli, M. Cortina-Escribano, H. Vanhanen and V. Marjomäki, *Front. Microbiol.*, 2018, **9**, 412077.
- 32 A. A. Brakhage, J. Schuemann, S. Bergmann, K. Scherlach, V. Schroeckh and C. Hertweck, *Prog. Drug Res.*, 2008, **66**, 1–12.
- 33 D. H. Demers, M. A. Knestrick, R. Fleeman, R. Tawfik, A. Azhari, A. Souza, B. Vesely, M. Netherton, R. Gupta, B. L. Colon, C. A. Rice, M. A. Rodríguez-Pérez, K. H. Rohde, D. E. Kyle, L. N. Shaw and B. J. Baker, *Mar. Drugs*, 2018, **16**, 376.
- 34 G. Niu, T. Annamalai, X. Wang, S. Li, S. Munga, G. Niu, Y. C. Tse-Dinh and J. Li, *PeerJ*, 2020, **8**, e10392.
- 35 T. A. K. Prescott, R. Hill, E. Mas-Claret, E. Gaya and E. Burns, *Biomolecules*, 2023, **13**, 986.
- 36 H. B. Tiwari, P. Tiwari and H. Bae, *Microorganisms*, 2022, **10**, 360.
- 37 F. Kempken, *PLoS Pathog.*, 2023, **19**, e1011624.
- 38 L. Marquez and C. L. Quave, *Antibiotics*, 2020, **9**, 150.
- 39 M. Barbero, E. Artuso and C. Prandi, *Curr. Med. Chem.*, 2017, **25**, 141–185.
- 40 K. Sułkowska-Ziaja, M. Trepa, A. Olechowska-Jarząb, P. Nowak, M. Ziaja, K. Kała and B. Muszyńska, *Pharmaceuticals*, 2023, **16**, 1200.
- 41 A. N. Wethalawe, Y. V. Alwis, D. N. Udukala and P. A. Paranagama, *Molecules*, 2021, **26**, 3901.
- 42 D. Jakubczyk and F. Dussart, *Molecules*, 2020, **25**, 911.
- 43 K. M. G. O'Connell, J. T. Hodgkinson, H. F. Sore, M. Welch, G. P. C. Salmond and D. R. Spring, *Angew. Chem. Int. Ed.*, 2013, **52**, 10706–10733.
- 44 P. Pasrija, M. Girdhar, M. Kumar, S. Arora and A. Katyal, *Phytomed. Plus*, 2022, **2**, 100249.
- 45 T. O. Lawal, N. Raut, S. M. Wicks, G. B. Mahady and G. B. Mahady, *Med. Res. Arch.*, 2018, **6**(1), 1–22.
- 46 S. Banerjee and S. B. Paruthy, *Fungal Metabolites*, 2017, pp. 669–700.
- 47 J. A. Cooper, *J. Cell Biol.*, 1987, **105**, 1473–1478.
- 48 M. Binder and C. Tamm, *Angew. Chem. Int. Ed.*, 1973, **12**, 370–380.
- 49 A. A. Ismaiel and J. Papenbrock, *Agriculture*, 2015, **5**, 492–537.
- 50 J. Zhu, L. Song, S. Shen, W. Fu, Y. Zhu and L. Liu, *Molecules*, 2023, **28**, 7789.
- 51 C. C. Gu, J. Zeng, X. P. Peng, Y. J. Sun, S. Z. Yuan, X. N. Wang, R. S. Zhang, H. X. Lou and G. Li, *J. Org. Chem.*, 2023, **88**, 3185–3192.
- 52 R. Chen, L. J. Guo, X. D. Li, X. R. Li, K. Hu, J. W. Tang, Z. N. Ye, B. C. Yan and P. T. Puno, *Org. Chem. Front.*, 2023, **10**, 2218–2225.



53 H. Zhu, *et al.*, Progress in the Chemistry of Cytochalasans, in *Progress in the Chemistry of Organic Natural Products 114*, ed. A. D. Kinghorn, H. Falk, S. Gibbons, J. Kobayashi, Y. Asakawa and J. K. Liu, Springer, Cham, 2021, vol. 114, DOI: [10.1007/978-3-030-59444-2_1](https://doi.org/10.1007/978-3-030-59444-2_1).

54 D. C. Aldridge, J. J. Armstrong, R. N. Speake and W. B. Turner, *Chem. Commun.*, 1967, 26–27.

55 B. M. Kemkuignou, C. Lambert, K. Schmidt, L. Schweizer, E. G. M. Anoumedem, S. F. Kouam, M. Stadler, T. Stradal and Y. Marin-Felix, *Fitoterapia*, 2023, **166**, 105434.

56 B. B. Shi, C. Tian, X. Lv, J. Schinnerl, K. Ye, H. Guo, F. Xu, Y. He, H. L. Ai and J. K. Liu, *J. Org. Chem.*, 2023, **88**, 13926–13933.

57 X. Hu, X. Li, S. Yang, X. Li, B. Wang and L. Meng, *Chin. Chem. Lett.*, 2023, **34**, 107516.

58 K. Scherlach, D. Boettger, N. Remme and C. Hertweck, *Nat. Prod. Rep.*, 2010, **27**, 869–886.

59 G. Ding, H. Lou Wang, L. Chen, A. J. Chen, J. Lan, X. D. Chen, H. W. Zhang, H. Chen, X. Z. Liu and Z. M. Zou, *J. Antibiot.*, 2012, **65**, 143–145.

60 E. Skellam, *Nat. Prod. Rep.*, 2017, **34**, 1252–1263.

61 X. Peng, Y. He, Y. Gao, F. Duan, J. Chen and H. Ruan, *Bioorg. Chem.*, 2020, **104**, 104317.

62 M. Zaghouani, O. Gayraud, V. Jactel, S. Prévost, A. Dezaire, M. Sabbah, A. Escargueil, T. L. Lai, C. Le Clainche, N. Rocques, S. Romero, A. Gautreau, F. Blanchard, G. Frison and B. Nay, *Chem.-Eur. J.*, 2018, **24**, 16686–16691.

63 M. Trendowski, *Anticancer Agents Med. Chem.*, 2015, **15**, 327–335.

64 X. Y. Hu, X. M. Li, S. Q. Yang, B. G. Wang and L. H. Meng, *Chem. Biodivers.*, 2022, **19**, e202200550.

65 Y. Zhang, R. Tian, S. Liu, X. Chen, X. Liu and Y. Che, *Bioorg. Med. Chem.*, 2008, **16**, 2627–2634.

66 K. J. S. Farias, P. R. L. Machado, R. F. d. A. Júnior and B. A. L. da Fonseca, *Access Microbiol.*, 2019, **1**, e000041.

67 D. S. Chulpanova, Z. E. Gilazieva, S. K. Kletukhina, A. M. Aimaletdinov, E. E. Garanina, V. James, A. A. Rizvanov and V. V. Solovyeva, *Biology*, 2021, **10**, 141.

68 Y. Liu, Q. Ruan, S. Jiang, Y. Qu, J. Chen, M. Zhao, B. Yang, Y. Liu, Z. Zhao and H. Cui, *Fitoterapia*, 2019, **137**, 104187.

69 Z. Feng, X. Zhang, J. Wu, C. Wei, T. Feng, D. Zhou, Z. Wen and J. Xu, *Mar. Drugs*, 2022, **20**, 526.

70 W. X. Wang, G. G. Cheng, Z. H. Li, H. L. Ai, J. He, J. Li, T. Feng and J. K. Liu, *Org. Biomol. Chem.*, 2019, **17**, 7985–7994.

71 M. Zhao, Y. Ge, C. Zhou, X. Liu and B. Wu, *Fitoterapia*, 2023, **168**, 105523.

72 R. Fujii, A. Minami, K. Gomi and H. Oikawa, *Tetrahedron Lett.*, 2013, **54**, 2999–3002.

73 C. Wang, C. Lambert, M. Hauser, A. Deuschmann, C. Zeilinger, K. Rottner, T. E. B. Stradal, M. Stadler, E. J. Skellam and R. J. Cox, *Chem.-Eur. J.*, 2020, **26**, 13578–13583.

74 K. M. Fisch, *RSC Adv.*, 2013, **3**, 18228–18247.

75 C. Lambert, K. Schmidt, M. Karger, M. Stadler, T. E. B. Stradal and K. Rottner, *Biomolecules*, 2023, **13**, 1247.

76 M. A. Tammam and A. El-Demerdash, *Curr. Res. Biotechnol.*, 2023, **6**, 100145.

77 J. Reed, A. Orme, A. El-Demerdash, C. Owen, L. B. B. Martin, R. C. Misra, S. Kikuchi, M. Rejzek, A. C. Martin, A. Harkess, J. Leebens-Mack, T. Louveau, M. J. Stephenson and A. Osbourn, *Science*, 2009, **325**, 161–165.

78 M. A. Tammam, M. I. Gamal El-Din, A. Abood and A. El-Demerdash, *RSC Adv.*, 2023, **13**, 8049–8089.

79 M. A. Tammam, M. Sebak, C. Greco, A. Kijjoa and A. El-Demerdash, *J. Mol. Struct.*, 2022, **1268**, 133711.

80 M. Sebak, F. Molham, C. Greco, M. A. Tammam, M. Sobeh and A. El-Demerdash, *RSC Adv.*, 2022, **12**, 24887–24921.

81 A. El-Demerdash, C. Borde, G. Genta-Jouve, A. Escargueil and S. Prado, *Nat. Prod. Res.*, 2022, **36**, 1273–1281.

82 A. El-Demerdash, *J. Fungi*, 2018, **4**, 130.

83 A. El-Demerdash, G. Genta-Jouve, M. Bärenstrauch, C. Kunz, E. Baudouin and S. Prado, *Phytochemistry*, 2019, **166**, 112056.

84 M. Binder, J. -R Kiechel and C. Tamm, *Helv. Chim. Acta*, 1970, **53**, 1797–1812.

85 J. -L Robert and C. Tamm, *Helv. Chim. Acta*, 1975, **58**, 2501–2504.

86 J. C. Vederas and C. Tamm, *Helv. Chim. Acta*, 1976, **59**, 558–566.

87 A. Probst and C. Tamm, *Helv. Chim. Acta*, 1981, **64**, 2065–2077.

88 H. Oikawa, Y. Murakami and A. Ichihara, *J. Chem. Soc., Perkin Trans. 1*, 1992, 2955–2959.

89 D. Boettger and C. Hertweck, *Chem. Biol. Chem.*, 2013, **14**, 28–42.

90 K. Ishiuchi, T. Nakazawa, F. Yagishita, T. Mino, H. Noguchi, K. Hotta and K. Watanabe, *J. Am. Chem. Soc.*, 2013, **135**, 7371–7377.

91 K. Qiao, Y. H. Chooi and Y. Tang, *Metab. Eng.*, 2011, **13**, 723–732.

92 J. Collemare, M. Pianfetti, A. E. Houlle, D. Morin, L. Camborde, M. J. Gagey, C. Barbisan, I. Fudal, M. H. Lebrun and H. U. Böhnert, *New Phytol.*, 2008, **179**, 196–208.

93 H. U. Böhnert, I. Fudal, W. Dioh, D. Tharreau, J. L. Notteghem and M. H. Lebrun, *Plant Cell*, 2004, **16**, 2499–2513.

94 N. Khaldi, J. Collemare, M. H. Lebrun and K. H. Wolfe, *Genome Biol.*, 2008, **9**, 1–10.

95 Z. Song, W. Bakeer, J. W. Marshall, A. A. Yakasai, R. M. Khalid, J. Collemare, E. Skellam, D. Tharreau, M. H. Lebrun, C. M. Lazarus, A. M. Bailey, T. J. Simpson and R. J. Cox, *Chem. Sci.*, 2015, **6**, 4837–4845.

96 M. L. Nielsen, T. Isbrandt, L. M. Petersen, U. H. Mortensen, M. R. Andersen, J. B. Hoof and T. O. Larsen, *PLoS One*, 2016, **11**, e0161199.

97 C. Wang, V. Hantke, R. J. Cox and E. Skellam, *Org. Lett.*, 2019, **21**, 4163–4167.

98 H. Li, H. Wei, J. Hu, E. Lacey, A. N. Sobolev, K. A. Stubbs, P. S. Solomon and Y. H. Chooi, *ACS Chem. Biol.*, 2020, **15**, 226–233.



99 S. C. Heard, G. Wu and J. M. Winter, *J. Antibiot.*, 2020, **73**, 803–807.

100 C. Wang, K. Becker, S. Pfütze, E. Kuhnert, M. Stadler, R. J. Cox and E. Skellam, *Org. Lett.*, 2019, **21**, 8756–8760.

101 J. M. Zhang, X. Liu, Q. Wei, C. Ma, D. Li and Y. Zou, *Nat. Commun.*, 2022, **13**, 1–10.

102 B. Perlatti, C. B. Nichols, N. Lan, P. Wiemann, C. J. B. Harvey, J. A. Alspaugh and G. F. Bills, *Front. Microbiol.*, 2020, **11**, 564149.

103 J. Qi, L. Jiang, P. Zhao, H. Chen, X. Jia, L. Zhao, H. Dai, J. Hu, C. Liu, S. H. Shim, X. Xia and L. Zhang, *Appl. Microbiol. Biotechnol.*, 2020, **104**, 1545–1553.

104 G. G. Moore, J. Collemare, M. H. Lebrun and R. E. Bradshaw, *Natural Products: Discourse, Diversity, and Design*, 2014, pp. 341–356.

105 V. Hantke, E. J. Skellam and R. J. Cox, *Chem. Commun.*, 2020, **56**, 2925–2928.

106 M. Cheng, S. Zhao, H. Liu, Y. Liu, C. Lin, J. Song, C. Thawai, S. Charoensettasilp and Q. Yang, *Fungal Biol.*, 2021, **125**, 201–210.

107 C. L. M. Gilchrist and Y. H. Chooi, *Bioinformatics*, 2021, **37**, 2473–2475.

108 J. Schümann and C. Hertweck, *J. Am. Chem. Soc.*, 2007, **129**, 9564–9565.

109 H. Heinemann, H. Zhang and R. J. Cox, *Chem.-Eur. J.*, 2023, e202302590.

110 H. Zhang, V. Hantke, P. Bruhnke, E. J. Skellam and R. J. Cox, *Chem.-Eur. J.*, 2021, **27**, 3106–3113.

111 Y. Hu, D. Dietrich, W. Xu, A. Patel, J. A. J. Thuss, J. Wang, W. B. Yin, K. Qiao, K. N. Houk, J. C. Vederas and Y. Tang, *Nat. Chem. Biol.*, 2014, **10**, 552–554.

112 Z. Shang, R. Raju, A. A. Salim, Z. G. Khalil and R. J. Capon, *J. Org. Chem.*, 2017, **82**, 9704–9709.

113 H. Guo, Q. P. Diao, B. Zhang and K. H. Wang, *Phytochem. Lett.*, 2021, **46**, 162–165.

114 S.-Q. Teng, X.-F. Zhang, H.-F. Li, X.-W. Luo, Y.-S. Zhou, H. Liu, J.-K. Liu and T. Feng, *Phytochemistry*, 2023, **215**, 113861.

115 A. Evidente, A. Andolfi, M. Vurro, M. C. Zonno and A. Motta, *J. Nat. Prod.*, 2003, **66**, 1540–1544.

116 A. Cimmino, A. Andolfi, A. Berestetskiy and A. Evidente, *J. Agric. Food Chem.*, 2008, **56**, 6304–6309.

117 A. Evidente, A. Cimmino, A. Andolfi, A. Berestetskiy and A. Motta, *Tetrahedron*, 2011, **67**, 1557–1563.

118 X. Peng, J. Chang, Y. Gao, F. Duan and H. Ruan, *Chin. Chem. Lett.*, 2022, **33**, 4572–4576.

119 D. Zhang, H. Ge, D. Xie, R. Chen, J. H. Zou, X. Tao and J. Dai, *Org. Lett.*, 2013, **15**, 1674–1677.

120 D. Zhang, X. Tao, R. Chen, J. Liu, L. Li, X. Fang, L. Yu and J. Dai, *Org. Lett.*, 2015, **17**, 4304–4307.

121 D. Zhang, X. Tao, J. Liu, R. Chen, M. Zhang, L. Li, X. Fang, L. Y. Yu and J. Dai, *Tetrahedron Lett.*, 2016, **57**, 796–799.

122 J. Liu, D. Zhang, M. Zhang, X. Liu, R. Chen, J. Zhao, L. Li, N. Wang and J. Dai, *Tetrahedron Lett.*, 2016, **57**, 5794–5797.

123 A. Evidente, A. Andolfi, M. Vurro, M. C. Zonno and A. Motta, *Phytochemistry*, 2002, **60**, 45–53.

124 R. Kretz, L. Wendt, S. Wongkanoun, J. J. Luangsa-Ard, F. Surup, S. E. Helaly, S. R. Noumeur, M. Stadler and T. E. B. Stradal, *Biomolecules*, 2019, **9**, 73.

125 C. Zhao, G. Liu, X. Liu, L. Zhang, L. Li and L. Liu, *RSC Adv.*, 2020, **10**, 40384–40390.

126 K. Y. M. Garcia, M. T. J. Quimque, C. Lambert, K. Schmidt, G. Primahana, T. E. B. Stradal, A. Ratzenböck, H. M. Dahse, C. Phukhamsakda, M. Stadler, F. Surup and A. P. G. Macabeo, *J. Fungi*, 2022, **8**, 560.

127 D. Xu, M. Luo, F. Liu, D. Wang, X. Pang, T. Zhao, L. Xu, X. Wu, M. Xia and X. Yang, *Sci. Rep.*, 2017, **7**, 1–9.

128 D. Xu, X. Zhang, X. Shi, P. J. Xian, L. Hong, Y. D. Tao and X. L. Yang, *Phytochem. Lett.*, 2019, **32**, 52–55.

129 A. Sallam, M. A. Sabry and A. A. Galala, *Chem. Biodivers.*, 2021, **18**, e2000957.

130 A. Höltzel, D. G. Schmid, G. J. Nicholson, P. Krastel, A. Zeeck, K. Gebhardt, H. P. Fiedler and G. Jung, *J. Antibiot.*, 2004, **57**, 715–720.

131 K. Gebhardt, J. Schimana, A. Höltzel, K. Dettner, S. Draeger, W. Beil, J. Rheinheimer and H. P. Fiedler, *J. Antibiot.*, 2004, **57**, 707–714.

132 J. Liu, Z. Hu, H. Huang, Z. Zheng and Q. Xu, *J. Antibiot.*, 2011, **65**, 49–52.

133 H. Zhu, C. Chen, Y. Xue, Q. Tong, X. N. Li, X. Chen, J. Wang, G. Yao, Z. Luo and Y. Zhang, *Angew. Chem. Int. Ed.*, 2015, **54**, 13374–13378.

134 L. Yu, W. Ding and Z. Ma, *Nat. Prod. Res.*, 2016, **30**, 1718–1723.

135 Z. Wu, Q. Tong, X. Zhang, P. Zhou, C. Dai, J. Wang, C. Chen, H. Zhu and Y. Zhang, *Org. Lett.*, 2019, **21**, 1026–1030.

136 L. Wang, J. Yang, J. P. Huang, J. Li, J. Luo, Y. Yan and S. X. Huang, *Org. Lett.*, 2020, **22**, 7930–7935.

137 R. Orfali, S. Perveen, M. F. Khan, A. F. Ahmed, S. Tabassum, P. Luciano, G. Chianese and O. Taglialatela-Scafati, *Phytochemistry*, 2021, **192**, 112952.

138 X. Zhang, Z. Wu, A. Bao, Z. Zhao, Y. Chen, H. Zhao, J. Wang, C. Chen, Q. Tong, H. Zhu and Y. Zhang, *Org. Chem. Front.*, 2022, **9**, 2585–2592.

139 Y. C. Li, J. Yang, Y. Z. Zhao, Q. Di Ma, B. G. Liu and J. L. Sun, *J. Fungi*, 2023, **9**, 374.

140 C. Iwamoto, T. Yamada, Y. Ito, K. Minoura and A. Numata, *Tetrahedron*, 2001, **57**, 2997–3004.

141 X. Ding, W. Ye, B. Tan, Q. Song, Y. Chen, W. Liu, L. Sun, W. Tang, Y. Qiao, Q. Zhang, H. Zhang, Y. Wang, W. Zhang, C. Zhang and W. Zhang, *Chin. J. Chem.*, 2023, **41**, 915–923.

142 T. Lin, G. Wang, D. Zeng and H. Chen, *Phytochem. Lett.*, 2015, **13**, 206–211.

143 S. Xu, M. G. Hui, C. S. Yong, Y. Shen, H. Ding and X. T. Ren, *Chem. Biodivers.*, 2009, **6**, 739–745.

144 Q. L. Mou, S. X. Yang, T. Xiang, W. W. Liu, J. Yang, L. P. Guo, W. J. Wang and X. L. Yang, *Tetrahedron Lett.*, 2021, **87**, 153207.

145 X. Yang, P. Wu, J. Xue, H. Li and X. Wei, *Fitoterapia*, 2020, **145**, 104611.

146 S. Gao, P. Wu, J. Xue, H. Li and X. Wei, *Phytochemistry*, 2022, **202**, 113295.



147 B. C. Yan, W. G. Wang, D. B. Hu, X. Sun, L. M. Kong, X. N. Li, X. Du, S. H. Luo, Y. Liu, Y. Li, H. D. Sun and J. X. Pu, *Org. Lett.*, 2016, **18**, 1108–1111.

148 Y. F. Luo, M. Zhang, J. G. Dai, P. Pedpradab, W. J. Wang and J. Wu, *Phytochem. Lett.*, 2016, **17**, 162–166.

149 Y. Hsiao, H.-S. Chang, T.-W. Liu, S.-Y. Hsieh, G.-F. Yuan, M.-J. Cheng and I.-S. Chen, *Rec. Nat. Prod.*, 2016, **10**, 189–194.

150 J. wei Tang, K. Hu, X. zheng Su, X. nian Li, B. chao Yan, H. dong Sun and P. tenzin Puno, *Tetrahedron*, 2020, **76**, 131475.

151 B. C. Yan, W. G. Wang, L. M. Kong, J. W. Tang, X. Du, Y. Li and P. T. Puno, *J. Fungi*, 2022, **8**, 543.

152 Z. Lin, T. Zhu, H. Wei, G. Zhang, H. Wang and Q. Gu, *Eur. J. Org. Chem.*, 2009, **2009**, 3045–3051.

153 J. Kornsakulkarn, P. Auncharoen, A. Khonsanit, N. Boonyuen and C. Thongpanchang, *RSC Adv.*, 2023, **13**, 10564–10576.

154 G. Ding, L. Chen, A. Chen, X. Tian, X. Chen, H. Zhang, H. Chen, X. Z. Liu, Y. Zhang and Z. M. Zou, *Fitoterapia*, 2012, **83**, 541–544.

155 G. Ding, H. Wang, L. Li, A. J. Chen, L. Chen, H. Chen, H. Zhang, X. Liu and Z. Zou, *Eur. J. Org. Chem.*, 2012, **2012**, 2516–2519.

156 G. Ding, H. Wang, L. Li, B. Song, H. Chen, H. Zhang, X. Liu and Z. Zou, *J. Nat. Prod.*, 2014, **77**, 164–167.

157 L. Chen, Y. T. Liu, B. Song, H. W. Zhang, G. Ding, X. Z. Liu, Y. C. Gu and Z. M. Zou, *Fitoterapia*, 2014, **96**, 115–122.

158 C. Von Wallbrunn, H. Luftmann, K. Bergander and F. Meinhardt, *J. Gen. Appl. Microbiol.*, 2001, **47**, 33–38.

159 G. Ding, Y. C. Song, J. R. Chen, X. Chen, H. M. Ge, X. T. Wang and R. X. Tan, *J. Nat. Prod.*, 2006, **69**, 302–306.

160 C. M. Cui, X. M. Li, C. S. Li, P. Proksch and B. G. Wang, *J. Nat. Prod.*, 2010, **73**, 729–733.

161 H. Dou, Y. Song, X. Liu, W. Gong, E. Li, R. Tan and Y. Hou, *Biol. Pharm. Bull.*, 2011, **34**, 1864–1873.

162 S. Thohinung, S. Kanokmedhakul, K. Kanokmedhakul, V. Kukongviriyapan, O. Tusskorn and K. Soytong, *Arch. Pharm. Res.*, 2010, **33**, 1135–1141.

163 G. B. Xu, L. M. Li, T. Yang, G. L. Zhang and G. Y. Li, *Org. Lett.*, 2012, **14**, 6052–6055.

164 M. Xue, Q. Zhang, J. M. Gao, H. Li, J. M. Tian and G. Pescitelli, *Chirality*, 2012, **24**, 668–674.

165 H. Li, J. Xiao, Y. Q. Gao, J. J. Tang, A. L. Zhang and J. M. Gao, *J. Agric. Food Chem.*, 2014, **62**, 3734–3741.

166 C. Chen, J. Wang, J. Liu, H. Zhu, B. Sun, J. Wang, J. Zhang, Z. Luo, G. Yao, Y. Xue and Y. Zhang, *J. Nat. Prod.*, 2015, **78**, 1193–1201.

167 C. Chen, H. Zhu, J. Wang, J. Yang, X. N. Li, J. Wang, K. Chen, Y. Wang, Z. Luo, G. Yao, Y. Xue and Y. Zhang, *Eur. J. Org. Chem.*, 2015, **2015**, 3086–3094.

168 C. Chen, H. Zhu, X. N. Li, J. Yang, J. Wang, G. Li, Y. Li, Q. Tong, G. Yao, Z. Luo, Y. Xue and Y. Zhang, *Org. Lett.*, 2015, **17**, 644–647.

169 R. K. Dissanayake, P. B. Ratnaweera, D. E. Williams, C. D. Wijayarathne, R. L. C. Wijesundera, R. J. Andersen and E. D. de Silva, *Mycology*, 2016, **7**, 1.

170 Z. Zhang, X. Min, J. Huang, Y. Zhong, Y. Wu, X. Li, Y. Deng, Z. Jiang, Z. Shao, L. Zhang and F. He, *Mar. Drugs*, 2016, **14**, 233.

171 C. Chen, Q. Tong, H. Zhu, D. Tan, J. Zhang, Y. Xue, G. Yao, Z. Luo, J. Wang, Y. Wang and Y. Zhang, *Sci. Rep.*, 2016, **6**, 18711–18719.

172 X. Yan, L. J. Wang, Z. Wu, Y. L. Wu, X. X. Liu, F. R. Chang, M. J. Fang and Y. K. Qiu, *J. Chromatogr. B*, 2016, **1033–1034**, 1–8.

173 X. Y. Wang, X. Yan, M. J. Fang, Z. Wu, D. Wang and Y. K. Qiu, *Nat. Prod. Res.*, 2017, **31**, 1669–1675.

174 W. Gao, W. Sun, F. Li, C. Chai, Y. He, J. Wang, Y. Xue, C. Chen, H. Zhu, Z. Hu and Y. Zhang, *Phytochemistry*, 2018, **156**, 106–115.

175 W. Gao, Y. He, F. Li, C. Chai, J. Zhang, J. Guo, C. Chen, J. Wang, H. Zhu, Z. Hu and Y. Zhang, *Bioorg. Chem.*, 2019, **83**, 98–104.

176 H. H. Wang, G. Li, Y. N. Qiao, Y. Sun, X. P. Peng and H. X. Lou, *Org. Lett.*, 2019, **21**, 3319–3322.

177 Q. F. Guo, Z. H. Yin, J. J. Zhang, W. Y. Kang, X. W. Wang, G. Ding and L. Chen, *Molecules*, 2019, **24**, 3240.

178 X. W. Luo, C. H. Gao, H. M. Lu, J. M. Wang, Z. Q. Su, H. M. Tao, X. F. Zhou, B. Yang and Y. H. Liu, *Molecules*, 2020, **25**, 1237.

179 X. G. Peng, J. Liu, Y. Gao, F. Cheng, J. L. Chang, J. Chen, F. F. Duan and H. L. Ruan, *Org. Lett.*, 2020, **22**, 9665–9669.

180 J. Qi, D. Wang, X. Yin, Q. Zhang and J. M. Gao, *Nat. Prod. Commun.*, 2020, **15**, 7.

181 J. Ji, C. Liu, X. He, G. Chen, L. Qin and C. Zheng, *Fitoterapia*, 2021, **151**, 104874.

182 J. F. Wang, R. Huang, S. S. Liu and S. H. Wu, *Chem. Nat. Compd.*, 2021, **57**, 1169–1174.

183 T. Li, Y. Wang, L. Li, M. Tang, Q. Meng, C. Zhang, E. Hua, Y. Pei and Y. Sun, *Mar. Drugs*, 2021, **19**, 438.

184 Q. Guo, J. Chen, Y. Ren, Z. Yin, J. Zhang, B. Yang, X. Wang, W. Yin, W. Zhang, G. Ding and L. Chen, *Front. Chem.*, 2021, **9**, 620589.

185 A. X. Zhang, L. Feng, J. Wang, N. H. Tan and Z. Wang, *J. Asian Nat. Prod. Res.*, 2022, **24**, 769–776.

186 W. Gao, R. Jiang, H. Zeng, J. Cao, Z. Hu and Y. Zhang, *Nat. Prod. Res.*, 2024, **38**, 1599–1605.

187 X. Peng, J. Liu, C. Qin, Q. Wu, W. Li, F. Mohammadipanah and H. Ruan, *Chin. J. Chem.*, 2022, **40**, 1909–1916.

188 J. Wang, Z. Wang, Z. Ju, J. Wan, S. Liao, X. Lin, T. Zhang, X. Zhou, H. Chen, Z. Tu and Y. Liu, *Planta Med.*, 2015, **81**, 160–166.

189 Y. Shu, J. P. Wang, B. X. Li, J. L. Gan, H. Ding, R. Liu, L. Cai and Z. T. Ding, *Phytochemistry*, 2022, **194**, 113009.

190 J. T. Liu, B. Hu, Y. Gao, J. P. Zhang, B. H. Jiao, X. L. Lu and X. Y. Liu, *Chem. Biodivers.*, 2014, **11**, 800–806.

191 Y. Zhou, Y. X. Zhang, J. P. Zhang, H. B. Yu, X. Y. Liu, X. L. Lu and B. H. Jiao, *Nat. Prod. Res.*, 2017, **31**, 1676–1681.

192 D. N. Quang, T. Hashimoto, M. Tanaka, M. Baumgartner, M. Stadler and Y. Asakawa, *J. Nat. Prod.*, 2002, **65**, 1869–1874.



193 L. J. Yang, H. X. Liao, M. Bai, G. L. Huang, Y. P. Luo, Y. Y. Niu, C. J. Zheng and C. Y. Wang, *Nat. Prod. Res.*, 2018, **32**, 208–213.

194 A. Narmani, S. Pichai, P. Palani, M. Arzanlou, F. Surup and M. Stadler, *Mycol. Prog.*, 2019, **18**, 175–185.

195 K. T. Yuyama, L. Wendt, F. Surup, R. Kretz, C. Chepkirui, K. Wittstein, C. Boonlarppradab, S. Wongkanoun, J. Luangsa-Ard, M. Stadler and W. R. Abraham, *Biomolecules*, 2018, **8**, 129.

196 H. Van Trung, P. C. Kuo, N. N. Tuan, N. T. Ngan, N. Q. Trung, N. T. Thanh, H. V. Hai, D. L. Phuong, B. L. Giang, Y. C. Li, T. S. Wu and T. D. Thang, *Nat. Prod. Commun.*, 2019, **14**, 5.

197 S. Wongkanoun, L. Wendt, M. Stadler, J. Luangsa-ard and P. Srikitkulchai, *Mycol. Prog.*, 2019, **18**, 553–564.

198 M. Stadler, D. N. Quang, A. Tomita, T. Hashimoto and Y. Asakawa, *Mycol. Res.*, 2006, **110**, 811–820.

199 M. Stadler, J. Fournier, D. N. Quang and A. Y. Akulov, *Nat. Prod. Commun.*, 2007, **2**, 287–304.

200 C. Lambert, M. J. Pourmoghaddam, M. Cedeño-Sanchez, F. Surup, S. A. Khodaparast, I. Krisai-Greilhuber, H. Voglmayr, T. E. B. Stradal and M. Stadler, *J. Fungi*, 2021, **7**, 131.

201 N. Sharma, M. Kushwaha, D. Arora, S. Jain, V. Singamaneni, S. Sharma, R. Shankar, S. Bhushan, P. Gupta and S. Jaglan, *J. Appl. Microbiol.*, 2018, **125**, 111–120.

202 M. Kushwaha, A. Qayum, S. K. Jain, J. Singh, A. K. Srivastava, S. Srivastava, N. Sharma, V. Abrol, R. Malik, S. K. Singh, R. A. Vishwakarma and S. Jaglan, *ACS Omega*, 2021, **6**, 3717–3726.

203 M. Kushwaha, A. Qayum, N. Sharma, V. Abrol, P. Choudhary, M. Murtaza, S. K. Singh, R. A. Vishwakarma, U. Goutam, S. K. Jain and S. Jaglan, *ACS Omega*, 2022, **7**, 29135–29141.

204 M. J. Pourmoghaddam, G. Ekiz, C. Lambert, F. Surup, G. Primahana, K. Wittstein, S. A. Khodaparast, H. Voglmayr, I. Krisai-Greilhuber, T. E. B. Stradal and M. Stadler, *Mycol. Prog.*, 2022, **21**, 1–14.

205 Q. Zhang, J. Xiao, Q. Q. Sun, J. C. Qin, G. Pescitelli and J. M. Gao, *J. Agric. Food Chem.*, 2014, **62**, 10962–10969.

206 W. X. Wang, Z. H. Li, T. Feng, J. Li, H. Sun, R. Huang, Q. X. Yuan, H. L. Ai and J. K. Liu, *Org. Lett.*, 2018, **20**, 7758–7761.

207 C. W. Lei, Z. Q. Yang, Y. P. Zeng, Y. Zhou, Y. Huang, X. S. He, G. Y. Li and X. H. Yuan, *Nat. Prod. Res.*, 2018, **32**, 7–13.

208 W. X. Wang, T. Feng, Z. H. Li, J. Li, H. L. Ai and J. K. Liu, *Tetrahedron Lett.*, 2019, **60**, 150952.

209 W. X. Wang, X. Lei, Y. L. Yang, Z. H. Li, H. L. Ai, J. Li, T. Feng and J. K. Liu, *Org. Lett.*, 2019, **21**, 6957–6960.

210 W. X. Wang, Z. H. Li, J. He, T. Feng, J. Li and J. K. Liu, *Fitoterapia*, 2019, **137**, 104278.

211 W. X. Wang, X. Lei, H. L. Ai, X. Bai, J. Li, J. He, Z. H. Li, Y. S. Zheng, T. Feng and J. K. Liu, *Org. Lett.*, 2019, **21**, 1108–1111.

212 W. X. Wang, Z. H. Li, H. L. Ai, J. Li, J. He, Y. S. Zheng, T. Feng and J. K. Liu, *Fitoterapia*, 2019, **137**, 104253.

213 P. H. F. da Silva, F. M. A. da Silva and H. H. F. Koolen, *Chem. Nat. Compd.*, 2019, **55**, 592–593.

214 J. H. Su, M. Q. Wang, Y. Z. Li, Y. S. Lin, J. Y. Gu, L. P. Zhu, W. Q. Yang, S. Q. Jiang, Z. X. Zhao and Z. H. Sun, *Fitoterapia*, 2022, **157**, 105124.

215 W. Hinterdobler, M. Bacher, B. B. Shi, D. Baurecht, I. Krisai-Greilhuber, M. Schmoll, L. Brecker, K. Valant-Vetschera and J. Schinnerl, *Nat. Prod. Res.*, 2023, **37**, 85–92.

216 C. Lambert, L. Shao, H. Zeng, F. Surup, P. Saetang, M. C. Aime, D. R. Husbands, K. Rottner, T. E. B. Stradal and M. Stadler, *Mycologia*, 2023, **115**, 277–287.

217 A. Daina, O. Michielin and V. Zoete, *Sci. Rep.*, 2017, **7**(1), 1–13.

218 D. E. V. Pires, T. L. Blundell and D. B. Ascher, *J. Med. Chem.*, 2015, **58**, 4066–4072.

219 E. Urbanik and B. R. Ware, *Arch. Biochem. Biophys.*, 1989, **269**, 181–187.

220 L. Pampanella, G. Petrocelli, P. M. Abruzzo, C. Zucchini, S. Canaider, C. Ventura and F. Facchin, *Cells*, 2024, **13**, 400.

221 C. Hua, Y. Yang, L. Sun, H. Dou, R. Tan and Y. Hou, *Immunobiology*, 2013, **218**, 292–302.

222 L. Pampanella, P. M. Abruzzo, R. Tassinari, A. Alessandrini, G. Petrocelli, G. Ragazzini, C. Cavallini, V. Pizzuti, N. Collura, S. Canaider, F. Facchin and C. Ventura, *Pharmaceuticals*, 2023, **16**, 289.

223 M. Valli, J. M. Souza, R. C. Chelucci, C. R. Biassetto, A. R. Araujo, V. da Silva Bolzani and A. D. Andricopulo, *PLoS One*, 2022, **17**, e0275002.

224 M. Trendowski, T. D. Christen, C. Acquafondata and T. P. Fondy, *BMC Cancer*, 2015, **15**, 1–14.

225 S. MacLean-Fletcher and T. D. Pollard, *Cell*, 1980, **20**, 329–341.

226 P. A. Theodoropoulos, A. Gravanis, A. Tsapara, A. N. Margioris, E. Papadogiorgaki, V. Galanopoulos and C. Stournaras, *Biochem. Pharmacol.*, 1994, **47**, 1875–1881.

227 J. H. Hartwig and T. P. Stossel, *J. Mol. Biol.*, 1979, **134**, 539–553.

228 A. Forer, J. Emmersem and O. Behnke, *Science*, 1972, **175**, 774–776.

229 N. K. Wessells, B. S. Spooner, J. F. Ash, M. O. Bradley, M. A. Luduena, E. L. Taylor, J. T. Wrenn and K. M. Yamada, *Science*, 1971, **171**, 135–143.

230 D. W. Goddette and C. Frieden, *J. Biol. Chem.*, 1986, **261**, 15974–15980.

231 J. S. Choy, X. Lu, J. Yang, Z. Du Zhang and G. S. Kassab, *Am. J. Physiol. Heart Circ. Physiol.*, 2014, **306**, H69.

232 Z. A. Schiller, N. R. Schiele, J. K. Sims, K. Lee and C. K. Kuo, *Stem Cell Res. Ther.*, 2013, **4**, 1–10.

233 J. F. Casella, M. D. Flanagan and S. Lin, *Nature*, 1981, **293**(5830), 302–305.

234 K. Kobayashi, D. Matsuda, H. Tomoda and T. Ohshiro, *Drug Discov. Ther.*, 2022, **16**, 148–153.

235 B. B. Khomtchouk, Y. S. Lee, M. L. Khan, P. Sun, D. Mero and M. H. Davidson, *Expert Opin. Drug Discov.*, 2022, **17**, 443–460.



236 S. Bräse, F. Gläser, C. Kramer, S. Lindner, A. M. Linsenmeier, K.-S. Masters, A. C. Meister, B. M. Ruff and S. Zhong, *The Chemistry of Mycotoxins*, Springer, Wien Heidelberg New York Dordrecht London, 2013.

237 D. G. Menter, B. F. Sloane, B. W. Steinert, J. Onoda, R. Craig, C. Harkins, J. D. Taylor and K. V. Honn, *J. Natl. Cancer Inst.*, 1987, **79**, 1077–1090.

238 B. H. Choi, J. A. Park, K. R. Kim, G. I. Lee, Y. T. Lee, H. Choe, S. H. Ko, M. H. Kim, Y. H. Seo and Y. G. Kwak, *Am. J. Physiol. Cell Physiol.*, 2005, **289**, 425–436.

239 Y. Takanezawa, R. Nakamura, Y. Kojima, Y. Sone, S. Uraguchi and M. Kiyono, *Biochem. Biophys. Res. Commun.*, 2018, **498**, 603–608.

240 G. Van Goetsenoven, V. Mathieu, A. Andolfi, A. Cimmino, F. Lefranc, R. Kiss and A. Evidente, *Planta Med.*, 2011, **77**, 711–717.

241 S. Delebassée, L. Mambu, E. Pinault, Y. Champavier, B. Liagre and M. Millot, *Fitoterapia*, 2017, **121**, 146–151.

242 M. S. Reifenberger, L. Yu, H. F. Bao, B. J. Duke, B. C. Liu, H. P. Ma, A. A. Alli, D. C. Eaton and A. A. Alli, *Am. J. Physiol.*, 2014, **307**, 86–95.

243 T. Udagawa, J. Yuan, D. Panigrahy, Y.-H. Chang, J. Shah and R. J. D'Amato, *J. Pharmacol. Exp. Ther.*, 2000, **249**, 421–428.

244 K. C. Tjandra, N. McCarthy, L. Yang, A. J. Laos, G. Sharbeen, P. A. Phillips, H. Forgham, S. M. Sagnella, R. M. Whan, M. Kavallaris, P. Thordarson and J. A. McCarroll, *J. Med. Chem.*, 2020, **63**, 2181–2193.

245 K. E. Fischer, G. Nagaraj, R. Hugh Daniels, E. Li, V. E. Cowles, J. L. Miller, M. D. Bunger and T. A. Desai, *Biomaterials*, 2011, **32**, 3499–3506.

246 R. E. Serda, J. Gu, R. C. Bhavane, X. W. Liu, C. Chiappini, P. Decuzzi and M. Ferrari, *Biomaterials*, 2009, **30**, 2440–2448.

247 A. W. Baird, C. T. Taylor and D. J. Brayden, *Adv. Drug Deliv. Rev.*, 1997, **23**, 111–120.

248 A. Nair, J. Bu, P. A. Rawding, S. C. Do, H. Li and S. Hong, *Nanomaterials*, 2022, **12**, 3.

249 T. T. Morgan, H. S. Muddana, E. I. Altinoğlu, S. M. Rouse, A. Tabaković, T. Tabouillot, T. J. Russin, S. S. Shanmugavelandy, P. J. Butler, P. C. Eklund, J. K. Yun, M. Kester and J. H. Adair, *Nano Lett.*, 2008, **8**, 4108–4115.

250 K. G. Lehmann, J. J. Popma, J. A. Werner, A. J. Lansky and R. L. Wilensky, *J. Am. Coll. Cardiol.*, 2000, **35**, 583–591.

251 M. Trendowski, J. M. Mitchell, C. M. Corsette, C. Acquafondato and T. P. Fondy, *Invest. New Drugs*, 2015, **33**, 290–299.

252 F. Y. Huang, W. L. Mei, Y. N. Li, G. H. Tan, H. F. Dai, J. L. Guo, H. Wang, Y. H. Huang, H. G. Zhao, S. L. Zhou, L. Li and Y. Y. Lin, *Eur. J. Cancer*, 2012, **48**, 2260–2269.

253 J. Hwang, M. Yi, X. Zhang, Y. Xu, J. H. Jung and D. K. Kim, *Oncol. Rep.*, 2013, **30**, 1929–1935.

254 M. Y. Kim, J. H. Kim and J. Y. Cho, *Biol. Ther.*, 2014, **22**, 295–300.

255 J. Bylund, S. Pellmé, H. Fu, U. H. Mellqvist, K. Hellstrand, A. Karlsson and C. Dahlgren, *BMC Cell Biol.*, 2004, **5**, 1–14.

256 V. Betina, D. Mičeková and P. Nemec, *Microbiology*, 1972, **71**, 343–349.

257 J. He, Q. Zou, H. Deng, S. He, D. Yan, K. Pan, Y. Zhou, Z. Zhao, H. Cui and Y. Liu, *Fitoterapia*, 2024, **173**, 105804.

258 Z. Wu, W. Wang, J. Li, C. Ma, L. Chen, Q. Che, G. Zhang, T. Zhu and D. Li, *J. Nat. Prod.*, 2024, **26**, 87–91.

259 A. Ali, B. A. Malla, N. Sehar, S. B. Ahmad, Z. Imtiyaz, A. Arafah, M. U. Rehman and A. Nadeem, *J. Biol. Regul. Homeost. Agents*, 2023, 4555–4569.

260 K. Bhattacharai, M. E. Kabir, R. Bastola and B. Baral, *Adv. Genet.*, 2021, **107**, 193–284.

261 I. S. Asogwa, C. Osita Eze, A. I. Onah, C. A. Agbo, S. A. Evarani and A. A. Attama, *Int. J. Sci. Res. Arch.*, 2024, **2024**, 302–321.

262 X.-H. Si, R.-Y. Lyu, Z.-G. Sun, H. Dong and X.-Y. Liu, *Cancer Adv.*, 2023, **6**, e23021.

263 P. B. Devi, R. Jayaseelan, P. B. Devi and R. Jayaseelan, *Drug Design – Novel Advances in the Omics Field and Applications*, 2020, pp. 117–125.

